Heat flux and friction losses effects on natural circulation package boilers

— **Source link**

Syed A.M. Said, H. Al-Saqour, Mohamed A. Habib

Institutions: King Fahd University of Petroleum and Minerals, Saudi Aramco

Related papers:

- Experimental Study on Natural Circulation Heat Transfer of Square Channel in Water-Cooled Blanket

- Optimum structural design of a heat exchanger for gas-circulation systems

- Sensitivity studies in the optimal design of a natural-circulation boiling water loop.

- Experimental Investigations on Temperature Distribution and Heat Removal Capability of Residual Heat Exchanger

- Dynamic heat transfer analysis of a direct-expansion CO2 downhole heat exchanger

HEAT FLUX AND FRICTION LOSSES EFFECTS ON NATURAL CIRCULATION IN PACKAGE BOILERS

BY

HAMAD S. AL MEHTHEL AL SAQOUR

A Dissertation Presented to the

DEANSHIP OF GRADUATE STUDIES

KING FAHD UNIVERSITY OF PETROLEUM & MINERALS

DHAHRAN, SAUDI ARABIA

In Partial Fulfillment of the
Requirements for the Degree of
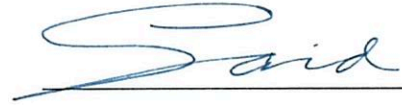
DOCTOR OF PHILOSOPHY

In

MECHANICAL ENGINEERING

MAY 2019

KING FAHD UNIVERSITY OF PETROLEUM & MINERALS

DHAHRAN- 31261, SAUDI ARABIA

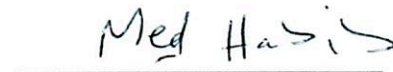**DEANSHIP OF GRADUATE STUDIES**

This thesis, written by **HAMAD SHATRAIN HAMAD AL MEHTHEL AL SAQOUR** under the direction of his thesis advisor and approved by his thesis committee, has been presented and accepted by the Dean of Graduate Studies, in partial fulfillment of the requirements for the degree of **DOCTOR OF PHILOSOPHY IN MECHANICAL ENGINEERING.**

Dr. Zuhair M. Gasem
Department Chairman

Dr. Salam A. H. Zummo
Dean of Graduate Studies

28/5/19
Date

Dr. Syed A. M. Said
(Advisor)

Dr. Mohamed A. M. Habib
(Co-Advisor)

Dr. Esmail M. A. Mokheimer
(Member)

Dr. Habib Ibrahim Abualhamayel
(Member)

Dr. Ahmet Ziyaettin Sahin
(Member)

Dedication

I dedicate this dissertation to my parents and my wife for their support, words of encouragement, and prayers throughout my PhD journey.

ACKNOWLEDGEMENTS

TABLE OF CONTENTS

LIST OF TABLES

LIST OF FIGURES

LIST OF ABBREVIATIONS

ANSYS	analysis system (CFD software)
CFD	computational fluid dynamics
CHF	critical heat flux
CR	circulation ratio
D-A	floor tubes of the D-Tubes circuit
D-B	vertical tubes of the D-Tubes circuit
D-C	roof tubes of the D-Tubes circuit
DC-A	primary downcomer circuit
DC-B	secondary downcomer circuit
DNB	departure from nucleate boiling
D-Tubes	circuit with D shape tubes
EVA1	first circuit of the evaporator tubes
EVA2	second circuit of the evaporator tubes
EVA3	third circuit of the evaporator tubes
EVA4	fourth circuit of the evaporator tubes
FW	front wall circuit
HRSG	heat recovery steam generator
MW	megawatts
NDH	net driving head
RW	rear wall circuit
SGG	sum of gray gases
TPFPD	two-phase friction pressure drop
WSGG	weighted-sum of gray gases

LIST OF SYMBOLS

A	Tube cross sectional area, m^2
B	Number of burners
BD	% boiler blowdown from steam output
c_{pg}	Specific heat of flue gas at T_g, kCal/(kg.°C)
$c_{pg-adia}$	Specific heat of flue gas at the adiabatic flame temperature, kCal/(kg.°C)
CR	Circulation ratio
$CR_{min-allow}$	Minimum allowable circulation ratio
C_t	Screen tube exposed circumference, mm
D_F	Furnace depth, m
D_i	Tube inside diameter, mm
D_o	Tube outside diameter, mm
D_{oF}	Feeder tubes outside diameter, mm
D_{oS}	Supply tubes outside diameter, mm
E/D_i	Diameter roughness factor, 1/mm
E_f	Fin extension on both sides of tube, mm
$EPRS$	Effective projected radiant surface of the furnace tubes, m^2
ESL	Total exposed surface length, mm
f_e	External fouling factor, $(m^2.hr.°C)/kCal$
f_{fouled}	Friction factor for fouled tube
f_i	Internal fouling factor, $(m^2.hr.°C)/kCal$
f_{incon}	Concentrated friction factor at the inlet

f_{outcon}	Concentrated friction factor at the outlet
f_{new}	Friction factor for new tube
h_{adia}	Adiabatic enthalpy, kCal/kg
h_{fg}	Latent heat of vaporization, kCal/kg
h_{fw}	Enthalpy at feed water temperature, kCal/kg
$h_{sat.s}$	Enthalpy of saturated steam, kCal/kg
$h_{sat.w}$	Enthalpy of saturated water, kCal/kg
$h_{sup.st}$	Enthalpy of superheated steam , kCal/kg
H_F	Furnace height, m
L_e	Equivalent tube length, m
L_f	Length of fin, m
LHV	Lower heating value of fuel gas, kCal/m^3
$\dot{m}_a$	Air mass flow rate, kg/hr
$m_{a/f}$	Specific combustion air flow (per fuel volume), kg/m^3
$\dot{m}_{fuel}$	Total fuel mass flow rate, kg/hr
$\dot{m}_g$	Flue gas mass flow rate, kg/hr
$m_{g/f}$	Specific flue gas flow (per fuel volume), kg/m^3
$\dot{m}_s$	total steam mass flow rate in a circuit, kg/hr
$\dot{m}_{s1}$	Steam generation in the circuit, kg/hr
$\dot{m}_{s2}$	Steam inlet flow (required for subcooling) in the circuit, kg/hr
$\dot{m}_{s-cons.}$	Steam consumption of the boiler due to economizer water subcooling, kg/hr
$\dot{m}_{s+cons.}$	Total steam produced by the boiler considering $\dot{m}_{s-cons.}$, kg/hr
$\dot{m}_w$	Water mass flow rate, kg/hr

N	Number of the tubes in a circuit
N_F	Number of the feeder tubes for Circuits 1 and 2
N_S	Number of the supply tubes for Circuits 1 and 2
NDH	Net driving head, kg/m^2
NDH_1	Total net driving head for the circuit, kg/m^2
NDH_2	Net driving head for the feeder tubes (Circuit 1 and 2), kg/m^2
NDH_3	Net driving head for the supply tubes (Circuit 1 and 2), kg/m^2
Nu	Nusselt number
p	Tube pitch, mm
P_d	Steam drum pressure, barg
P_{fw}	Feed water pressure, barg
ΔP_{dist}	Distributed pressure drop, kg/m^2
ΔP_{incon}	Concentrated pressure drop at the inlet, kg/m^2
$\Delta P_{internals}$	Seam drum internals pressure drop, kg/m^2
ΔP_{outcon}	Concentrated pressure drop at the inlet, kg/m^2
Pr	Prandtl number of water
P_s	Steam pressure, barg
ΔP_{tot}	Total pressure drop in the circuit, kg/m^2
q''	Heat flux, $kCal/(hr.m^2)$
Q_{abs}	Absorbed heat output, $kCal/hr$
Q_{bd}	Blowdown heat output, $kCal/hr$
Q_c	Total heat of combustion, $kCal/hr$
Q_{c-EPRS}	Combustion heat load on the furnace EPRS, $kCal/(hr.m^2)$

Q_{c-FV}	Combustion heat load on the furnace volume, $kCal/(hr.m^2)$	
Q_{fur}	Heat exchanged in the furnace, $kCal/hr$	
Q_g	Flue gas heat at furnace exit, $kCal/hr$	
Q_{rad}	Radiation heat from flue gas to tubes, $kCal/hr$	
Q_{rad-RL}	Radiation heat considering radiation loss, $kCal/hr$	
Q_{THO}	Total heat output, $kCal/hr$	
R_{conv}	Resistance of inner water film, $(m.^{\circ}C)/W$	
Re	Reynolds number	
RL	% Radiation loss of the absorbed heat	
R_{pipe}	Resistance of tube thickness, $(m.^{\circ}C)/W$	
S	Tube surface area, m^2	
SH	Static Head, m	
SH_i	Static Head at the inlet of the circuit, m	
SH_{iF}	Static Head at the inlet of the feeder tubes (Circuits 1 and 2), m	
SH_{iS}	Static Head at the inlet of the supply tubes (Circuits 1 and 2), m	
SH_o	Static Head at the outlet of the circuit, m	
SH_{oF}	Static Head at the outlet of the feeder tubes (Circuits 1 and 2), m	
SH_{oS}	Static Head at the outlet of the supply tubes (Circuits 1 and 2), m	
SO	Steam output, kg/hr	
t_f	Fin thickness, mm	
t_w	Tube wall thickness, mm	
t_{wF}	Feeder tubes thickness for Circuits 1 and 2, mm	
t_{wS}	Supply tubes thickness for Circuits 1 and 2, mm	

T_{adia}	Adiabatic flame temperature, °C
T_{amb}	Ambient air temperature, °C
ΔT_{ei}	Temperature difference from external to internal bulk, °C
T_{EO}	Water temperature at the economizer outlet, °C
T_f	Fin temperature, °C
ΔT_f	Temperature difference across the fin, °C
ΔT_{fe}	Temperature difference across fe, °C
ΔT_{fi}	Temperature difference across fi, °C
T_{fuel}	Fuel gas temperature, °C
T_{fw}	Feed Water Temperature, °C
TH	Thermosyphonic head (mixture average density multiplied by the static head column height difference), kg/m^2
T_i	Temperature of internal bulk, °C
T_{sat}	Saturation temperature at drum pressure, °C
T_{sup}	Superheated steam temperature, °C
T_{t-f}	Mean temperature of tube and fin, °C
ΔT_w	Temperature difference across tube wall, °C
T_{w-fur}	Furnace tube wall temperature, °C
T_{wi-eva}	Inside Tube wall temperature of the evaporator bank tubes, °C
T_{wo-eva}	Outside Tube wall temperature of the evaporator bank tubes, °C
v_{avg}	Mixture average velocity, m/s
v_i	Water inlet velocity, m/s
v_o	Water outlet velocity, m/s

$\dot{V}_a$ *Volumetric flow rate of combustion air, m^3/hr*

$\dot{V}_f$ *Volumetric flow rate of fuel gas, m^3/hr*

V_{fur} *Furnace volume, m^3*

$\dot{V}_g$ *Volumetric flow rate of flue gas, m^3/hr*

V_P *Mass velocity*

W_F *Furnace width., m*

x_i *Ratio of steam at the inlet to steam at the outlet of the circuit*

x_o *Ratio of steam output to steam at the outlet of the circuit*

Z_{avg} *Average velocity head, kg/m^2*

Z_i *Inlet velocity head, kg/m^2*

Z_o *Outlet velocity head, kg/m^2*

Greek Symbols

α_e *External heat transfer coefficient, $kCal/(hr.m^2.°C)$*

α_i *Internal heat transfer coefficient, $kCal/(hr.m^2.°C)$ in heat flux calculations or $W/(m^2.°C)$ in circulation ratio calculations*

α_o *Overall heat transfer coefficient, $kCal/(hr.m^2.°C)$*

δ *Fin factor*

$\in$ *Fuel emissivity*

ξ *Boiler efficiency, % based on LHV (ASME PTC4.1)*

λ *Thermal conductivity of tube and fin, $W/(m.°C)$*

$\mu_{mix-avg}$ *Average mixture viscosity, $kg/(m.hr)$*

μ_s *Steam viscosity at the drum design pressure, $kg/(m.hr)$*

μ_{s-avg}	*Average steam viscosity, kg/(m.hr)*
μ_w	*Water viscosity at the drum design pressure, kg/(m.hr)*
μ_{w-avg}	*Average water viscosity, kg/(m.hr)*
ρ_a	*Wet air density, kg/m³*
ρ_g	*Specific Flue gas density, kg/m³*
$\rho_{mix-avg}$	*Average mixture density, kg/m³*
ρ_{mix-i}	*Mixture density at the inlet of the circuit, kg/m³*
ρ_{mix-o}	*Mixture density at the outlet of the circuit, kg/m³*
ρ_s	*Steam density at the steam drum design pressure, kg/m³*
ρ_{si}	*Steam density at the inlet of the circuit, kg/m³*
ρ_{so}	*Steam density at the outlet of the circuit, kg/m³*
ρ_w	*Water density at the steam drum design pressure, kg/m³*
ρ_{wi}	*Water density at the inlet of the circuit, kg/m³*
ρ_{wo}	*Water density at the outlet of the circuit, kg/m³*
τ	*Density ratio factor*

ABSTRACT

Full Name	:	Hamad Shatrain Al Mehthel Al Saqour
Thesis Title	:	Heat Flux and Friction Losses Effects on Natural Circulation in Package Boilers
Major Field	:	Mechanical Engineering
Date of Degree	:	May 2019

Natural circulation boilers are generally preferred over forced circulation ones in the oil and gas industry due to potential pumping system breakdowns and high water treatment programs costs. However, water circulation in natural circulation boilers is a critical factor in boiler operation. Poor circulation may cause tube failures resulting in unplanned boiler shutdowns that may interrupt the whole plant operation. Such poor circulation may arise due to either an excessive pressure drop in some of the boiler tubes, resulting from losses in bends and other local resistances, or due to problems related to boiler operation resulting in sudden boiler load fluctuations. Excessive pressure drops are either a result of tube geometry or internal friction effects. Water side scale and deposits that build up inside the tubes is a significant contributor to friction increase and tube corrosion. Scaled tubes are susceptible to failure due to losing mixture cooling effect, as a result of the higher pressure drop, or starting the tube side corrosion. The published literature does not include a model that would perform calculations for each circuit and produce circulation parameters for all circuits at the same time. Hence, the overall objective of this dissertation was to develop a program that will size and analyze the performance of package boilers. The specific objectives include: 1) sizing of package boilers to meet a specific load, 2) identifying the most critical circuit of a package boiler, 3) determining the impact of heat flux on the circulation parameters and the wall temperature, 4) determining the impact of friction factor on circulation

parameters, and 5) determining the impact of plugging the D-tubes and boiler bank tubes on circulation parameters and tube wall temperature.

Excellent agreement was observed between the program results and the actual data of package boilers. The impact studies results revealed that: the D-Tubes (Circuit 3) is the most critical circuit. Plugging these tubes reduces the circulation ratio and increases the tube wall temperature significantly. Also, the results indicated that the distributed pressure drops play an adverse impact on circulation. The available driving head decreases as the pressure drop increases. Boiler operators and analysts need to ensure that all boiler circuits are operating above the minimum circulation ratio, pay special considerations for the D-Tubes circuit, have an effective water treatment program to minimize internal friction effects and minimize tube plugging in the D-Tubes circuit. Further, a number of design modifications can be made to achieve a reliable circulation.

ARABIC ABSTRACT

ملخص الرسالة

الاسـم الكامل	:	حمد شطرين حمد آل مهذل الصقور
عنوان الرسالة	:	تأثير التدفق الحراري والاحتكاك الداخلي في الأنابيب على غلايات الدوران

الطبيعي (المجمعة مسبقاً في المصنع)

التـخصـص	:	الهندسة الميكانيكية
تاريخ التخرج	:	مايو 2019م

غلايات الدوران الطبيعي مفضلة عمومًا على غلايات الدوران القسري في صناعة النفط والغاز نظرًا لاحتمال تعطل نظام الضخ وارتفاع تكاليف برامج معالجة المياه ، ومع ذلك ، فإن دوران الماء في غلايات الدوران الطبيعي يعد عاملاً بالغ الأهمية في تشغيل الغلاية. أعطال الأنبوب التي تؤدي إلى إغلاق الغلايات غير المخطط له والتي قد تعطل تشغيل المعمل بالكامل، وقد ينشأ هذا الدوران الضعيف نتيجة لانخفاض الضغط المفرط في بعض أنابيب الغلاية ، نتيجةً للخسارة في الانحناءات والمقاومات المحلية الأخرى، أو بسبب مشاكل متعلقة بتشغيل الغلاية تكون قد أدت إلى تقلبات مفاجئة في تحميل الغلاية. إن نزول الضغط الزائد إما أن يكون نتيجة للتصميم الهندسي للأنبوب أو تأثيرات الاحتكاك الداخلي في الأنبوب، يعتبر التقشر في جانب الماء والترسبات التي تتراكم داخل الأنابيب مساهماً كبيراً في زيادة الاحتكاك وتآكل الأنبوب. الأنابيب المتقشرة داخلياً أكثر عرضة للفشل بسبب فقدان تأثير تبريد خليط الماء والبخار ، باعتبارها نتيجة من انخفاض الضغط العالي أو بدء التآكل من جانب الأنبوب، إلى أفضل معرفة للمؤلفين ؛ لا تتضمن الأدبيات المنشورة نموذجًا من شأنه إجراء عمليات حسابية لكل دائرة ويأتي بعوامل الدوران لجميع الدوائر في نفس الوقت ، لذلك فالهدف العام لهذه الأطروحة هو تطوير برنامج لتنفيذ حسابات تصميم الدوران الطبيعي وتحليل الاداء للغلايات المجمعه في المصنع مسبقاً، وتشمل الأهداف المحددة ما يلي : 1) تغيير حجم غلايات العبوات لتتوافق مع الحمل المحدد ، 2) تحديد الدائرة الأكثر أهمية في الغلاية ، 3) تحديد تأثير تدفق الحرارة على عوامل الدوران الطبيعي ودرجة حرارة جدار الأنابيب ، 4) تسليط الضوء على تأثير عامل الاحتكاك الداخلي على عوامل الدوران الطبيعي ، و5) تحديد تأثير سد أنابيب D وأنابيب بنك الغلايات على عوامل الدوران ودرجة حرارة جدار الأنبوب .

وقد تم تطوير برنامج من شأنه تغيير حجم وتحليل أداء المراجل وقد أشارت النتائج إلى أن مخرجات البرنامج تتفق بشكل جيد مع البيانات المقاسة الفعلية ، وأن الدائرة الأكثر أهمية هي أنابيب ال D ، وأن سد هذه الانابيب يقلل من نسبة الدوران الطبيعي ويزيد من درجة حرارة جدار الانبوب بشكل كبير. اظهرت النتائج ايضا أن فوارق الضغط الموزعه لها تأثير سلبي على الدوران الطبيعي. يتناقص دفع السائل المتاح مع زيادة فوارق الضغط.

يحتاج مشغلوا ومحللوا الغلايه الى التأكد من أن جميع دوائر الغلايه تعمل فوق نسبة الحد الادنى للدوران الطبيعي ، وأن يكون هناك اعتبارات خاصه لدائرة أنابيب ال D ، وأن يوجد برنامج فعال لمعالجة المياه لتقليل آثار الاحتكاك الداخلي ، وان يتم تجنب سد الانابيب في دائرة D. علاوة على ذلك هناك العديد من التعديلات الممكن اجراؤها لتحقيق دوران طبيعي موثوق.

.

CHAPTER 1

INTRODUCTION

In recent years, oil and gas industries have preferred natural circulation boilers over forced circulation ones. This is because the breakdown of pumps used in forced circulation boilers could cause major failures in the boiler tubes and drums. Also, water treatment maintenance and operation costs are significant.

Water circulation in natural circulation boilers is a critical factor in boiler operation. Poor water circulation may cause tube failures resulting in unplanned boiler shutdowns which may interrupt the whole plant or refinery operation. Such poor circulation may arise due to either an excessive pressure drop in some of the boiler tubes, resulting from losses in bends and other local resistances, or due to problems related to operating the boiler resulting in sudden boiler load fluctuations. In fired boilers, each of the furnace tubes is exposed to unique heating conditions due to the non-uniform heat flux distribution. Concurrently, boiler tube geometry depends on its location in the furnace being at the front, side or rear walls.

Water side scale and deposits that build up inside the tubes comprise a significant contributor to friction increase and eventually tube corrosion. In both cases, tubes are susceptible to failure by reducing water cooling effect or starting the tube side corrosion, respectively.

1

This dissertation was aimed at developing a program that will carry out the design of circulation parameters for a 112,000 kg/hr package boiler, identify the most critical circuit in the boiler, determine the impact of heat flux on the circulation parameters and the tube wall temperature, and determine the internal friction impact on circulation.

The boiler tubes, excluding the downcomers, are divided into eight different circuits (front wall, rear wall, D-Tubes, division wall, and evaporators). Input data to the program included general information about the boiler to be designed, including steam drum design, economizer output water temperature, boiler blowdown rate, furnace, dimensions, tubes and fin materials, fuel specifications, combustion air and flue gas flow relative to fuel gas, boiler efficiency, excess air percentage, and radiation loss. Further, input data for every circuit included heat flux, heating surface (number of tubes), tube geometry (length, height, diameter size, and thickness), tube pitch, internal friction and fouling factors, and water mass flow rate. The output of the program for every circuit includes heat flux, steam generation and mass flow rates, circulation ratio, number of tubes, velocity, pressure drop, and net driving head.

CHAPTER 2

LITERATURE REVIEW

The published literature on the analysis of water circulation in boilers can be divided into several categories. These include natural water circulation in boiler tubes, numerical simulation of natural water circulation, heat flux in natural circulation, boiler internal friction in water tube boilers, furnace heat transfer and water circulation in natural circulation boilers, and boiler tube failures. The analysis of the literature on each category is presented in this section.

2.1 Natural Water Circulation in Boiler Tubes

Numerous investigations were conducted on the effect of various parameters on natural circulation in different energy conversion systems such as solar heaters, cooling systems of nuclear reactors, thermosiphon reboilers and many others. Zvirin [1] gave an excellent review of the studies conducted on various types of natural-circulation loops prior to 1981.

Ganapathy [2] presented a method for the calculation of various losses in a natural-circulation waste-heat boiler together with a discussion of the causes of boiler tube failure. He highlighted that high pressure natural circulation boilers (1,500 to 2,100 psig) normally operate within a CR range of 4 to 8. However, lower pressure waste-heat boilers (200 to 1,000 psig) operate in the range of 15 to 50 CR. He further explained that the whole circulation system needs to be analyzed rather than looking at the circulation ratio (CR)

3

only. Beside CR, a number of other parameters need to be analyzed to have an insight on dynamics and reliability of the boiling process. These parameters include heat flux, steam pressure, number of tubes, tube geometry (size, orientation, roughness, and location), quality of feed water, etc. Tube failures occur due to departure from nucleate boiling (DNB). DNB is a result of losing the cooling effect in the tube when the mixture does not remove the big number of bubbles formed; hence the tube is not cooled adequately. Determining the amount of water-steam mixture is achieved by calculating the CR. Considering the above mentioned parameters makes CR calculations involved and iterative. The main circuits of the boiler are comprised of down-comers, risers, and evaporator with possible multiple paths for each circuit. Each of these circuits has a different CR based on the amount of steam generated and the different system resistances associated with the tube geometry. The boiler bank evaporator tubes circuit can be further divided into various circuits of parallel paths, each with a different steam generation rate and CR. The division is made based on boilers operators and manufacturers' judgment and experience.

Kok et al. [3] developed a model that estimates the steady state variables involved in a boiling water reactor simulation loop including the natural-circulation mass flow rate, steam quality, and void fraction. The model was derived following the study carried out by Van de Graaf et al. [4] for investigating a natural-circulation loop consisting of a scaled version of an actual boiling water reactor. There was excellent agreement between the obtained values of the circulation flow rate and the experimental data except at very low power where the flow rate was over-predicted. The measured and predicted mass flow rates obtained for a much wider range of valve friction factors were in excellent agreement. As

a result, the authors suggested that the model correctly describes all relevant physics of the system. Wu et al. [5] conducted an experimental investigation of the stability of two-phase flow in the natural-circulation primary loop of a nuclear heating reactor. The effects of system inlet sub-cooling, pressure and steam quality on the system stability were investigated. Higher system inlet sub-cooling and pressures resulted in wider stable regions. It was also found that the steam quality at the exit of the heated section could be considered a dominant factor for the hydrodynamic stability of a low quality, two-phase natural circulation system. Ha et al. [6] studied the behavior of boiling-induced two-phase natural circulation flow in the insulation gap using a 1/21.6 scaled experimental facility to simulate an Advanced Power Reactor 1400 reactor vessel and the associated insulation system. Results were compared with analytical data given by simple loop analysis. Local recirculation convective flows in the minimum gap were detected by flow observation. The results indicated an increase in the mass flow rates as the flux and area increased and a generation of periodic intensive back flow in the case of high flux and small area. Also; the results indicated a qualitative agreement between the obtained mass flow rates using simple loop analysis and the experimental ones as the heat flux was varied.

Ganapathy [7] discussed measures for understanding and ensuring good natural boiler circulation. He provided guidance on determining the circulation ratio (CR) in package D-type shop-assembled boilers used in petro-chemical industries and power plants. He identified four steps for circulation calculation.

Roslyakov et al. [8] investigated the impact of various design solutions on the stability of natural circulation in a circuit with horizontal evaporator tubes of negative static head. A criteria was proposed for characterizing reliability and efficiency of the investigated

system. Also, a procedure for circulation calculations and an algorithm for checking reliability of the evaporator's performance were developed. The investigators concluded that more stable natural circulation in vertical HRSGs is achieved most efficiently by installing a U-shaped evaporator with as many number of tubes in the coil as possible, and that the commonly adopted criteria for stability of natural circulation is not suitable for determining reliable operation of a horizontal heater; therefore, indirect parameters have to be used.

De Mesquita et al. [9] investigated enhancing the accuracy of predicting transition shapes of two phase flows. Characteristics of images were used to classify two-phase flow instabilities in natural circulation designs. These classifications were used as input to an algorithm developed for grouping self-organizing maps. This system was used to analyze and obtain a more successful classification to allow for effective experimental studies on two-phase flow studies.

2.2   Numerical Simulation of Natural Water Circulation

Pereyra et al. [10] investigated the effect of the water circulation rate on tube burnout in a natural-circulation boiler. The results indicated that the critical heat flux (that may cause tube burnout) was much higher than the actual heat flux values, suggesting that the boiler failure from the general tube burnout was unlikely and that tube failure is more likely to be caused by corrosion in the presence of poor circulation which causes high tube metal temperature. Basu and Cheng [11] investigated theoretically and experimentally the heat transfer characteristics of a finned water wall tube in a circulating fluidized bed boiler. The numerical analysis indicated that the heat flux (based on the inner wall surface) around a

water tube increases when a lateral fin or longitudinal fin is welded on it and the influence of the inner heat transfer coefficient and the metal thermal conductivity is low. The heat transfer enhancement by fins was verified by experimental measurements and the temperature distribution of the finned water tube cross-section agreed well with the theoretical analysis.

Astrom and Bell [12] presented a nonlinear dynamic model for natural circulation drum boilers. The complicated dynamics of the drum, downcomer, and riser components were explained by the model. The model addressed the complex shrink and swell phenomena fairly well. Validation of the model results against unique plant data was presented. The model covers a wide range of operating conditions.

Gomez et al. [13] presented a mathematical model of the convection heat transfer section of a power plant boiler. Validation of the model was carried out in two stages. Initially, it was validated against simple heat exchanger geometries for which analytical solutions can be obtained. Then the model was applied to an actual 350 MW power-station boiler. P.J. Edge et al. [14] linked a 1D process model for steam generation in a natural circulation boiler (thermosiphon loop) to a 3D computational fluid dynamics (CFD) model of the coal-fired furnace. Data from a 500 MWe subcritical power plant was used to validate the CFD model. Physics of the furnace combined with the steam loop resulted in circulation flows of approximately four times the feed water flow. The heat transfer coefficient of the steam is predicted by the process model, then the overall heat transfer coefficient is estimated by the CFD model as a function of height. J. Krzywanski and W. Nowak [15] presented a model that utilizes an artificial neural network for estimating the local heat transfer

coefficient in the furnace of a circulating fluidized bed boiler. Results of the model were in agreement with numerical and experimental results.

Hou et al [16] investigated the water hammering (sudden changes in pressure and temperature) resulting from flashing instability in natural circulation systems. Factors impacting the phenomena were studied such as vertical channel, tube outlet temperature, inlet subcooling, loop structure, and non-condensable gases in water. Scope, intensity, start and exit of hammering were also considered. A numerical model was used to simulate the peak of hammering. Results of the simulation (with low inlet subcooling) were congruent with the experiments, however, they were not in the case of high inlet subcooling.

2.3   Heat Flux in Natural Circulation Boilers

Biasi et al [17] proposed a new empirical correlation for predicting the critical heat flux flow circular ducts. The correlation has been compared with nearly more than 5000 experimental burnout data provided by laboratories from all over the world. A comparison with the experimental data indicated that the new proposed correlation exhibits a mean error of -0.124 and a mean quadratic error of 7.26 %. Leung et al [18] developed a computer code for predicting the onset of critical heat flux (CHF) using a number of well-known correlations. The code was also used to predict transient CHF based on the local conditions. A majority of the thermal-hydraulic calculation results produced by the code demonstrated matched the in-core measurements, however, with some discrepancies.

Jan Taler [19] developed a method for determining the local heat flux, inside heat transfer coefficient and water-steam mixture temperature in power station boiler furnaces based on

the distribution of tube temperature. The calculated and measured values showed good agreement. The method is suited both to membrane wall and smooth tubes.

Critical heat flux (CHF) in vertical and annular tubes was investigated experimentally by Monde and Yamaji [20], Monde et al. [21] and Monde et al. [22]. Three correlations were proposed to estimate the critical heat flux in vertical and annular tubes. Monde et al. [22] measured critical heat flux in natural circulation boiling water in a uniformly heated vertical annular tube with an uncertainty of 5 %.

Hall and Mudawar [23] developed a CHF database considered to be the largest with 32,544 data points collected from over 100 sources. The assessment indicated that 93 of the data was acceptable. Hence, it's considered to be an invaluable tool for the development of more accurate CHF correlations.

Taler et al. [24] presented a device (flux-tube) that can operate for a long time in the destructive environment of high-temperature cool-fired boiler furnaces and a numerical method for estimating the heat flux in boiler furnaces based on inner tube wall temperature measurements. The device and the numerical method can be used for online monitoring of membrane wall slagging to optimize boilers' operation and efficiency.

Kim [25] investigated the effects of many parameters, such as system pressure, mass flow rate, sub-cooled temperature, and surface wettability, on CHF under sub-cooled flow boiling conditions. The CHF prediction model, based on physical bubble force balance developed in this study, was compared with a previous model (Katto et al., [26]). The comparison showed that the Katto model had a 30% maximum deviation for the current

experiment CHF data, while the proposed model's maximum deviation was 85% for predicting the CHF.

Kamel et al. [27] investigated applying nanofluids in critical heat flux in pool and convective type boiling. The study showed that high heat flux can be obtained in conjunction with small temperature increments. This results in lower limits of the heat flux and operation with higher safety and remaining life.

2.4   Internal Friction in Water Tube Boilers

Babcock and Wilcox [28] highlighted that corrosion and deposits arise in boilers because of preboiler corrosion products, condenser cooling water makeup impurities, preexisting oxides in new components, and corrosion products from boiler materials. Mitigation of these reasons include: makeup water treatment, preoperational cleaning, internal water treatment, condensate treatment, chemistry and corrosion control, and chemical cleaning. Campbell [29] investigated the effect of chemical composition of water on corrosion problems in plants. He indicated that demineralized oxygen-free water with a pH of 7–8 is practically non-corrosive to most metals.

Romeo et al. [30] developed a series of more general equations for a more accurate estimation of friction factor in rough and smooth pipes. Woodruff et al. [31] presented measures on how to minimize the effects of fouling on boiler tubes during operation and maintenance cycles.

Annaratone [32] classified pressure drops in tubes and ducts as concentrated and distributed drops. He highlighted the causes and the correlations needed to calculate each pressure drop classification.

Joseph and Yang [33] developed a correlation for friction factor in terms of Reynolds number for laminar, transition, and turbulent flow in smooth pipes. They indicated that their correlation is more accurate than other correlations in the range of Reynolds numbers in which the correlations overlap.

Using close to 600 experimental data points in tubes operating under microgravity; Xiande Fang and Yu Xu [34] developed a correlation for two-phase friction pressure drop (TPFPD) in such tubes. The authors' comparison of their correlation with others indicated far better results.

Slawomir and Karol [35] presented a number of methods to calculate two-phase pressure losses. These included the homogeneous model, the Lockhart-Martinelli [36] and the Chrisholm phase-slip models and the Martinelli-Nelson [37] graphical method. The calculations were run for the evaporator section of a power plant boiler with a production capacity of 210,000 kg/h. Results from the different models were presented in comparison to each other.

2.5 Furnace Heat Transfer and Water Circulation in Natural Circulation Boilers

Chine-Hsiung and Barkelew [38] designed a computer program to predict field measurements for modeling the turbulent flow in jet stirred reactions in two dimensional (plane, axisymmetric, or polar) geometries. The results indicated that the strength of the

11

re-circulating eddy caused by the jet entrainment has a dominant impact on reactor performance. Comparing the program results with available observations from one the refineries indicated the program capability of predicting changes of flow pattern and yield structure in different geometries or operating conditions.

Coelho and Carvalho [39] modeled a utility power station boiler numerically to predict the gas temperature, chemical species and to determine the influence of air/fuel ration and power load. The predicted gas species concentrations were in a good agreement with the available experimental data while the temperature was under-predicted, in the burner region.

Fan et al [40] investigated the characteristics of coal particle flow, heat transfer, and combustion processes in a W-shaped furnace. The investigation results showed the presence of steady high temperature zone under the arch of W-shaped flame boiler which indicates that W-shaped boiler is suitable for low quality coals and operation in changed load.

Milkhaliov and Batrakov [41] presented a study on the heat transfer modes in different furnace layouts for gas tube boilers. Factors such as dimensions, number of burners and location, environmental conditions influence heat transfer in the furnace. An experimental arrangement was fixed to investigate heat transfer modes in relation to the different combustion products mobile contours. This experimental arrangement severs as means for simulating and analyzing the heat transfer between furnace wall and the high temperature gases.

Liu et al [42] conducted a comparative study of radiative heat transfer in a gas fired furnace using Sum of Gray Gases (SGG) and Weighted-Sum of Gray Gases (WSGG) models. The paper presented three case studies. Their results indicated that the WSGG model predicted gas temperatures, wall temperatures and wall heat flux in better agreement with the experimental data, than the SGG model. The SGG model produced large errors in predicting the wall fluxes and the flux divergence. Hence the WSGG model was recommended for simulating large scale gas-fired combustion systems.

Coelho and Carvalho [39] and Chungen et al [43] involved the total flow and energy modeling of industrial gas furnaces. The focus in these studies was on improving the efficiency of furnaces and reducing NOx pollution among other considerations.

Prior to 2006, the published literature pertaining to investigations on the effects of various flow parameters on water circulation in boilers did not provide any focused work on the influence of the boiler load and the shape of the boiler tube geometry on the burnout of water tubes. Additionally, water circulation was not simulated to enable calculation of the variation of void fraction and tube surface temperature along different boiler tubes at different steam production rates. Further, no means were available to identify the critical areas in boiler wall tubes under full load conditions and provide recommendations for achieving optimum circulation that helps in minimizing tube failure due to long term overheating. Bader H et al [44] investigated water circulation in two industrial operating boilers at different loads. Two computational models were developed. The first model dealt with the combustion process in the furnace while the second one dealt with water circulation in the boiler tubes. The results indicated high temperature areas around the

edges of the side wall. A drift in the temperature contours toward the exit of the furnace along the horizontal plane of the upper and the lower burners was observed.

Heat flux data indicated high values in the lower part of the riser tube, reduction with elevation, and then increased again in the upper part of the tube. The addition of two bends and the semi-circular tube to avoid the peepholes resulted in less total mass flow rate but a higher rate of steam generation in comparison with a normal D-tube. Temperature data indicated increased temperature along the D-tube with the maximum on the side wall. The maximum temperature location moved up the tube as the distance from the burner wall increased. The results also indicated an increase in the rate of steam generation as the distance from the burner wall increased.

Habib et al. [45] presented development of a nonlinear dynamic model to determine maximum load swing rates in natural circulation package boilers. Two boilers were used to run experiments and collect data on steam demand fluctuations. The conservation equations of mass, energy, and momentum as well as thermal properties of the mixture were used to develop the model. Steam drum pressure, water volume, steam quality at the outlet of the risers, drum water level, and rise tubes temperatures were determined at different loads. A procedure and a numerical solution were developed for calculating the furnace heat flux and combustion calculations. An acceptable level of agreement between field data and calculations was obtained. An ANSYS model was developed and used to indicate that the thermal stress level resulting from swing rates could not be the limiting factor, while the drum water level could be. Based on the critical heat flux and the allowable steam quality calculations, the maximum boiler swing rates were defined with variations in the riser tube heat flux and friction factor and heat flux.

Moghari et al. [46] assessed the thermal performance of a D-type water-cooled natural gas-fired boiler. They obtained heat flux distribution on furnace walls, as well as flue gas and water-steam mixture temperatures in the convective stages. Their results were in agreement with measured data obtained from a utility site.

Azimi and Nazami [47] investigated the impact of replacing boiler fuel oil with natural gas without changing the temperature of products of combustion and furnace heat absorption. Results of the study revealed that NO produced with natural gas is significantly less than with fuel oil. However, CO_2 produced is about the same in both cases. Further, using natural gas results in significant cost reduction in operating and maintaining the boiler

2.6 Boiler Tube Failures

Zarrabi et al. [48] developed a non-dimensional parameter termed T* which can be used to estimate the tube temperature variation in the scarred tube section of a boiler and a method to estimate and characterize the tube scar for more accurate tube life assessment.

Ranjbar [49] made analysis on the failure of cold boiler and hot reheater tubes by conducting sediments chemical analysis, metallographic examinations, XRD, SEM, and EDX studies. The analysis results indicated that the failures were attributed mainly to the bad maintenance and feed water chemistry, which led to various corrosion mechanisms. The most common corrosion mechanisms noticed in the reheater tubes were found to be pitting, caustic corrosion, and stress corrosion cracking. The level of impurities in the feed water was much higher than the prescribed values. Hence, it was recommended that proper

15

maintenance and operation need to be followed to prevent such corrosion mechanisms and tube failures.

Khjavi et al. [50] indicated that there are two significant water corrosion mechanisms, caustic and phosphate corrosion, that took place in boiler bank front tubes. The root causes of boiler-tube failures were found to be caustic and phosphate corrosion.

Bulloch et al. [51] presented tube strain gauge data of failures in two 250 MW boilers as a result of active high stresses at certain boiler locations. These stresses reside between the yield and tensile strengths of the tube materials. The defect extension process was shown to be fatigue crack growth, the most common mode of water-wall boiler tubes.

Dominguez et al. [52] described the analysis of recurrent failures of 1%Cr – ½%Mo steam superheater tubes of two boilers at an oil refinery. Material failure analysis showed overheating of material (at around 540 ℃), high temperature oxidation, bulging, cracks and creep degradation due to deposits accumulation on the internal tube wall. Traces of sodium sulfate were present in the deposits as a result of water carry-over to the superheater tubes.

Emara-Shabaik et al. [53] developed a model for prediction of riser tubes temperature of water tube boiler under different operating conditions. Results of the simulation provided an insight of the dynamic interactions between the main boiler variables including the drum pressure, water volume, steam quality and risers' temperature. The approach used is general and can be adapted to many steam generators configurations.

Purbolaksono et al. [54] evaluated two failure cases of a reheater and superheater tubes, made of typical SA213-T22 steel material. Increased temperature and decreased hardness

of tube metal, and formation of oxide scale on the inner surface of the tubes over prolonged periods of time are typical problems in power plant boilers. The temperature and hardness values were determined for the two cases in the study. The estimations obtained from the numerical simulation agreed with the actual values.

Kembaiyan et al. [55] evaluated a boiler tube failure of a 40-year old, 200-psig, O-Type package boiler operating at an oil refinery. The evaluation covered past failure record, roles of mechanical and water chemistry issues, and corrective measures taken to address such failures. The evaluation releveled that the predominant mode of failures are long-term overheating, thermal fatigue, localized corrosion gouging, and in-situ gouging. The local tube overheating is attributed to the insufficient water cooling effect as a result of steam blanketing conditions. Corrective actions to balance circulation and prevent steam blanketing as well as to optimize burners' characteristics were recommended.

Malik et al. [56] presented some particular failures of boiler tubes that had been studied previously and highlighted some lessons to address operation and maintenance practices to help ensure integrity of boiler tubes.

2.7   Conclusions

The take-away from the published literature on natural convection boilers includes:

1. Natural circulation circuits were modeled to identify critical heat flux, departure from nucleate boiling, and its effect on tube burn out and pressure losses across package boilers.

2. The local heat flux in power boilers was determined based on distribution of the tube wall temperature from interior thermocouples with good agreement for some tubes.

3. An empirical correlation for the critical heat flux was developed with expanded range of applicability and good accuracy.

4. Investigation of water circulation in two operating boilers at different loads was addressed; two computational models were developed for furnace combustion and water circulation in tubes.

5. The impact of chemical composition of water on corrosion problems depends on the combination of metal and water composition.

6. Measures to minimize effects of waterside scale include water treatment and boiler tube chemical cleaning.

7. Distributed pressure drops are a result of friction between fluid and wall; concentrated pressure drops originate from sectional changes along the flow path.

8. A model for two-phase flow was developed to predict riser tube temperatures under different operating conditions

CHAPTER 3

PROBLEM DEFINITION AND OBJECTIVES

3.1   Problem Definition

Poor water circulation is a primary cause of tube failures in natural circulation water tube package boilers. Heat flux and internal friction are among the main contributors to poor circulation. Varying heat flux causes significant interruption to the established circulation ratio inside the tubes. Sudden increase in the flux, prior to introducing enough water-steam mixture to keep a minimum cooling effect, results in tube failures. Internal tube friction, the second contributor to poor circulation, is experienced frequently in boiler tubes. Accumulation of deposits on the water side flow results in higher friction and reduction of water-steam mixture leading to a higher rate of localized heat transfer and steam generation. This eventually results in tube overheating and rupture. Additionally, tube corrosion is likely to take place and contribute further to tube rupture.

Despite the fact that several published models closely addressed natural circulation in package type boilers, they did not simultaneously consider grouping boiler tubes into a number of circuits, geometry and dimensions for each circuit tubes, accounting for sub-cooling of water in the economizer, average properties of steam-water mixture, heat flux, circulation ratio, pressure losses and net driving head. The published literature does not include a model that would perform calculations for each circuit and come up with

19

circulation parameters for all circuits at the same time to identify the minimum circulation ratio, the critical heat flux, and the ultimate critical circuit among all circuits. Hence, development of such model would contribute and add value to the literature on the subject.

3.2   Objectives

The overall objective of this dissertation is to develop a program that will size and analyze the performance of package boilers. Specific objectives include 1) sizing of a package boiler to meet a specific load of steam, 2) identifying the most critical circuit in the boiler, 3) determining the impact of heat flux on the circulation parameters and the wall temperature, 4) determining the impact of friction factor on circulation parameters, and 5) determining the impact of plugging the D-Tubes and boiler bank tubes on circulation parameters and tube wall temperature.

CHAPTER 4

METHODOLOGY

Developing a program to size and analyze the performance of package boilers involves

considering many variables. The most important are the combustion process in the boiler,

the boiler furnace configuration, and tube arrangement, as well as the required design

conditions. Figure 4-1 [28] shows a photo of a typical water tube package boiler and

Figure 4-2 shows a sectional view of a typical water tube package boiler [57].
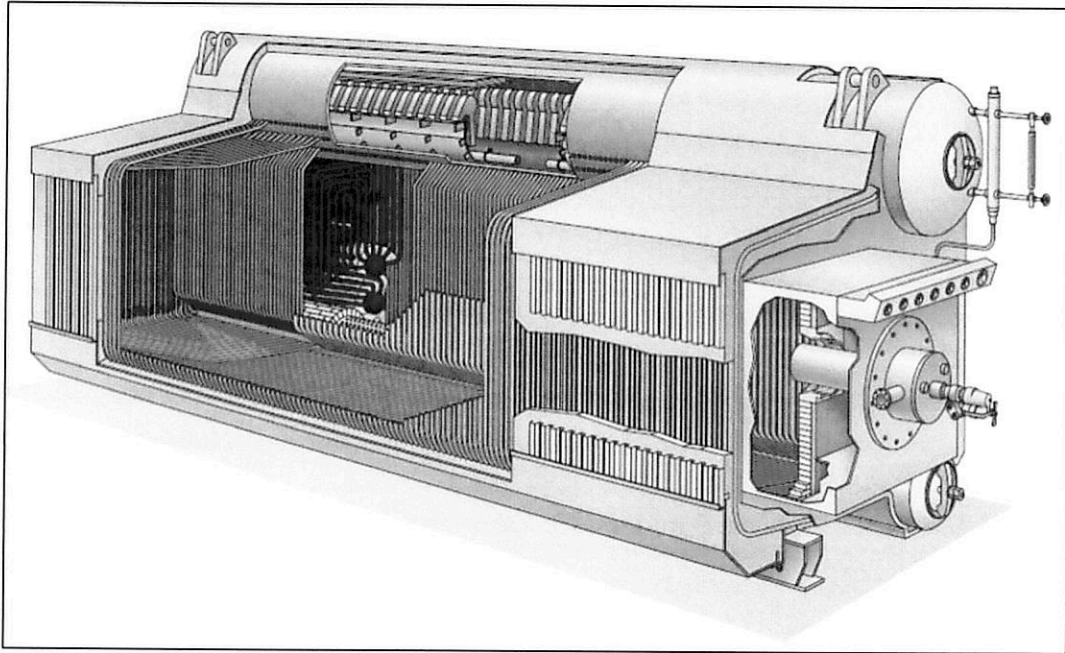
Figure 4-1:   typical water tube package boiler
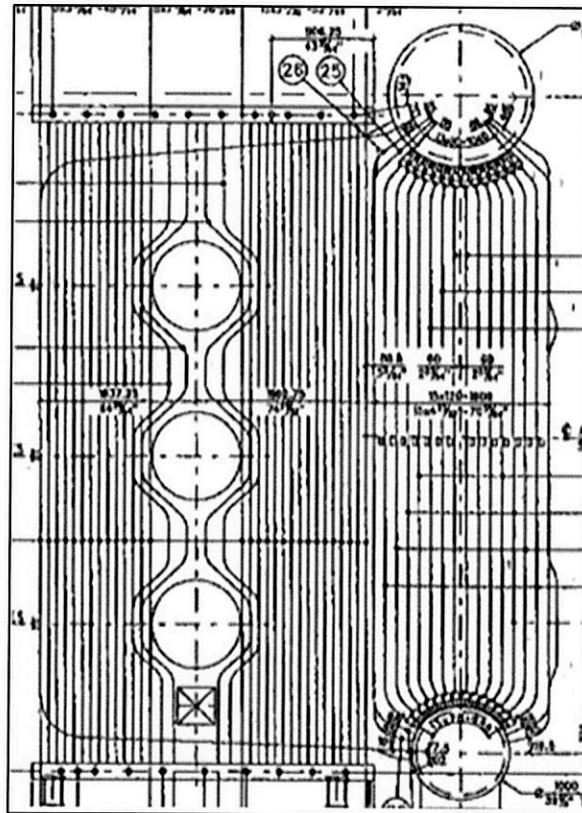
Figure 4-2: Sectional view of a typical water tube package boiler

The main elements that were considered in developing the program and performing the needed calculations were:

1) A number of correlations were used in conducting the boiler combustion calculations. These included boiler fuel emissivity, local and overall heat transfer coefficients, and adiabatic flame temperature. [2, 7]

2) An iteration process that starts with assuming initial values based on experience was used to estimate the tube wall and the flue gas temperatures. The calculations were repeated until the values of temperatures converged to final ones [2, 7].

3) Heat flux values for every circuit were used as input to the circulation parameter calculations to ensure steam generation from every circuit [2, 7]

4) In conducting the circulation calculations, the boiler tubes need to be divided into different circuits based on the experience of such boilers [2, 7]. In the current study, the package boiler was divided into a number of circulation circuits as shown in Figure 4-3. The circuits included the following:

    i.   Front wall tubes, Circuit 1

    ii.   Rear wall tubes, Circuit 2

    iii.   Furnace floor, side wall and roof tubes (D-Tubes)

        a.   Floor tubes, Circuit 3A

        b.   Furnace left wall tubes, Circuit 3B

        c.   Roof tubes, Circuit 3C

    iv.   Division (intermediate) wall tubes, Circuit 4

    v.   Bank evaporating tubes, EVA1, Circuit 5

    vi.   Bank evaporating tubes, EVA2, Circuit 6

vii.   Bank evaporating tubes, EVA3, Circuit 7

viii.   Bank evaporating tubes, EVA4, Circuit 8

ix.   Downcomer A (downcomer bank tubes)

x.   Downcomer B (downcomer side wall tubes)
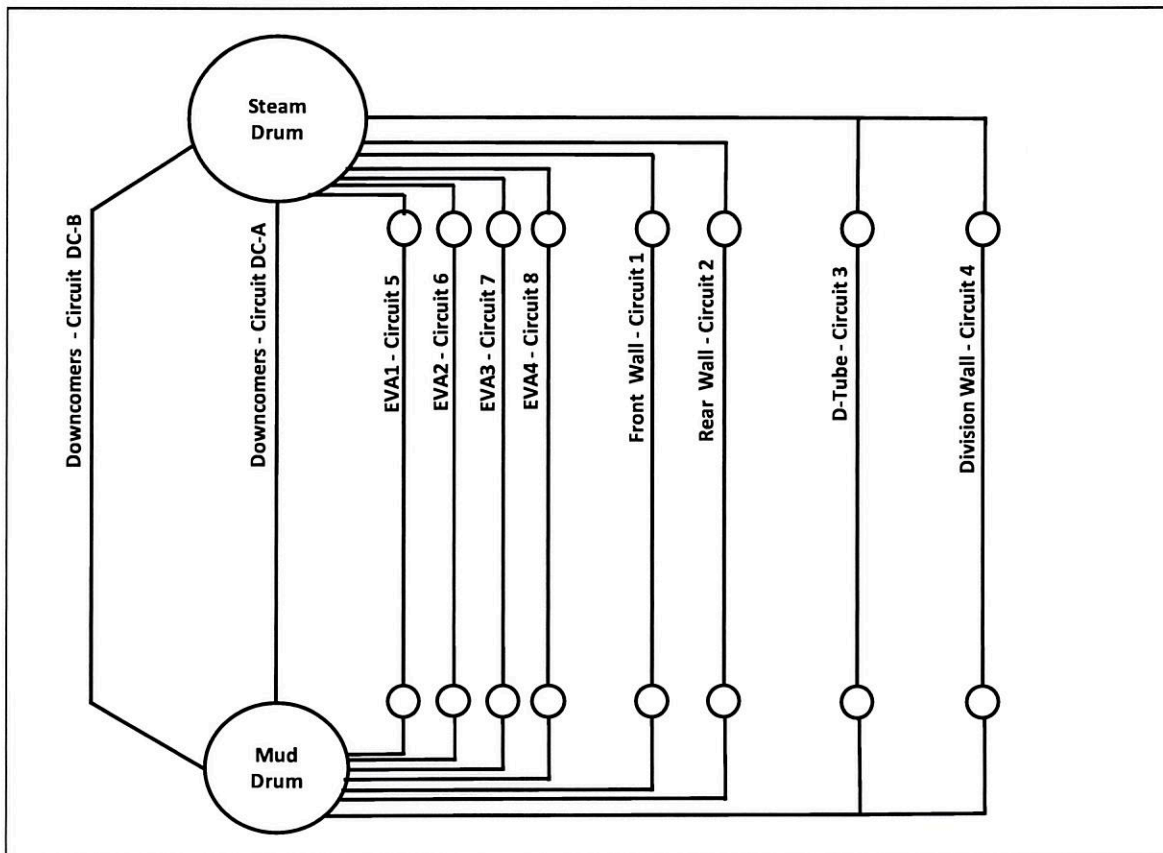
Figure 4-3: Schematic of circulation circuits

5) The circulation ratios are calculated for every circuit and compared to the minimum allowable value based on the industry practice. The minimum allowable circulation ratio used in this study is taken from Babcock and Wilcox [28] based on the steam pressure of the boiler.

6) The net driving head between the downcomer tubes and remaining tubes (risers) is balanced so that the head for the downcomer circuits is equal to the head in every other circuit taking into consideration all pressure losses [2, 32, 58].

7) A number of correlations were used to estimate the average mixture properties and pressure losses [32].

8) The following design parameters were determined [2, 7]:

1. Furnace size (typical value are initially used)
2. Number of tubes and size for each circuit (typical values are initially used)
3. Mass flow rates for each circuit (typical values are initially used)
4. Circulation ratio for each circuit
5. Pressure drop for each circuit

9) The results analysis included:

- Heat flux impact on circulation parameters of each circuit
- Impact of internal friction on all circuits
- Identifying the most critical circuit
- Impact of tube plugging on circulation parameters

4.1 Program Development

A program that utilizes Excel as a platform and Visual Basic to establish the logic of the program was developed and used to determine the required design parameters. The algorithm of the program is shown in Figure 4-4. The main elements of the program that need to be satisfied are summarized as follows [2, 7]:

25

- Steam output of the furnace and evaporator tubes circulation circuits must meet the required production capacity of the boiler.

- Total steam production must account for steam consumed due to subcooling. Hence, the rate of generation should be increased to produce the total required steam in addition to that required to overcome subcooling.

- The net driving head for each circuit should offset the net driving head in the downcomer circuits.

- The net driving head of the two downcomer circuits is equal.

- Flow in the first 8 circuits must be equal to that going to downcomer circuits.

Input

- Steam pressure
- Feed water temperature
- EPRS and volume
- Steam drum internals pressure drop

All Circuits:

- Heat flux (all circuits)
- Tube diameter and thickness
- Number of tubes
- Length of tubes
- Height of steam-water (inlet & outlet)

Check

- Circuits steam output matches the required production capacity
- Net driving head of downcomer circuits is equal to that of each other circuit
- Water flow rates in riser circuits is equal to that in downcomer circuits

No / Yes

Output

- Total steam production
- Total steam consumed due to subcooling

All Circuits:

- Steam mass flow rates
- Water mass flow rate
- Steam consumption
- Circulation ratio
- Minimum circulation ratio
- Steam, water, and mixture properties
- Concentrated pressure losses
- Distributed pressure losses
- Net driving head
- Tube wall temperature

Figure 4-4: Program algorithm

Heat flux and circulation parameters calculations are presented by a simple flow chart shown in Figure 4-5. The heat flux is calculated first and the results were used as input to circulation parameters calculations. Input and output of the heat flux calculations are listed in Table 4-1 and Table 4-2 respectively. The heat flux and other boiler data used as an input to the circulation calculations are shown in Table 4-3. The output of the circulation parameters calculations are listed in Table 4-4.

26
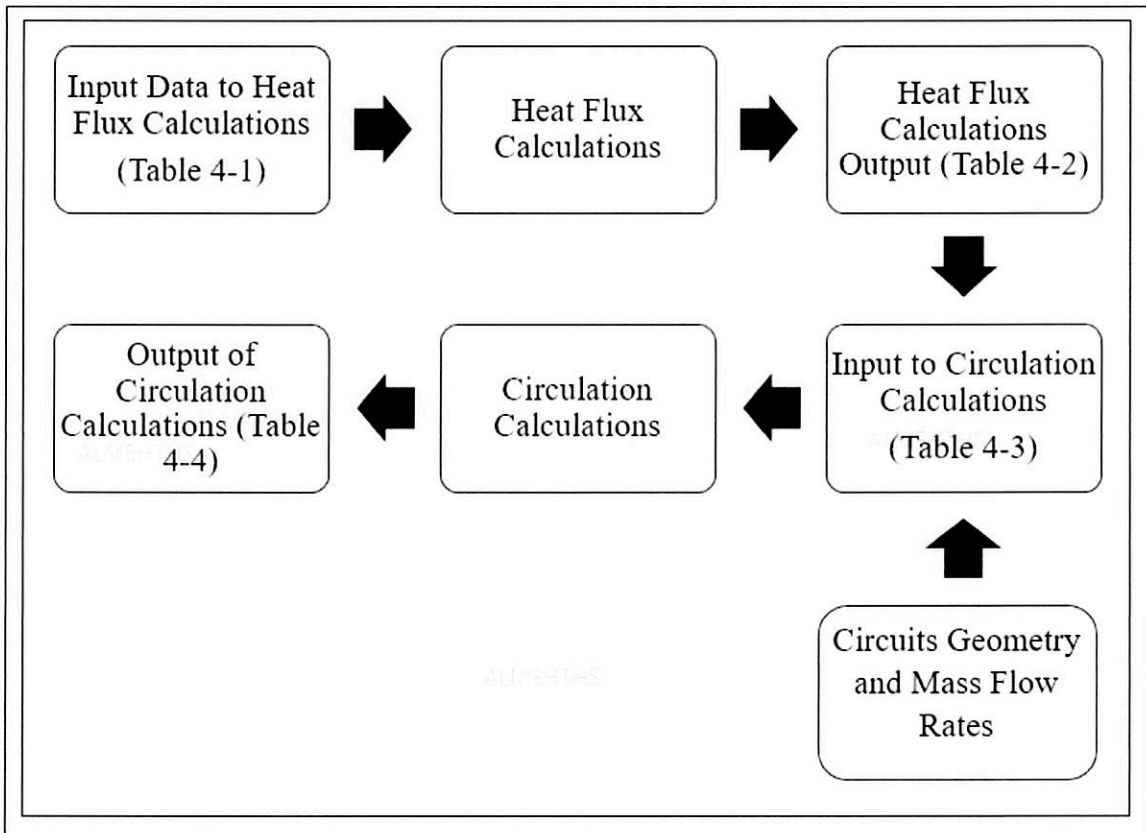
Figure 4-5: Flow chart of heat flux and circulation calculations

4.2 Heat Flux and Circulation Calculations

The heat flux in each circuit is calculated and its value is used to determine the circulation parameters.

4.2.1 Heat Flux Calculations

The input data needed to determine the heat flux in the boiler circuits are given in Table 4-1.

Table 4-1: Heat Flux Calculations Input Data

Variable	Description	Unit
BD	% boiler blowdown from boiler steam output	% of SO
B	Number of burners	-
c_{pg}	Specific heat of flue gas at T_g	kCal/(kg.°C)
$c_{pg-adia}$	Specific heat of flue gas at the adiabatic flame temperature	kCal/(kg.°C)
D_F	Furnace depth	m
D_o	Tube outside diameter	mm
f_i	Internal fouling factor	$(m^2.hr.°C)/kCal$
f_e	External fouling factor	$(m^2.hr.°C)/kCal$
H_F	Furnace height	m
L_f	Length of fin	m
LHV	Lower heating value of fuel gas	$kCal/m^3$
-	Tube material	-
-	Fin material	-
$m_{a/f}$	Specific combustion air flow (per fuel volume)	kg/m^3

$m_{g/f}$	Specific flue gas flow (per fuel volume)	kg/m^3
p	Tube pitch	mm
P_d	Steam drum pressure	$barg$
P_{fw}	Feed water pressure	$barg$
P_s	Steam pressure	$barg$
RL	Radiation loss % from absorbed heat	% from Q_{abs}
SO	Steam output	kg/hr
t_f	Fin thickness	mm
t_w	Tube wall thickness	mm
T_{sup}	Superheated steam temperature	$°C$
T_{fw}	Feed Water Temperature	$°C$
T_{fuel}	Fuel gas temperature	$°C$
T_{amb}	Ambient air temperature	$°C$
W_F	Furnace width	m
α_i	Internal heat transfer coefficient	$kCal/(hr.m^2.°C)$
δ	Fin factor	-

$\in$	Fuel emissivity	-
ξ	Boiler efficiency	%
λ	Thermal conductivity of tube and fin	$kCal/(hr.m^2.^{\circ}C)$
ρ_a	Wet air density	kg/m^3
ρ_g	Flue gas density	kg/m^3

The required steam properties (T_{sat} , $h_{sat.s}$, $h_{sat.w}$, h_{fw} , $h_{sup.st}$) are obtained from the built-in properties subroutine:

Calculations

The total heat output of the boiler is determined using equations 4.1 to 4.3. The total heat output of the boiler is the sum of the absorbed heat (gained by the boiler) and the boiler blowdown heat:

$$Q_{THO} = Q_{abs} + Q_{bd} \tag{4.1}$$

Where,

The absorbed heat (gained in the boiler) is calculated first [58, 59]:

$$Q_{abs} = SO\left(h_{sup.steam} - h_{fw}\right) \tag{4.2}$$

The heat lost in the boiler blowdown is given by:

$$Q_{bd} = BD \left(h_{sw} - h_{fw} \right) \tag{4.3}$$

The heat of combustion is determined in terms of the heat input [59, 60] and given as:

$$Q_c = Q_{THO} / \xi \tag{4.4}$$

The fuel, air and flue gas mass flow rates are determined by equations 6 to 10. The fuel flow rate is given by [59, 60]:

$$\dot{m}_f = Q_c / LHV \tag{4.5}$$

The combustion air mass flow rate is determined by multiplying the fuel flow rate by the specific air mass per unit fuel volume [59, 60]:

$$\dot{m}_a = \dot{m}_f * m_{a/f} \tag{4.6}$$

The air volumetric flow rate is then given as [59, 60]:

$$\dot{V}_a = \dot{m}_a / \rho_a \tag{4.7}$$

The flue gas mass flow rate is calculated by multiplying the fuel flow rate by the specific flue gas mass per unit fuel volume [59, 60]:

$$\dot{m}_g = \dot{m}_f * m_{g/f} \tag{4.8}$$

The flue gas volumetric flow rate is then calculated as [59, 60]:

$$\dot{V}_g = \dot{m}_g / \rho_g \tag{4.9}$$

Heat liberation (load) on the furnace tubes and volume are calculated using equations 4.10 and 4.11 [59]:

$$Q_{c-EPRS} = Q_c / EPRS \tag{4.10}$$

$$Q_{c-FV} = Q_c / V_{fur} \tag{4.11}$$

Where,

The effective projected radiant surface (EPRS) is determined first using equation 4.12. The area for each burner opening is estimated as 1.8 m2 [59].

$$EPRS = =(H_F*W_F*2)+(D_F*H_F*2)+(W_F*D_F+W_F*D_F*0.1)-B*1.8 \tag{4.12}$$

The furnace volume is given by

$$V_{fur} = W_F * H_F * D_F \tag{4.13}$$

The radiation heat transfer calculations are presented by equations 4.14 to 4.18 [32, 59].

$$Q_{rad} = 4.96 * \in * [(T_g + 273)/100]^4 - [(T_{t-f} + 273)/100]^4 \tag{4.14}$$

Where,

The mean temperature of the fin and the tube is estimated:

$$T_{t-f} = \{(C_t * T_w) + (ESL * T_f)\}/ESL \tag{4.15}$$

The total tube exposed surface length is calculated

$$ESL = (C_t + E_f) \tag{4.16}$$

32

The tube exposed circumference is given by:

$$C_t = \left(\pi * D - 2 * t_f\right)/2 \tag{4.17}$$

The fin side extensions are determined:

$$E_f = (2 * f_w) \tag{4.18}$$

T_{w-fur}, T_f and T_g are initially assumed.

Hence, the external heat transfer coefficient is given as:

$$\alpha_e = Q_{rad} / \{ \text{EPRS} *(T_g - T_{t-f})\} \tag{4.19}$$

The overall heat transfer coefficient is given by:

$$\alpha_o = 1 / \{ 1 /\alpha_e + 1/ \alpha_i + t_w / \lambda + f_e + f_i\} \tag{4.20}$$

The radiation heat considering the radiation loss is determined:

$$Q_{rad-RL} = Q_{rad} / \{1+ RL\} \tag{4.21}$$

The first estimate of T_{w-fur} is made by calculating the temperature differences between the external and the internal bulk using equation 4.22 [32]:

$$T_{w-fur} = T_{sat} + \Delta T_{w-fur} + \Delta T_{fi} + \Delta T_{fe} + \Delta T_{ei} \tag{4.22}$$

Where,

The temperature differences across the tube wall, across internal fouling, across external fouling, and between the external and internal films are given by equations 4.23 to 4.26 [32].

$$\Delta T_{w-fur} = Q_{rad} \text{ / EPRS } * t_w \text{ / } \lambda \qquad (4.23)$$

$$\Delta T_{fi} = Q_{rad} \text{ / EPRS } * f_i \qquad (4.24)$$

$$\Delta T_{fe} = Q_{rad} \text{ / EPRS } * f_e \qquad (4.25)$$

$$\Delta T_{ei} = \alpha_e \text{ / } (\alpha_e + \alpha_i) * (T_g - T_{sat} - \Delta T_{w-fur} - \Delta T_{fi} - \Delta T_{fe}) \qquad (4.26)$$

The value of T_{w-fur} is checked against the assumed value. If it is not within a certain accuracy, the iterations are continued [59].

The fin temperature is calculated using equations 4.27 to 4.29 [32, 59]

$$T_f = T_{w-fur} + \Delta T_f \qquad (4.27)$$

Where,

The temperature difference across the fin is given by [32, 59]:

$$\Delta T_f = [(0.85 * Q_{rad} * L_f \text{^}2)/(24*\lambda*\delta)]/1.8 \qquad (4.28)$$

Where,

34

The radiation heat transfer and the thermal conductivity of the fin are substituted in English units [Q_{rad} *is in Btu/(hr.ft²) and* λ *is in Btu/(hr.ft.°F)*] ; the result of the temperature difference across the fin is given in °C.

The fin factor δ is given as part of the input data.

The heat flux is obtained using equations 4.29 and 4.30 [32, 59]:

$$q'' = \alpha_o \, (T_g - T_i) \tag{4.29}$$

Where,

$$T_i = 0.375 * \Delta T_{ei} + T_{sat} \tag{4.30}$$

T_g is the initial assumed value and α_o is the value determined from equation 4.20.

The heat exchanged in the furnace is given by [32, 59]:

$$Q_{fur} = q'' * EPRS \tag{4.31}$$

The flue gas temperature at the furnace exit T_g is then determined and checked against the assumed value to repeat the calculations until the desired accuracy is achieved [28, 59]:

$$T_g = Q_g \, / \, (\dot{m}_g * c_{pg}) \tag{4.32}$$

Where,

The heat of the flue gas is calculated as the difference between the heat of combustion and the radiation heat (absorbed in the furnace) [59, 60]:

35

$$Q_g = Q_c - Q_{rad} \tag{4.33}$$

An estimate of the specific heat of the flue gas is given as part of the input data.

The flue gas mass flue rate $\dot{m}_g$ was determined using equation 4.8.

The adiabatic flame temperature is determined next using equations 4.34 and 4.35 [28, 59]:

$$T_{adia} = h_{adia}/c_{pg-adia} \tag{4.34}$$

Where,

The enthalpy at the adiabatic flame temperature is given by:

$$h_{adia} = Q_c/\dot{m}_g \tag{4.35}$$

An estimate of the specific heat of the flue gas at T_{adia} is given as part of the input data.

Another way of calculating the heat flux is from the heat mass balance [28, 59]:

$$q'' = \frac{\Delta Q}{EPRS} \tag{4.36}$$

Where,

$$\Delta Q = Q_{in} - Q_{out} \tag{4.37}$$

The heat input to the furnace is the same as the flue gas mass flow rate multiplied by the enthalpy at the adiabatic flame temperature:

$$Q_{in} = \dot{m}_f * LHV = \dot{m}_g * h_{adia} \tag{4.38}$$

The heat at the exit of the furnace is given by:

$$Q_g = Q_{out} = \dot{m}_g * h_g \qquad (4.39)$$

Flue gas mass flow rate is the mixture of air and fuel gas flow rates:

$$\dot{m}_g = \dot{m}_a + \dot{m}_f \qquad (4.40)$$

Equation 4.6 is used to determine the air mass flow rate:

$$\dot{m}_a = m_{a/f} * \dot{V}_f$$

Fuel gas flow rate $\dot{m}_f$ is given as part of the input data.

The adiabatic enthalpy is determined from equation 4.39 upon determining the adiabatic flame temperature:

$$h_{adia} = \frac{Q_{in}}{m_g}$$

T_{adia} is back calculated from the given $h - T$ curves based on the flue gas constituents [28].

T_g is calculated from flue gas temperature calculations (equations 4.1 to 4.32). Then h_g is obtained from the h-T curves of the flue gas in the same way T_{adia} was determined.

The output of the heat flux calculations is listed in Table 4-2. A detailed sample of the heat flux calculations using equations 4.1 to 4.35 is shown in Appendix A.

Table 4-2: Heat Flux Calculations Output

Variable	Description	Unit
C_t	Screen tube exposed circumference	mm
E_f	Fin extension on both sides of tube	mm
ESL	Total exposed surface length	mm
EPRS	Effective projected radiant surface of the furnace tubes	m^2
h_{adia}	Adiabatic enthalpy	kCal/kg
$h_{sat.s}$	Enthalpy of saturated steam	kCal/kg
$h_{sat.w}$	Enthalpy of saturated water	kCal/kg
h_{fw}	Enthalpy at feed water temperature	kCal/kg
$h_{sup.st}$	Enthalpy of superheated steam	kCal/kg
$\dot{m}_{fuel}$	Total fuel mass flow rate	m^3/hr
$\dot{m}_a$	Air mass flow rate	Kg/hr
$\dot{m}_g$	Flue gas mass flow rate	Kg/hr
Q_{abs}	Absorbed heat output	kCal/hr
Q_{bd}	Blowdown heat output	kCal/hr

Q_{THO}	Total heat output	$kCal/hr$
Q_c	Total heat of combustion	$kCal/hr$
Q_{rad}	Radiation heat from flue gas to tubes	$kCal/hr$
Q_{fur}	Heat exchanged in the furnace	$kCal/hr$
Q_g	Flue gas heat at furnace exit	$kCal/hr$
Q_{c-EPRS}	Combustion heat load on the furnace EPRS	$kCal/(hr.m^2)$
Q_{c-FV}	Combustion heat load on the furnace volume	$kCal/(hr.m^3)$
Q_{rad-RL}	Radiation heat considering radiation loss	$kCal/hr$
q''	Heat flux	$kCal/(hr.m^2)$
T_{sat}	Saturation temperature at drum pressure	^oC
T_{t-f}	Mean temperature of tube and fin	^oC
T_g	Flue gas temperature (assumed initial value)	^oC
T_{w-fur}	Furnace tube wall temperature (assumed initial value)	^oC
T_f	Fin temperature (assumed initial value)	^oC
ΔT_w	Temperature difference across tube wall	^oC
ΔT_{fi}	Temperature difference across fi	^oC

ΔT_{fe}	Temperature difference across fe	$^{\circ}C$
ΔT_{ei}	Temperature difference from external to internal bulk	$^{\circ}C$
T_i	Temperature of internal bulk	$^{\circ}C$
T_{w-fur}	Furnace tube wall temperature	$^{\circ}C$
ΔT_f	Temperature difference across the fin	$^{\circ}C$
T_f	Fin temperature	$^{\circ}C$
T_g	Flue gas temperature	$^{\circ}C$
T_{adia}	Adiabatic flame temperature	$^{\circ}C$
$\dot{V}_a$	Volumetric flow rate of combustion air	m^3/hr
$\dot{V}_g$	Volumetric flow rate of flue gas	m^3/hr
$\dot{V}_f$	Volumetric flow rate of fuel gas	m^3/hr
V_{fur}	Furnace volume	m^3
α_e	External heat transfer coefficient	$kCal/(hr.m^2.^{\circ}C)$
α_o	Overall heat transfer coefficient in furnace	$kCal/(hr.m^2.^{\circ}C)$

4.2.2 Circulation Calculations

The following input data and equations are used to determine the circulation ratio in each circuit.

Table 4-3: Input Data to Circulation Calculations

Variable	Description	Unit
D_o	Tube outside diameter	mm
EPRS	Effective projected radiant surface of the furnace tubes	m^2
f_{incon}	Concentrated friction factor at the inlet	-
f_{outcon}	Concentrated friction factor at the outlet	-
L_e	Equivalent tube length	m
$\dot{m}_w$	Water mass flow rate (assumed initially)	kg/hr
N	Number of the tubes in Circuit 1 (assumed initially)	-
p	Tube pitch	mm
$\Delta P_{internals}$	Steam drum internals pressure drop	kg/m^2
P_s	Steam pressure	$barg$
q''	Heat flux	$kcal/(hr.m^2)$
SO	Steam output	Kg/hr

SH_i	Static head column height at the inlet of the circuit	m
SH_o	Static head column height at the outlet of the circuit	m
t_w	Tube thickness	mm
T_{EO}	Water temperature at the economizer outlet	$°C$
λ	Thermal conductivity of fin and tube	$W/(m.°C)$
α_i	Internal heat transfer coefficient	$W/(m^2.°C)$

Information of feeder tubes (Circuit 1 and 2):

D_{oF}	Feeder tubes outside diameter	mm
N_F	Number of the feeder tubes (assumed initially)	-
SH_{iF}	Static head column height at the inlet of the feeder tubes	m
SH_{oF}	Static head column height at the outlet of the feeder tubes	m
t_{wF}	Feeder tubes thickness	mm

Information of supply tubes (Circuit 1 and 2):

D_{oS}	Supply tubes outside diameter	mm
N_S	Number of the supply tubes (assumed initially)	-
SH_{iS}	Static head column height at the inlet of the supply tubes	m

SH_{oS}	*Static head column height at the outlet of the supply tubes*	*m*
t_{wS}	*Supply tubes thickness*	*mm*

The following equations are used to determine the circulation parameters in each circuit [7, 32].

The total steam generation in the circuit is determined using:

$$\dot{m}_s = \dot{m}_{s1} + \dot{m}_{s2} \tag{4.41}$$

Where,

Steam generated at the outlet of a circuit $\dot{m}_{s1}$ is calculated as follows:

$$\dot{m}_{s1} = \frac{q'' * S}{h_{fg}} \tag{4.42}$$

The surface area of the circuit tubes is given by:

$$S = N * \pi * D * L \tag{4.43}$$

N is the number of tubes in a circuit; it is assumed initially based on experience for similar types of boilers; q'' is was determined in the heat flux calculations and h_{fg} is obtained from the steam tables.

Steam required to account for subcooling $\dot{m}_{s2}$ is given by:

$$\dot{m}_{s2} = \frac{steam\ generated\ in\ the\ circuit}{steam\ genertaed\ in\ all\ circuits\ except\ downcomers}\ steam\ generated\ in\ downcomers \tag{4.44}$$

The circulation ratio (CR) is determined by:

$$CR = \frac{\dot{m}_w}{\dot{m}_s}$$

(4.45)

Where,

Water mass flow rate $\dot{m}_w$ into the circuit is also assumed initially.

The mass velocity is given as:

$$V_P = \frac{\dot{m}_w}{A*N}$$

(4.46)

Where,

A is the cross sectional area of one tube.

Inlet Sections

The inlet to outlet steam ratio, density of the water steam mixture, velocity and velocity head are calculated at the inlet of any circuit as follows [32],

$$x_i = \frac{\dot{m}_{s2}}{\dot{m}_{s1}}$$

(4.47)

$$\rho_{mix-i} = \frac{1}{\left[\frac{m_{s2}}{\rho_{si}} + \frac{m_w}{\rho_{wi}}\right]*\left[\frac{1}{m_{s2}+m_w}\right]}$$

(4.48)

$$v_i = \frac{V_P}{\rho_{mix-i}}$$

(4.49)

$$Z_i = \frac{(\rho_{mix-i})v_i^2}{2g}$$

(4.50)

Outlet Sections

44

Similarly the following properties are determined at the outlet of each circuit [32],

$$x_o = \frac{Total\ steam\ generated\ from\ Circuit\ \#\ 1}{Steam\ generated\ at\ the\ exit\ of\ Circuit\ \#\ 1} = 1.0 \qquad (4.51)$$

$$\rho_{mix-o} = \frac{CR}{\left[\frac{1}{\rho_{so}} + \frac{(CR-1)}{\rho_{wo}}\right]} \qquad (4.52)$$

$$v_o = \frac{V_P}{\rho_{mix-o}} \qquad (4.53)$$

$$Z_o = \frac{(\rho_{mix-o})v_o^2}{2g} \qquad (4.54)$$

Average Properties:

Average properties between the inlet and the outlet of each circuit are calculated as follows [32],

$$\rho_{mix-avg} = \frac{\frac{(\rho_{wi} * \frac{CR}{x_o})}{(1-\frac{x_i}{x_o})}}{(\frac{\rho_{wi}}{\rho_{si}}-1)} * ln\left[\frac{(\frac{\rho_{wi}}{\rho_{si}}-1)+\frac{CR}{x_o}}{\frac{CR}{x_o}+\frac{x_i}{x_o}*\frac{\rho_{wi}}{\rho_{si}}-1}\right] \qquad (4.55)$$

$$\mu_{mix-avg} = \tau * \mu_{s-avg} + (1-\tau) * \mu_{w-avg} \qquad (4.56)$$

Where,

$$\tau = \frac{(\rho_{wi} - \rho_{mix-avg})}{(\rho_{wi}-\rho_{si})} \qquad (4.57)$$

$$\mu_{w-avg} = \frac{\mu_{wi}+\mu_{wo}}{2} \qquad (4.58)$$

$$\mu_{s-avg} = \frac{\mu_{si}+\mu_{so}}{2} \qquad (4.59)$$

$$Re = \frac{V_P * D_i}{\mu_{mix-avg}} \qquad (4.60)$$

45

$$v_{avg} = \frac{V_P}{\rho_{mix-avg}} \tag{4.61}$$

$$Z_{avg} = \frac{(\rho_{mix-avg})v_{avg}^2}{2g} \tag{4.62}$$

Evaporator tubes wall temperature calculations (applicable only for Circuits 5-8)

Equations 4.63 and 4.64 were used to calculate the tube wall temperature in the evaporator bank tubes [45]

$$q'' \pi D_o = \frac{T_{wi\text{-}eva}\text{-}T_{sat}}{R_{conv}} \; ; \; q'' \pi D_o = \frac{T_{wo-eva}-T_{wi-eva}}{R_{pipe}} \tag{4.63}$$

$$R_{pipe} = \frac{\ln (D_o/ D_i)}{2\pi\lambda} \; ; \; R_{conv} = \frac{1}{\pi D_i \alpha_i} \tag{4.64}$$

The heat transfer coefficient in the water circulation loop typical value is used as an input.

Pressure Drop Calculations

The net driving head for each circuit is then calculated using [32, 58]:

$$NDH = TH - \Delta P_{tot} \tag{4.65}$$

Where,

The total pressure drop is calculated by equations 4.66 to 4.73 [32, 58].

$$\Delta P_{tot} = \Delta P_{dist} + \Delta P_{incon} + \Delta P_{outcon} + \Delta P_{internals} \tag{4.66}$$

The distributed pressure drop is given by:

$$\Delta P_{dist} = f_{fouled} * Z_{avg} * \frac{L_e}{D_i} \tag{4.67}$$

46

The value of the friction factor for a fouled tube is assumed to be 20% more than the value of friction factor of a new tube; it is determined by:

$$f_{fouled} = 1.2 * f_{new} \tag{4.68}$$

The friction factor for a new tube is obtained by:

$$f_{new} = 8 * \left(\left(\frac{8}{Re} \right)^{12} + \left(\left(\left(2.457 * LN \left(\frac{1}{\left(\frac{7}{Re} \right)^{0.9} + 0.27 * \left(\frac{E}{D_i} \right)} \right) \right)^{16} + \left(\frac{37.53}{Re} \right)^{16} \right)^{-1.5} \right)^{\frac{1}{12}} \right) \tag{4.69}$$

The tube roughness factor (E/D_i) is determined to calculate the friction factor for a new tube. E/D_i is given by:

$$\frac{E}{D_i} = \frac{0.044}{D_i} \tag{4.70}$$

The tube equivalent length is taken as an input value based on experience. Its value ranges between 4 and 8 miters depending on location of the tube in the boiler. The equivalent length to internal diameter L_e/D_i ratio is determined by:

$$\frac{L_e}{D_i} = \frac{L + 0.1}{D_i} \tag{4.71}$$

The concentrated pressure drops at the inlet and outlet of the circuit are given by equations 4.73 and 4.74:

$$\Delta P_{incon} = f_{incon} * Z_i \tag{4.72}$$

$$\Delta P_{outcon} = f_{outcon} * Z_o \tag{4.73}$$

f_{incon} and f_{outcon} range from 0 to 2 and are used as input values.

Pressure drop across the steam drum internals ($\Delta P_{internals}$) is given by the boiler manufacturer.

The thermosyphonic head is the average mixture density multiplied by the static head column height difference (between the inlet and outlet of the circuit) and is given by:

$$TH = \rho_{mix-avg} * (SH_i - SH_o) \qquad (4.74)$$

The net driving head given by equation 4.65 should be equal for the downcomer tubes circuits and other circuits.

Using the above listed equations and the input data a number of parameters will be determined. These parameters are listed for each circuit in Table 4-4.

Table 4-4: Output Parameters of Circulation Calculations

Variable	Description	Unit
CR	Circulation ratio	-
$CR_{min-allow}$	Minimum allowable circulation ratio	-
h_{fg}	Latent heat of vaporization	kCal/kg
h_{fw}	Enthalpy at feed water temperature (economizer outlet)	kCal/kg
$h_{sat.w}$	Enthalpy of saturated water	kCal/kg
$\dot{m}_{s-cons.}$	Total internal steam consumption of the boiler	kg/hr
$\dot{m}_{s+cons.}$	Total steam produced by the boiler considering $\dot{m}_{s-cons.}$	kg/hr

$\dot{m}_{s1}$	Steam Output per circuit	kg/hr
$\dot{m}_{s2}$	Steam inlet flow per circuit	kg/hr
$\dot{m}_w$	Water mass flow rate per circuit	kg/hr
$\dot{m}_s$	Total steam mass flow rate per circuit	kg/hr
N	Number of the tubes in Circuit 1 (final)	-
S	Tube surface area	m2
T_{sat}	Saturation temperature at drum pressure	C
V_P	Mass velocity	$kg/(hr.m^2)$
Circuit Inlet		
v_i	Water inlet velocity	m/s
x_i	Ratio of steam at the inlet to steam at the outlet	-
Z_i	Inlet velocity head	kg/m^2
ρ_{wi}	Inlet water density at the steam drum design pressure	kg/m^3
ρ_{si}	Inlet steam density at the steam drum design pressure	kg/m^3
ρ_{mix-i}	Inlet mixture density at the steam drum design pressure	kg/m^3
μ_{wi}	Inlet water viscosity at the drum design pressure	$kg/(m\ hr)$

μ_{si}	Inlet steam viscosity at the drum design pressure	kg/(m hr)

Circuit Outlet

v_o	Water outlet velocity	m/s
x_o	Ratio of steam output to steam at the outlet	-
Z_o	Outlet velocity head	kg/m^2
ρ_{wo}	Outlet water density at the steam drum design pressure	kg/m^3
ρ_{so}	Outlet steam density at the steam drum design pressure	kg/m^3
ρ_{mix-o}	Outlet mixture density at the steam drum design pressure	kg/m^3
μ_{wo}	Outlet water viscosity at the drum design pressure	kg/(m hr)
μ_{so}	Outlet steam viscosity at the drum design pressure	kg/(m hr)

Average Mixture Properties

Re	Reynolds number	-
v_{avg}	Mixture average velocity	m/s
Z_{avg}	Average velocity head	kg/m^2
$\rho_{mix-avg}$	Average mixture density	kg/m^3
τ	Density ratio factor	-

μ_{w-avg}	Average water viscosity	kg/(m hr)
μ_{s-avg}	Average steam viscosity	kg/(m hr)
$\mu_{mix-avg}$	Average mixture viscosity	kg/(m hr)
Pressure Drop (ΔP)		
E/D_i	Tube roughness factor	1/mm
f_{new}	Friction factor for new tube	-
f_{fouled}	Friction factor for fouled tube	-
L_e/D_i	Equivalent tube length to diameter ratio	-
NDH_1	Net driving head for the main circuit tubes	kg/m²
ΔP_{dist}	Distributed pressure drop	kg/m²
ΔP_{incon}	Concentrated pressure drop at the inlet	kg/m²
ΔP_{outcon}	Concentrated pressure drop at the inlet	kg/²
ΔP_{tot}	Total pressure drop in the circuit	kg/m²
TH	The thermosyphonic head (average mixture density by the static head column height difference)	kg/m²
ΔP for the feeder and supply tubes (Circuits 1 and 2)		

NDH_2	Net driving head for the supply tubes	kg/m^2
NDH_3	Net driving head for the supply tubes	kg/m^2
NDH for the circuit		
NDH	Total net driving head	kg/m^2

A detailed sample of calculations being carried out is shown in Appendix A.

CHAPTER 5

VALIDATION

The results of the program were compared with the actual data for two package boilers with different production capacities and geometries. Specifications of the first boiler are given in Table 5-1 [57]. The program was used to determine circulation parameters for the first boiler.

Table 5-1: Characteristics of the first boiler used in validation

Steam Production (kg/hr)	145,000
Fuel Type	Fuel gas
Steam Pressure (barg)	52
EPRS (m^2)	300
Number of burners	3

The calculated parameters are the heat flux, the mass flow rate, the circulation ratio, and the mixture average velocity. The calculated parameters are compared with the actual values as shown in Figures 5-1, 5-2, 5-3, and 5-4. The comparisons indicate a very good agreement between the calculated and actual parameters.
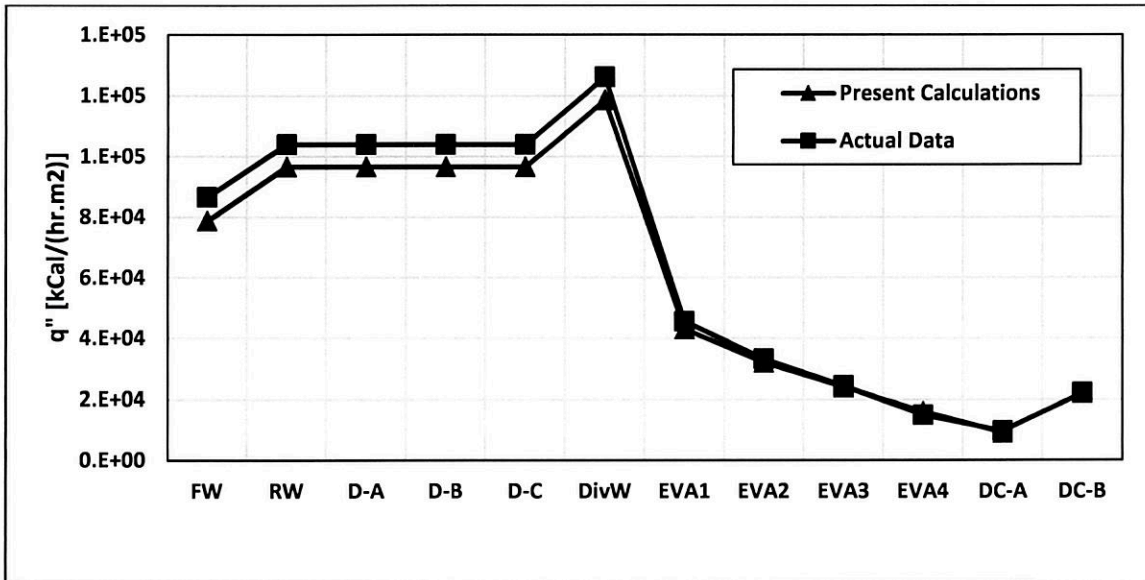
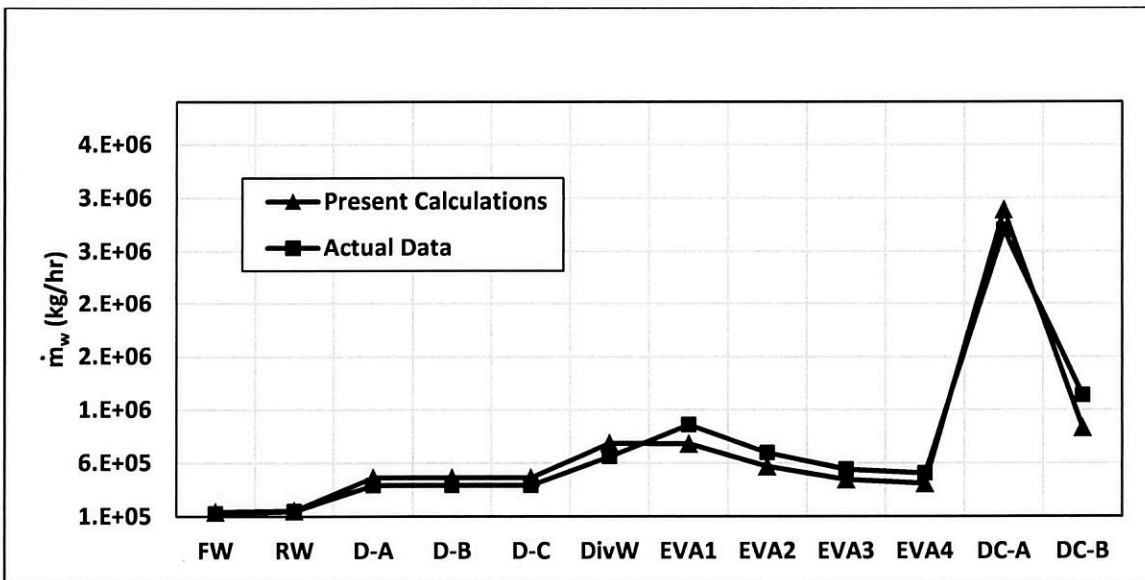**Figure 5-1: Comparison of calculated and actual heat flux values for the first boiler**

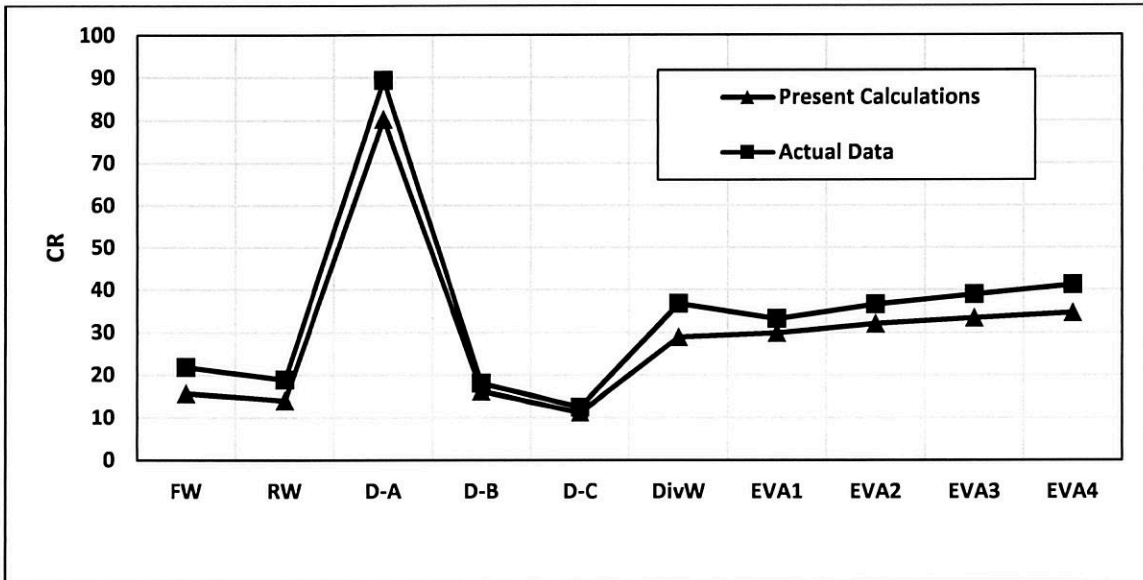**Figure 5-2: Comparison of calculated and actual mass flow rate values for the first boiler**

Figure 5-3: Comparison of calculated and actual circulation ratio values for the first boiler
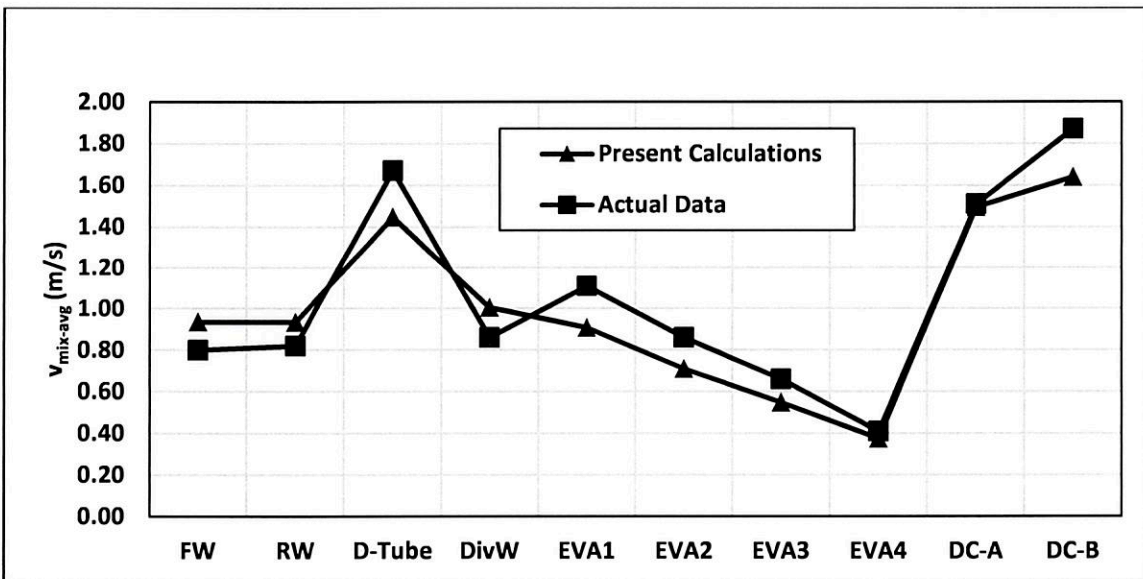

Figure 5-4: Comparison of calculated and actual circulation ratio values for the first boiler

Further validation of the developed program was carried out by comparing the calculated circulation parameters of a 244,463 kg/hr package boiler (boiler 2) using the developed program with the actual circulation parameters. The specifications of the package boiler are given in Table 5-2 [57].

Table 5-2: Characteristics of the second boiler used in validation

Steam Production (kg/hr)	244,463
Fuel Type	Fuel gas
Steam Pressure (barg)	48
EPRS (m^2)	400
Number of burners	2

The compared circulation parameters included the heat flux, mass flow rates, circulation ratio, and mixture average velocity. The comparisons of the calculated and actual data are presented in Figures 5-5, 5-6, 5-67 and 5-8. The comparison for the heat flux and actual mass flow rates indicate excellent agreement as shown by Figures 5-5 and 5-6. The comparison of calculated and actual circulation ratios and mixture average velocity indicate a very good agreement; except for the values of circulation ratio for Circuits 4, 5, and 6 which exhibited a maximum difference of 20%. This relatively high difference is due to possible modification to the circuits' geometry during commissioning of the boiler such as the number of the tubes which impacts steam generation in the circuits and therefore changes the circulation ratio.
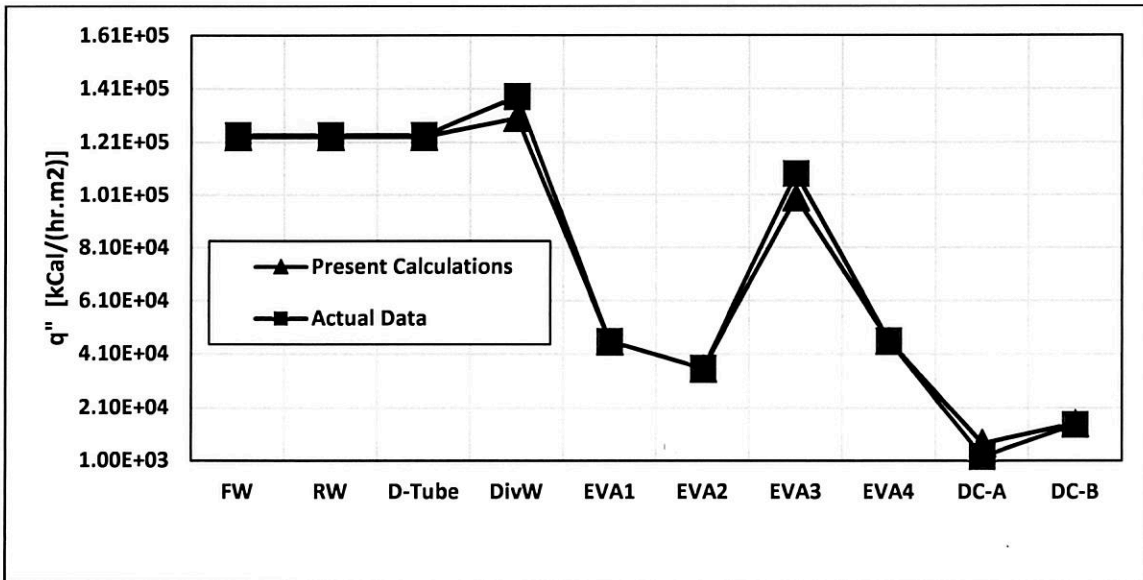
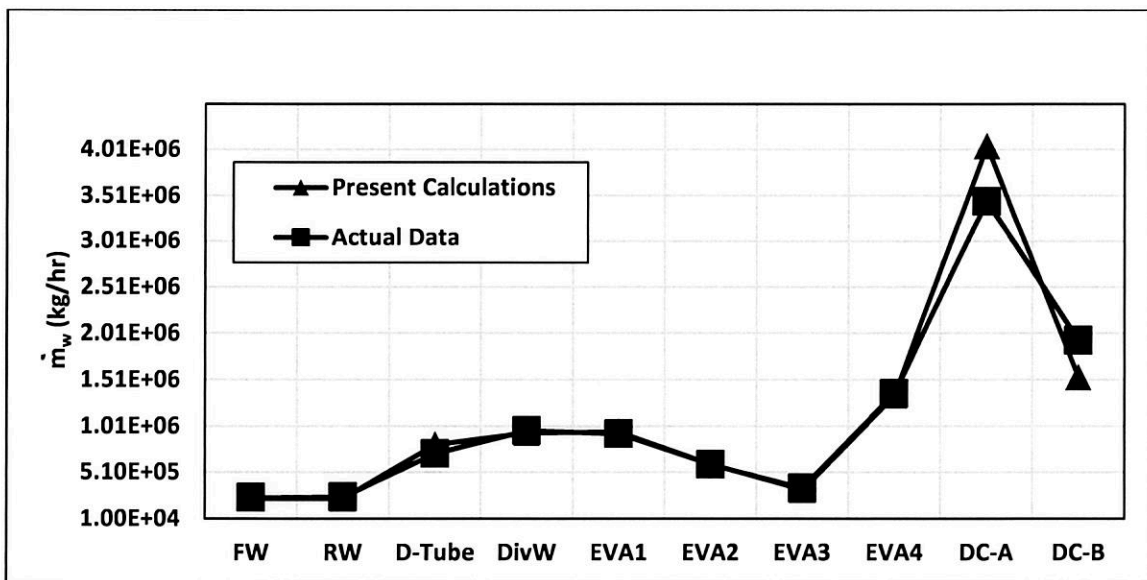**Figure 5-5:** Comparison of calculated and actual heat flux values for the second boiler

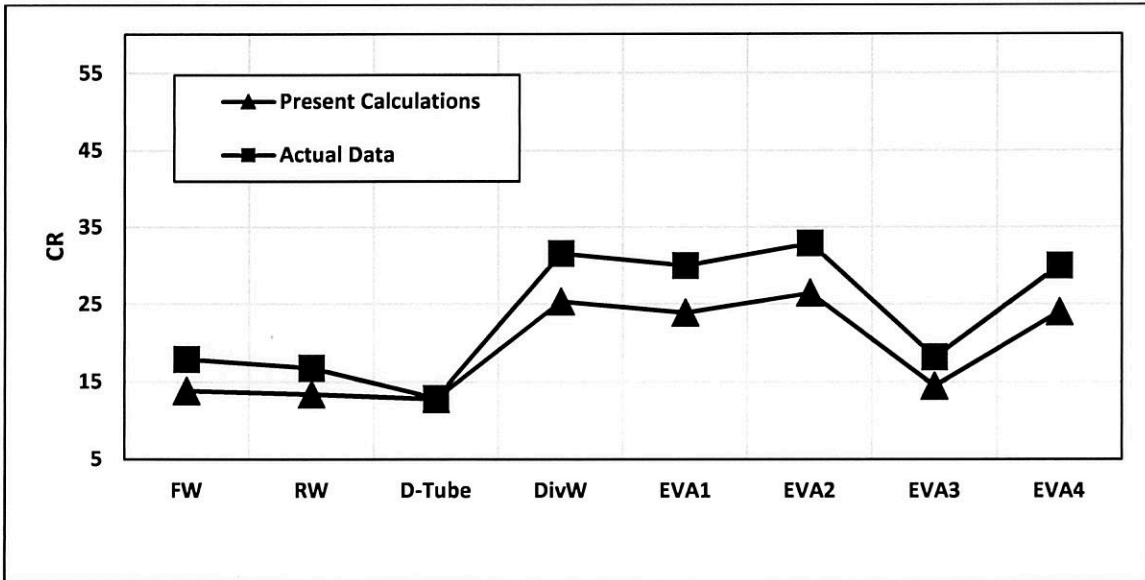**Figure 5-6:** Comparison of calculated and actual mass flow rate values for the second boiler

Figure 5-7: Comparison of calculated and actual circulation ratio values for the second boiler
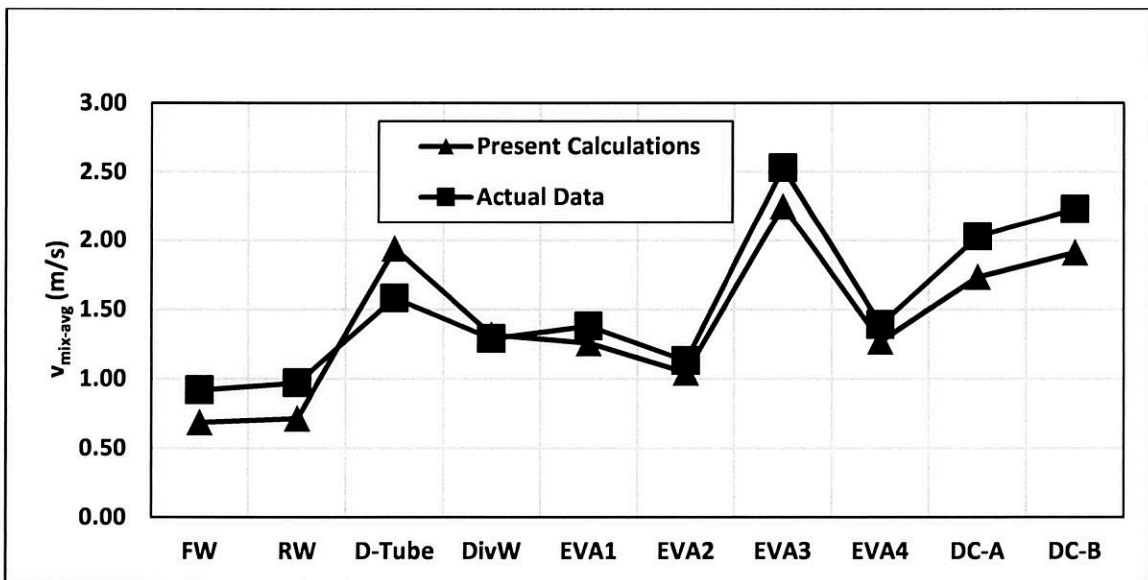

Figure 5-8: Comparison of calculated and actual mixture average velocity values for the second boiler

CHAPTER 6

RESULTS AND DISCUSSIONS

The boiler was divided into circuits (see Figure 4-3). Details of the boiler including the furnace layout and number of tubes in each circuit are shown in Figure 6-1 [57].
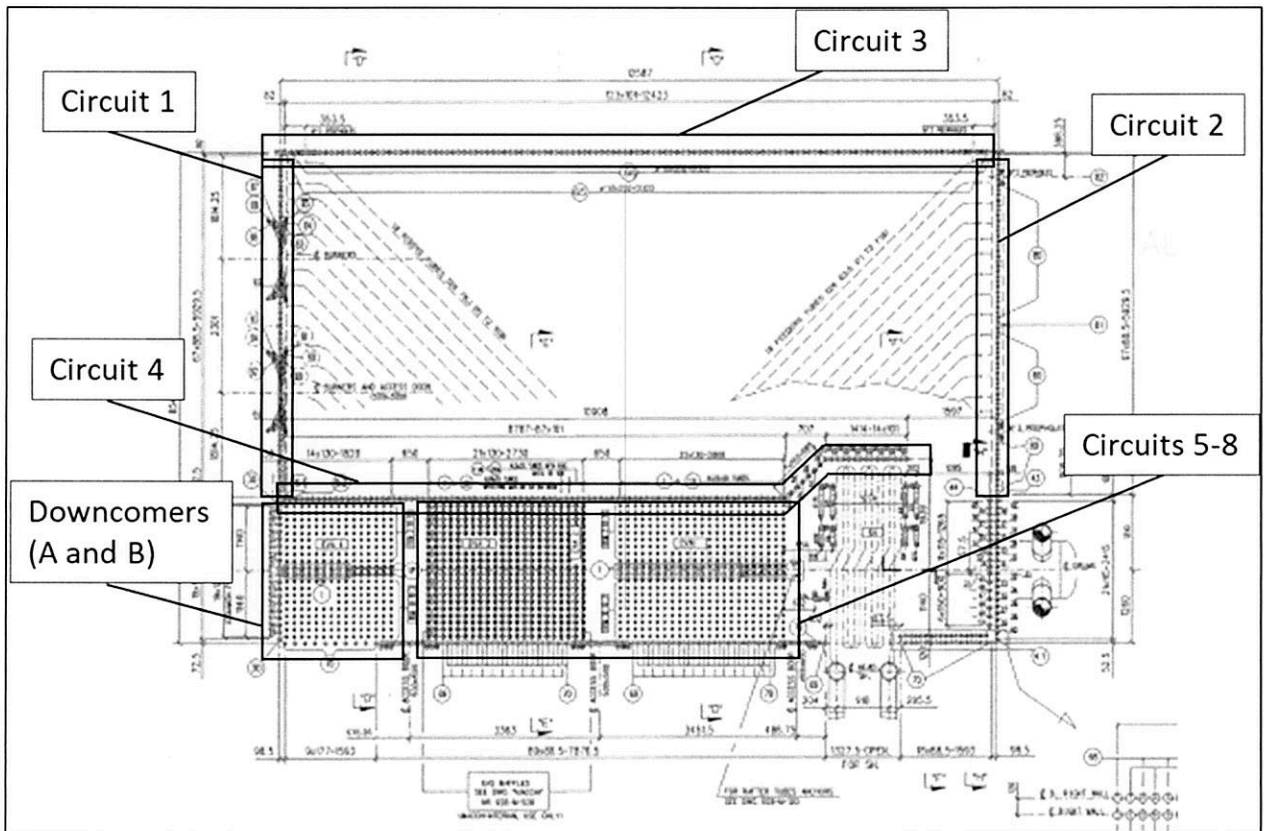

Figure 6-1: Cross section of the boiler with the circulation circuits marked

Each circuit has been analyzed to determine the impact of increasing heat flux on the following parameters:

1. Circulation ratio and the circuit with minimum circulation ratio

2. Minimum allowable circulation ratio

3. Net driving head across the circuits

4. Mass flow rate

5. Tube wall temperature

The impact results were used to identify the most critical circuit and associated critical parameters.

The first set of results pertain to the effect of heat flux and friction factor in each circuit on the circulation ratio (CR), net driving head (NDH) and mass flow rate. These results were analyzed to be able to identify the critical circuit. Figure 6-2 shows the change in the circulation ratio as a result of increasing the heat flux. The results indicate that the circulation ratio decreases as the heat flux increases for all circuits. The highest circulation ratios are those of Circuits 5, 6, 7, and 8. Circuits of lower circulation ratio are values close to the minimum allowable values are Circuits 1, 2, and 3. The circuit with circulation ratio value closet to the minimum allowable value one is Circuit 3.
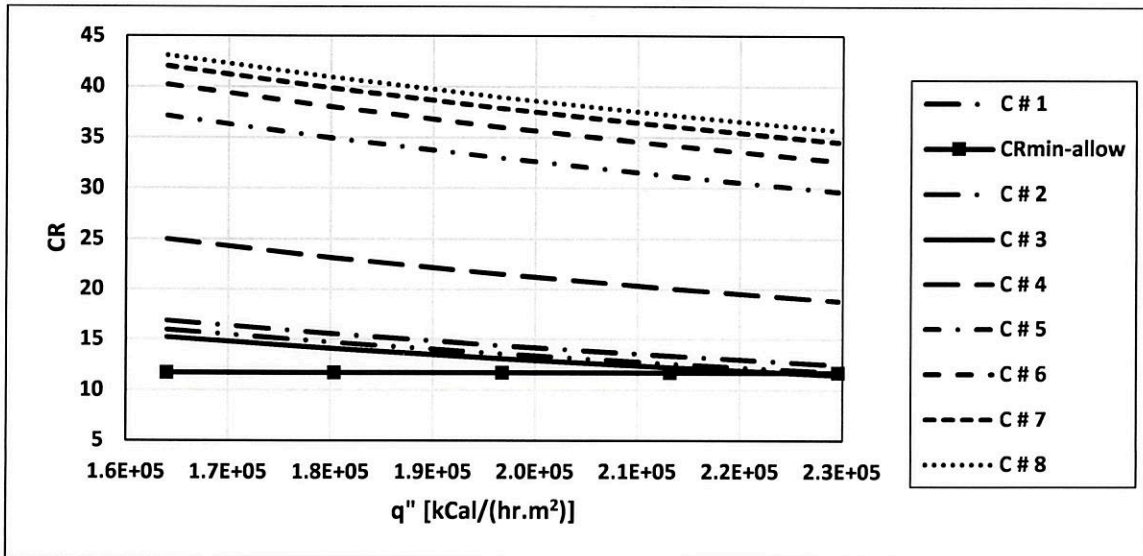
Figure 6-2: Effect of heat flux on circulation ratio for all circuits

Figures 6-3 to 6-7 show the variation of circulation parameters as a result of friction factor variation for all circuits. The parameters include: mass flow rate, the circulation ratio, and the water inlet, outlet and mixture velocities. The results indicate that the mass flow rate and velocities for Circuit 3C are the most impacted ones among other circuits. The minimum allowable CR for the boiler is 11.7 based on steam pressure [32]. Further, the circulation ratio values approach the minimum allowable value at higher friction factor values for Circuit 3. Hence, it can be concluded that Circuit 3 is the critical circuit and further analysis need to be conducted. The minimum required circulation velocity that needs to be maintained is 0.4 m/s [28].
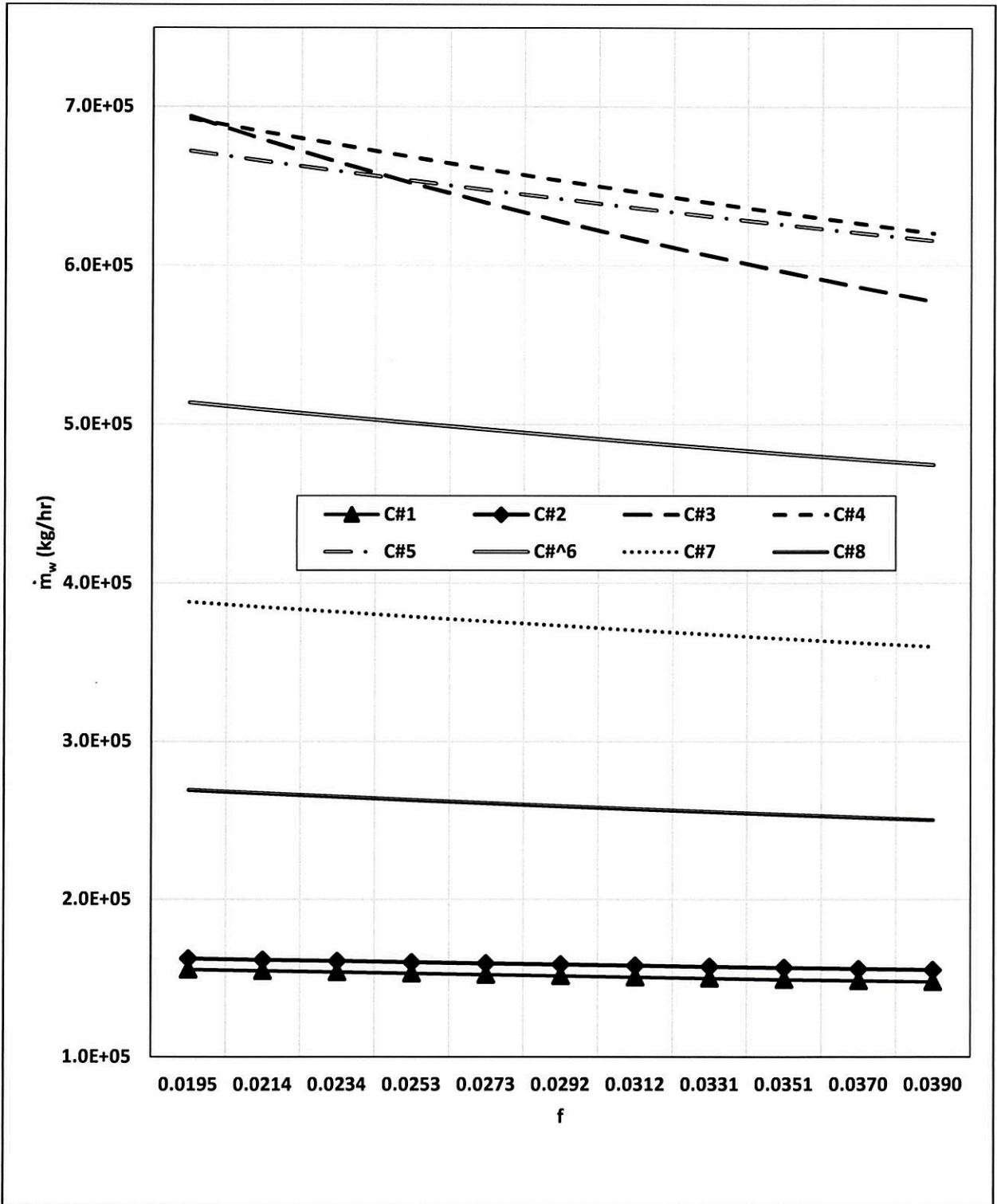
Figure 6-3: The impact of varying friction factor on mass flow rate in all circulation circuits
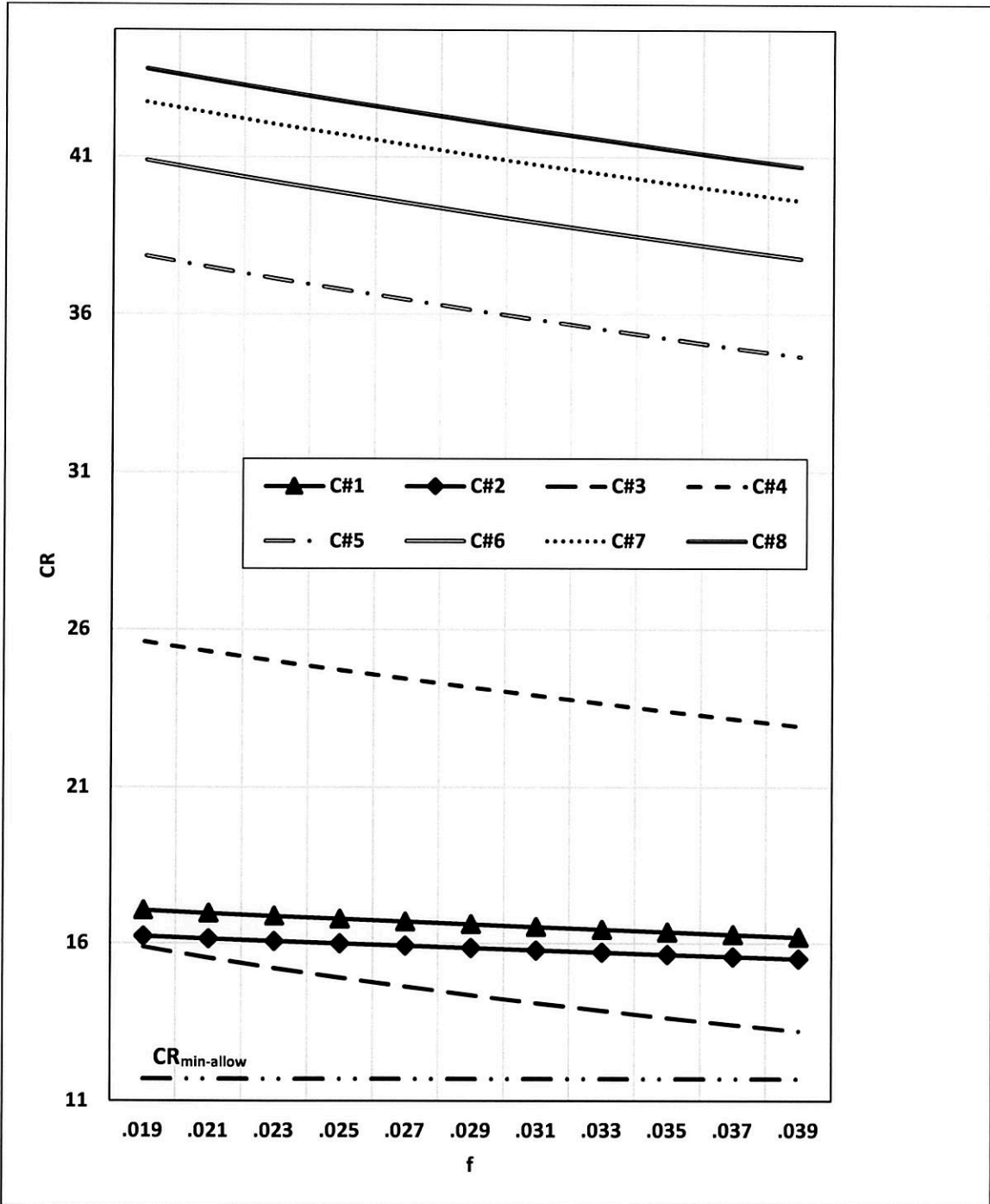
Figure 6-4: The impact of varying friction factor on circulation ratio in all circuits
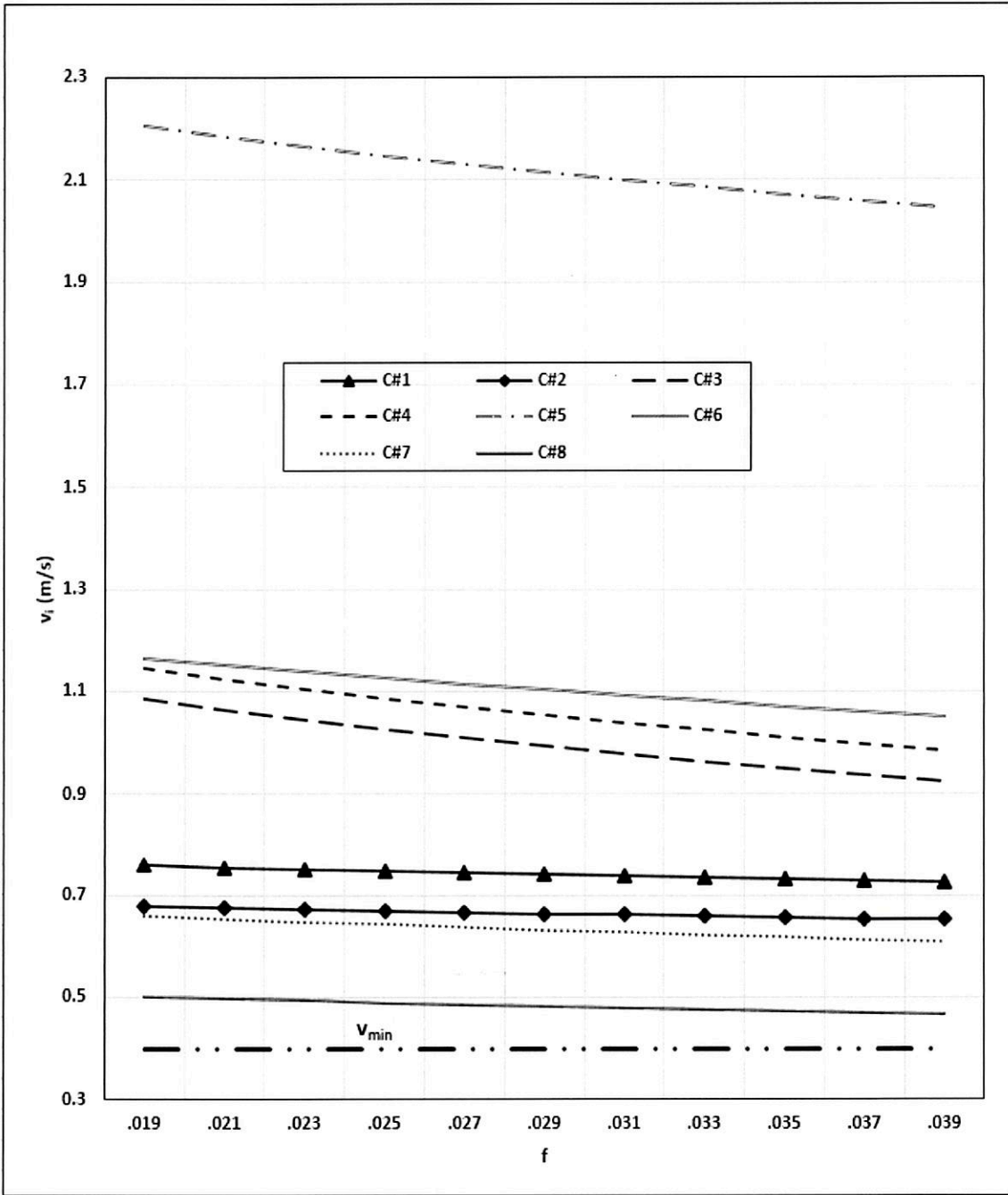
Figure 6-5: The impact of varying friction factor on inlet velocity in all circulation circuits
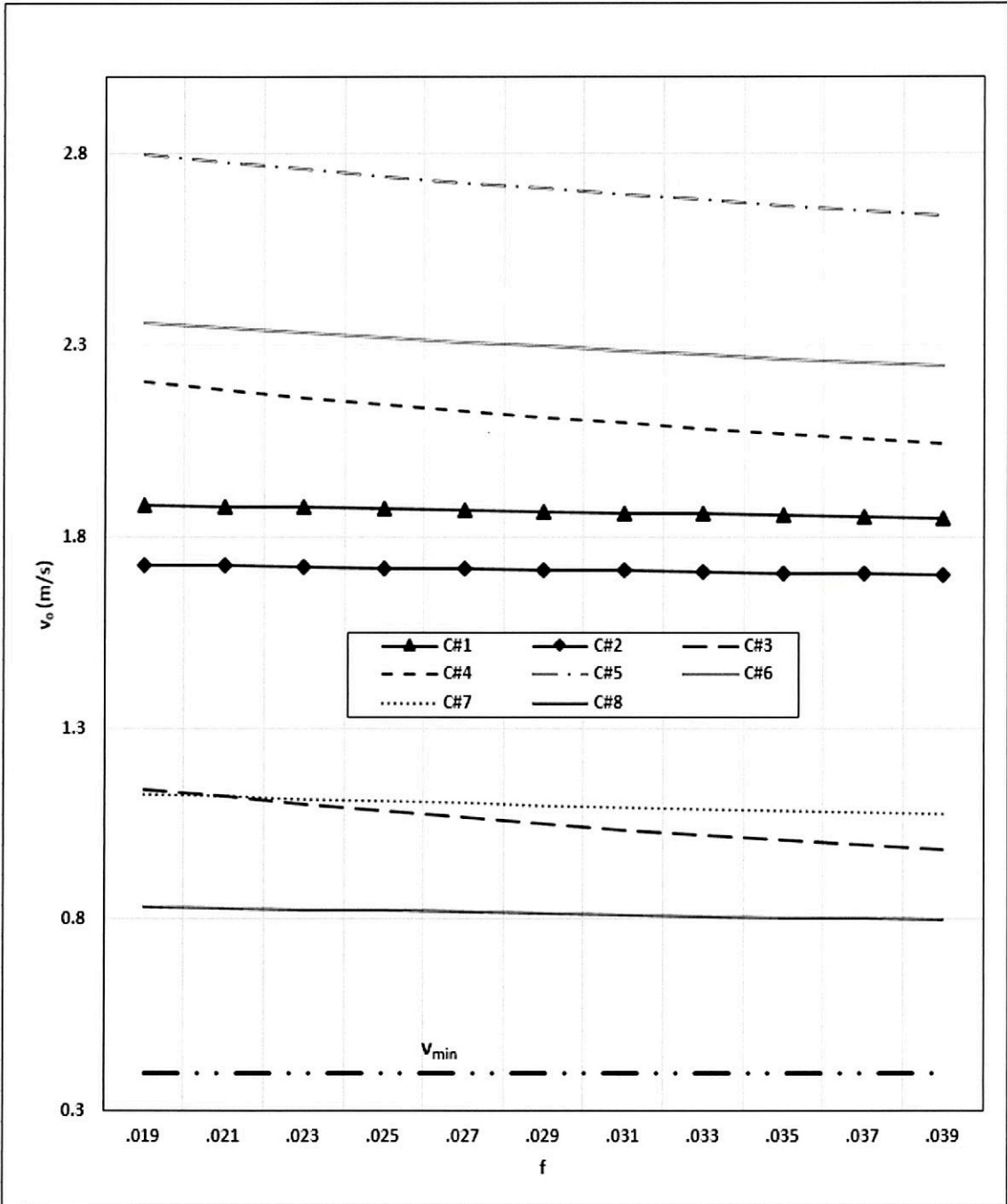
Figure 6-6: The impact of varying friction factor on outlet velocity in all circulation circuits
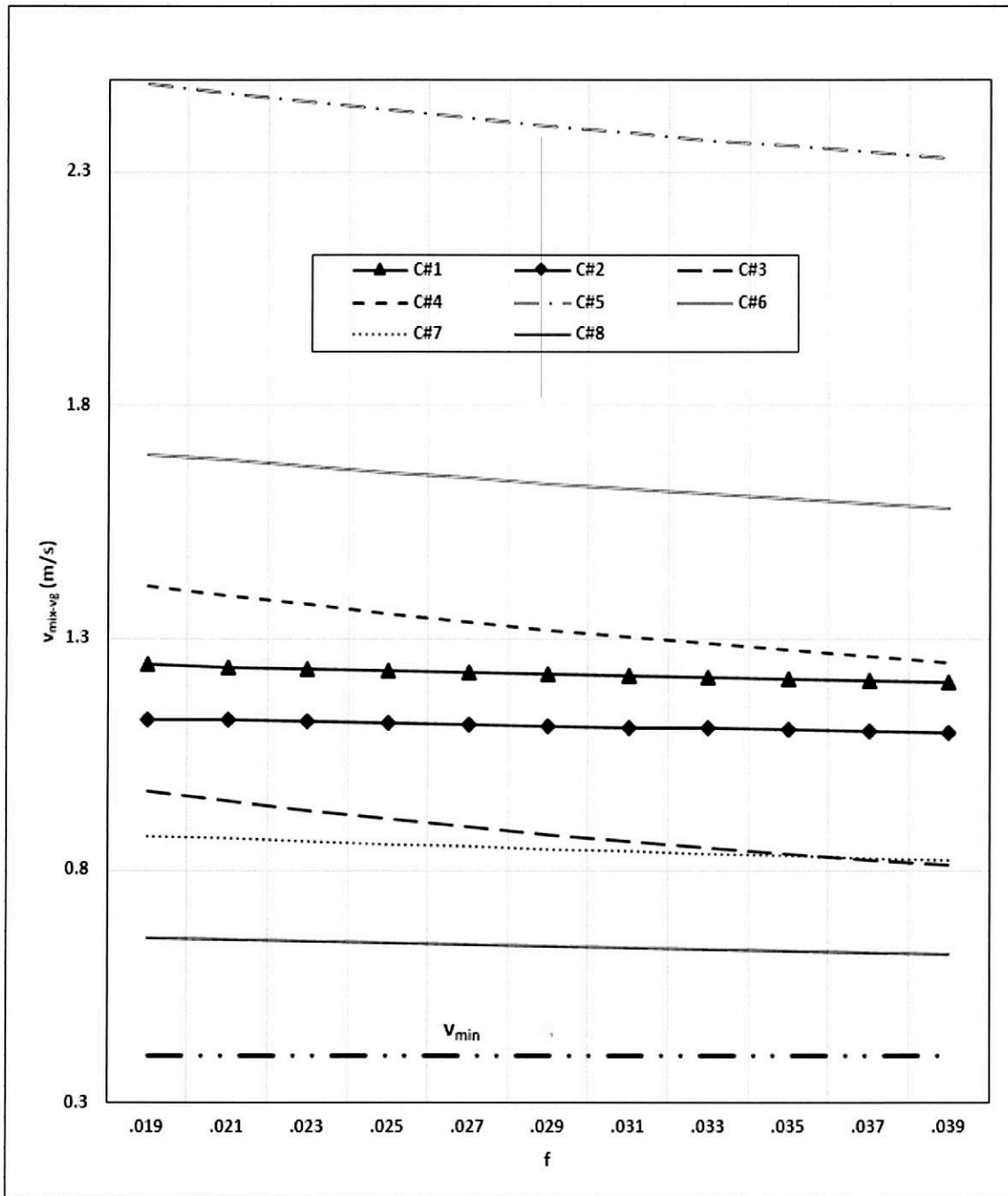
Figure 6-7: The impact of varying friction factor on average velocity in all circulation circuits

Figure 6-8 indicates that the net driving head decreases with increasing heat flux.

66
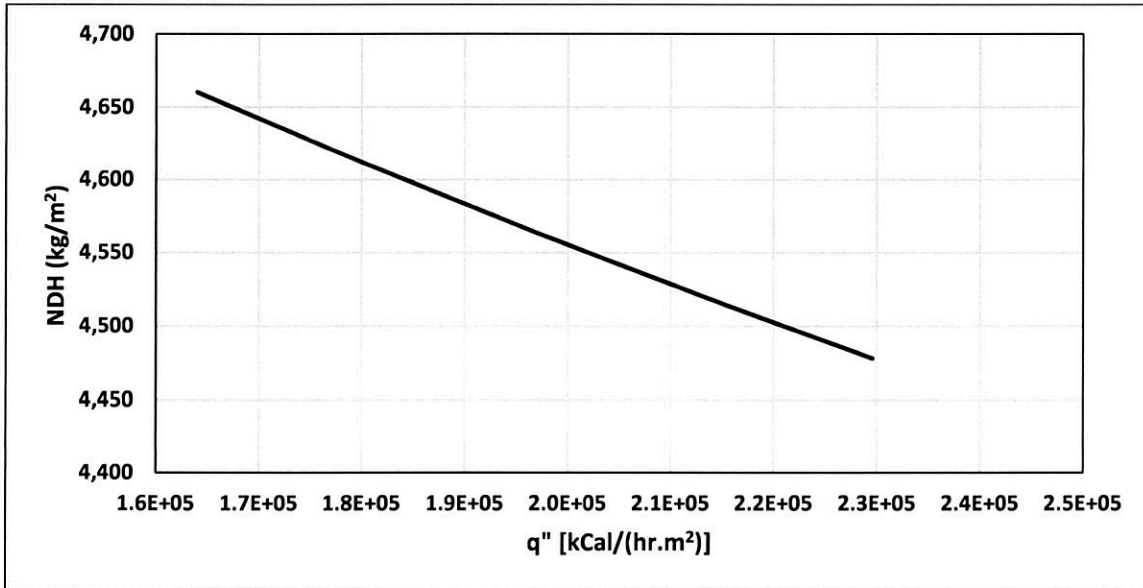
Figure 6-8: Effect of heat flux on the boiler net driving head

The variation of mass flow rate due to variation of heat flux is shown in Figure 6-9. The results indicate that the mass flow rate increases in all circuits upon increasing the heat flux due to increase in steam generation in all circuits. However, the increase is the highest in circuits 3, 5, 6, 7, and 8 (D-Tubes and evaporator or boiler bank tubes).
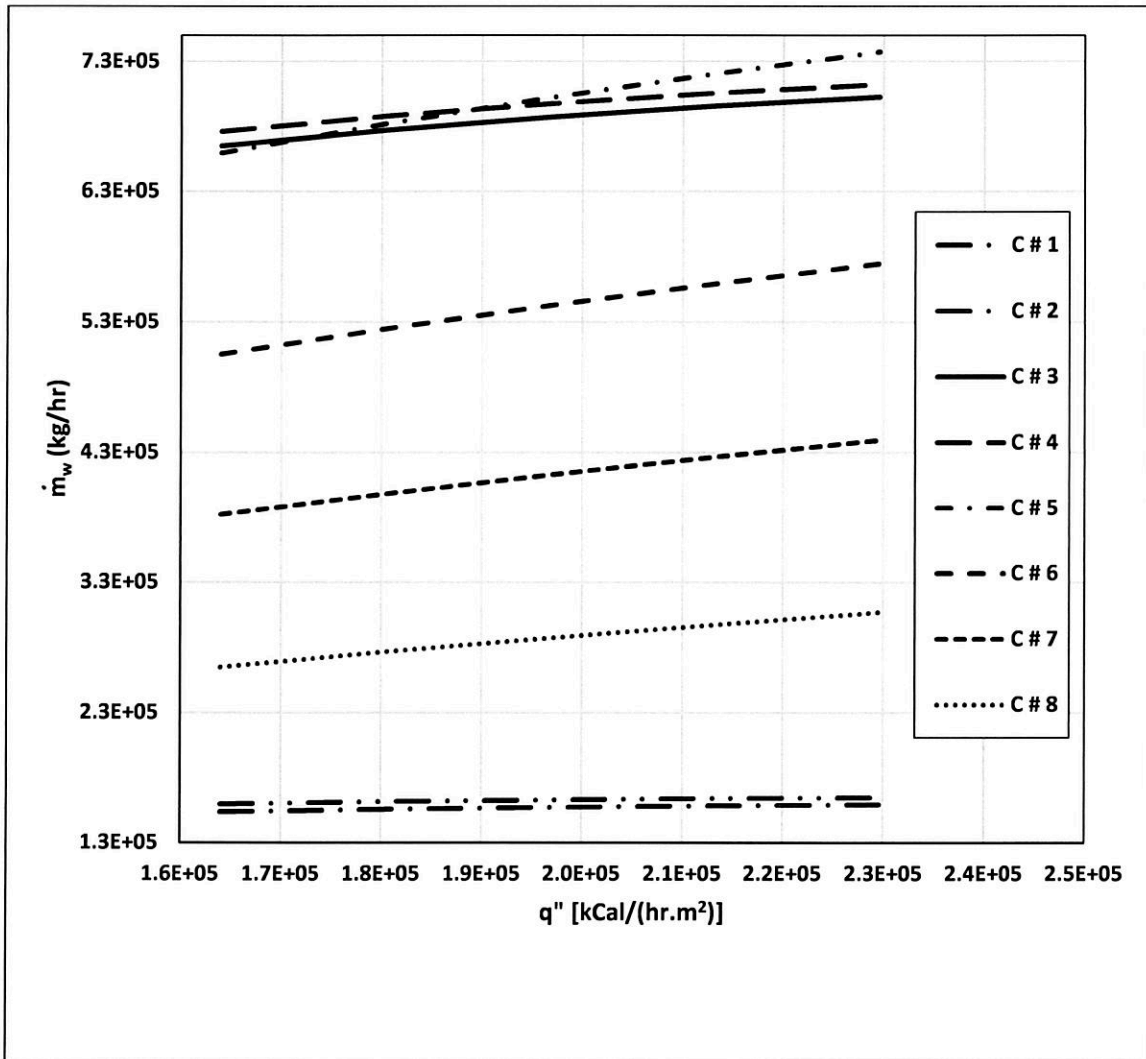
Figure 6-9: Effect of heat flux on mass flow rate for all circuits

6.1 Results for Circuits 1 and 2

More analysis is carried out for Circuits 1, 2 and 3; since they are the ones which experienced minimum circulation ratios at higher heat flux.

The second set of results pertain to the effect of heat flux on circulation ratio, mass flow rate, net driving head and tube wall temperature in Circuit 1. The results indicate that increasing heat flux results in more steam generation and hence higher mass flow rate and lower circulation ratios as shown in Figure 6-10. The results also indicate increase in the

wall temperature as a result of heat flux increase. The minimum allowable circulation ratio for this type of boiler is 11.7 [32] and the maximum temperature is 400 °C as per API-534 534 for carbon steel tubes. Figure 6-11 shows the net driving head as a result of increase in the magnitude of the change in mass flow rate.

Figure 6-10: Variation of mass flow rate, circulation ratio, and tube wall temperature in Circuit 1
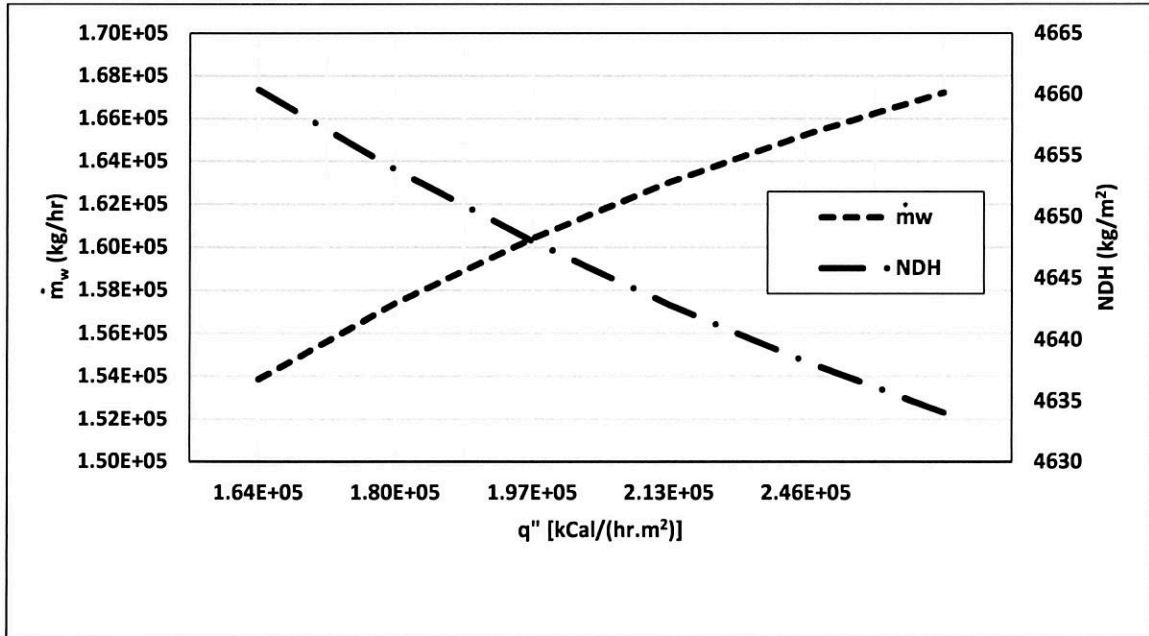
Figure 6-11: Effect of heat flux on mass flow rate and net driving head in Circuit 1

The third set of results pertain to the effect of heat flux (varied from 163,986 to 262,377 kCal/(hr.m^2) on circulation ratio, mass flow rate, net driving head and tube wall temperature in Circuit 2. Similar trends of results obtained for Circuit 1 have been obtained for Circuit 2 as shown in Figure 6-12. The only observed difference is that the two curves of the net driving head and mass flow rate cross at a lower heat flux value compared to the results of Circuit 1 as shown in Figure 6-13.

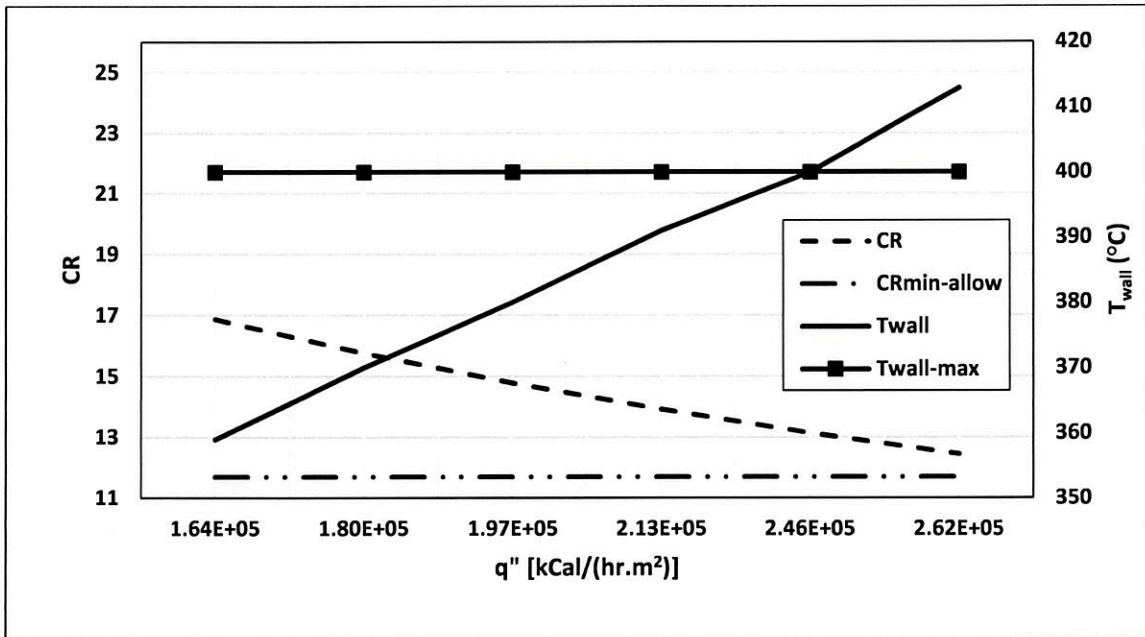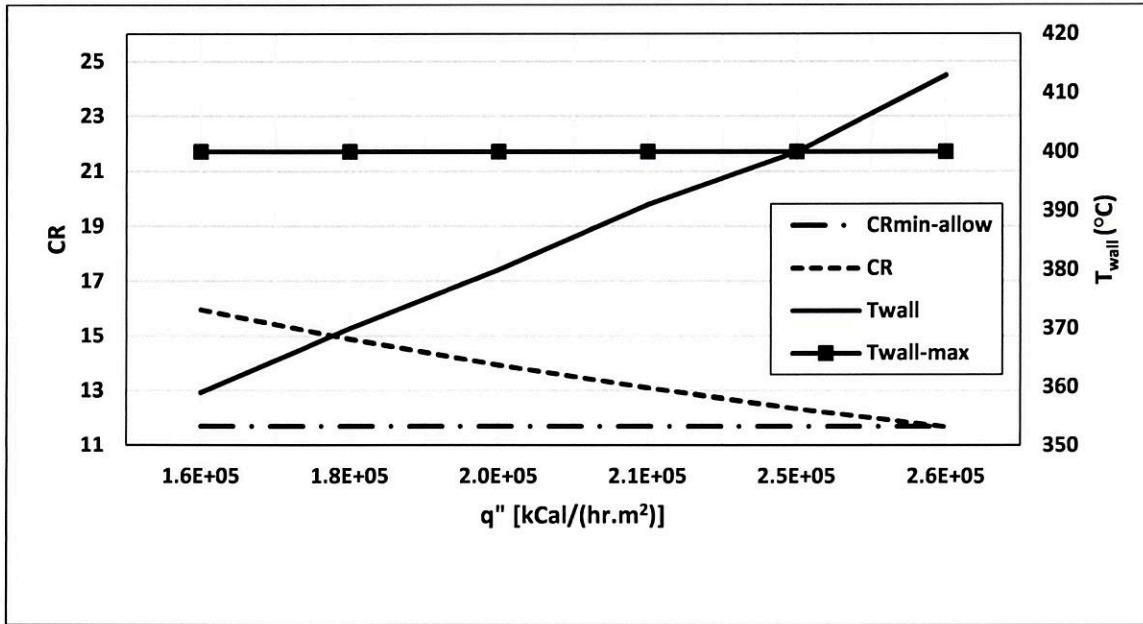**Figure 6-12: Variation of mass flow rate, circulation ratio, and tube wall temperature in Circuit 2**
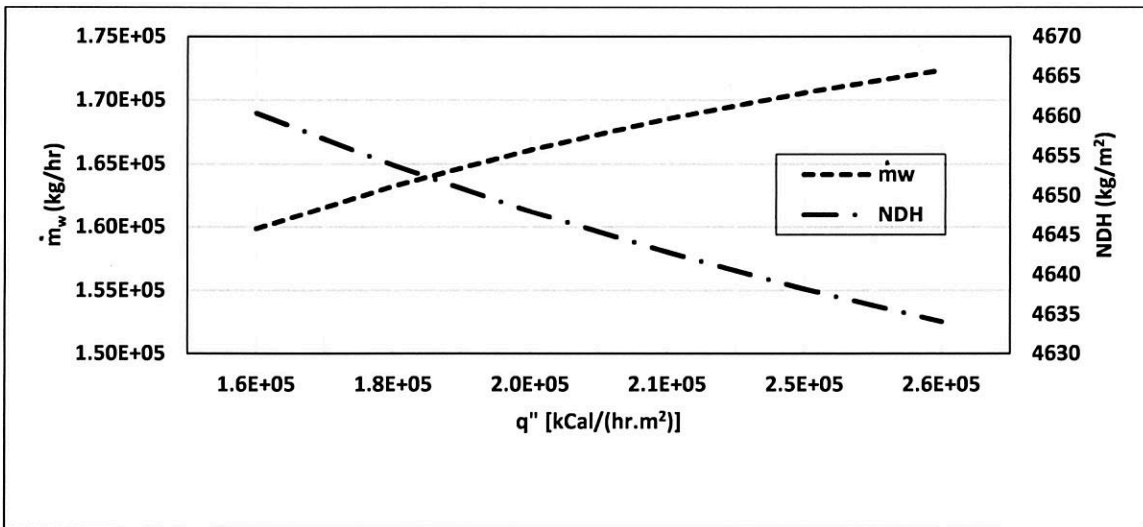
Figure 6-13: Effect of heat flux on mass flow rate and net driving head in Circuit 2

6.2 Results for Circuit 3

The fourth set of results pertain to Circuit 3 which is considered to be the critical circuit among all circuits because of its lowest circulation ratio. The analysis covered the

different sections of the circuit which are the floor horizontal tubes (Circuit 3A), left wall vertical tubes (Circuit # 3B), and roof horizontal tubes (Circuit # 3C).

6.2.1 Results for Circuit 3A

Figure 6-14: Variation of circulation ratio and tube wall temperature in Circuit 3A

Figure 6-14 shows the variation of circulation ratio and wall temperature versus heat flux in Circuit 3A (floor tubes). The results indicate that the circulation ratio decreases slightly as the heat flux increases but it does not reach the minimum circulation ratio over the range of heat flux variation. Although the heat flux was increased by 50%, the circulation ratio exhibited a slight decrease due to the fact that the floor tubes are covered with refractory. The wall temperature increase observed for Circuit 3A (the floor tubes) is negligible compared to the increase exhibited by the wall in Circuits 1 and 2.

6.2.2 Results for Circuit 3B
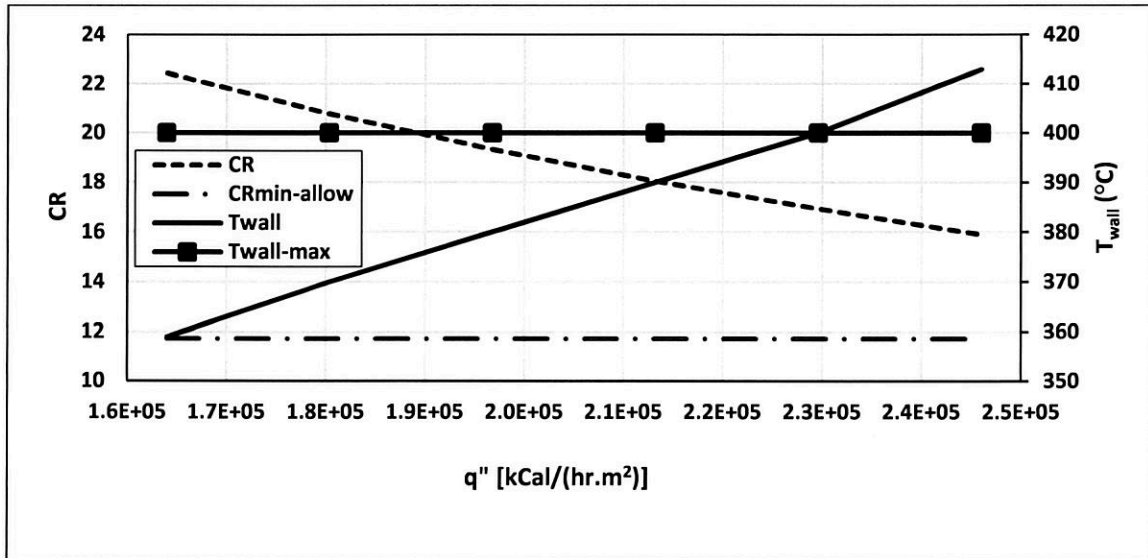
Figure 6-15: Variation of circulation ratio and tube wall temperature in Circuit 3B

Figure 6-15 shows variation of the circulation ratio and wall temperature versus heat flux in Circuit 3B (vertical tubes). The results exhibit a similar trend as the results of floor tubes (Circuit 3A); except that the rate of decrease of CR with increase in heat flux is larger. An increase in the heat flux by 40%, reduces the circulation ratio to a magnitude of 16.9 which is close to the minimum allowable value of 11.7

6.2.3 Results for Circuit 3C
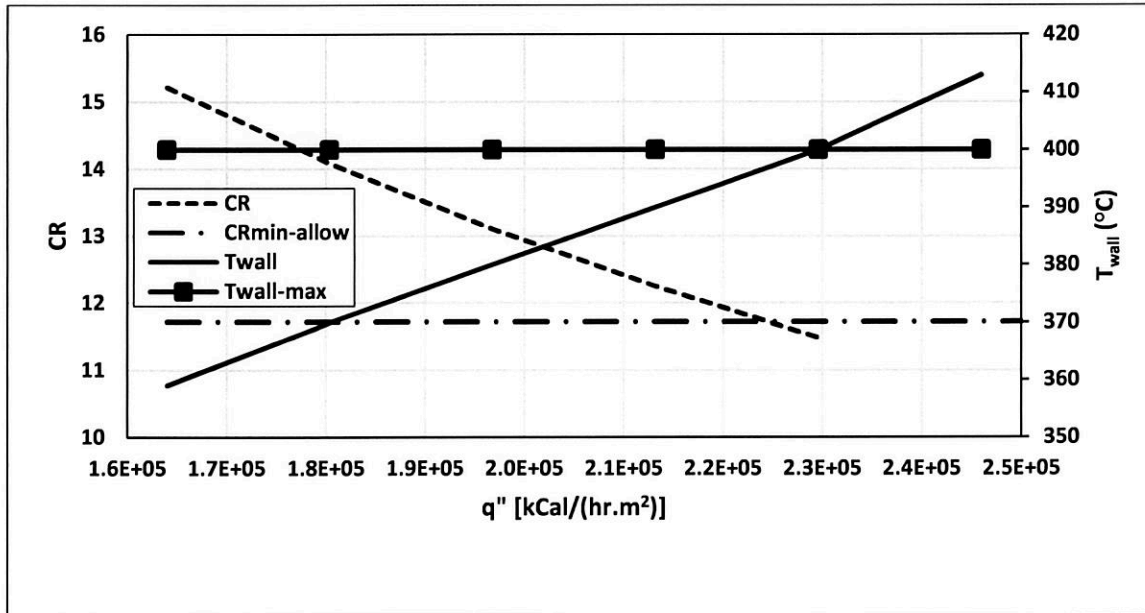
Figure 6-16: Variation of circulation ratio and tube wall temperature in Circuit 3C

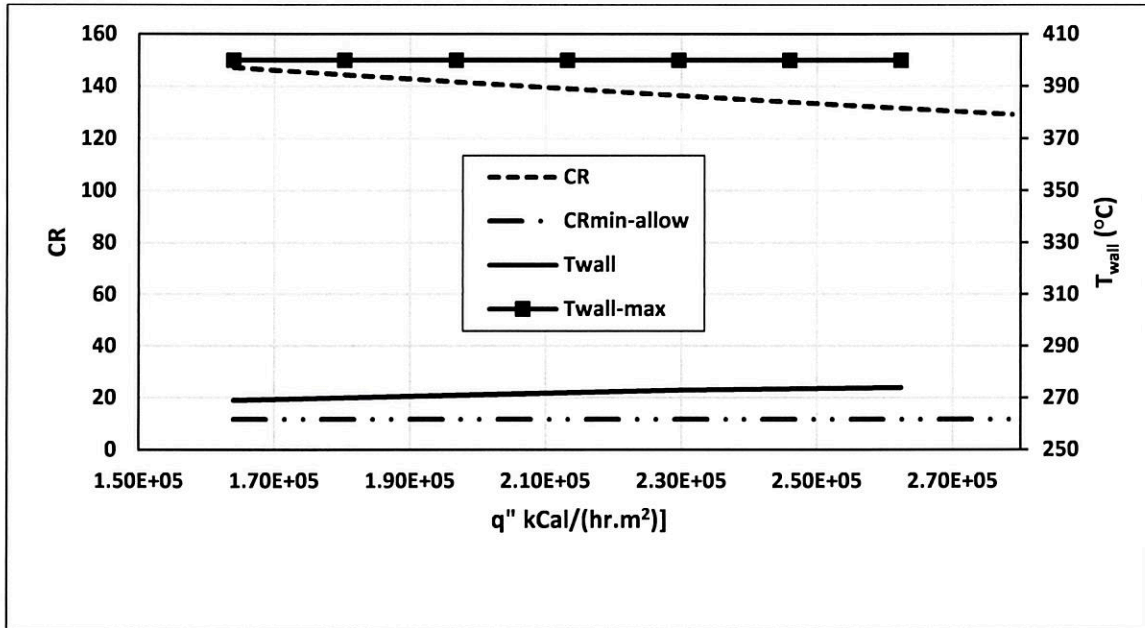The variation of circulation ratio and wall temperature with heat flux in the roof tubes

(Circuit 3C) is shown in Figure 6-16. An increase in the heat flux by 40% results in a

circulation ratio value of below the minimum allowable value of 11.7. This is the most

critical circuit as the circulation ratio starts to go below the minimum allowable value at

the heat flux of 2.25E5 kCal/(hr.m^2). Hence, this is the value of the critical heat flux. The

roof tubes wall temperature exhibits the same trend as other circuits' wall temperature

when the heat flux is increased.

6.3 Tube Plugging Impact on Critical Circuit 3C

The fifth set of results pertain to the effect of tube plugging on the circulation ratio and

tube wall temperature of the critical section of the D-Tubes (Circuit # 3C). Plugging a

certain number of the tubes in the circuit is investigated. The impact of the heat flux on

the circulation ratio and the tube wall temperature, with increasing the number of plugged

tubes, will be analyzed. Figure 6-17 shows the variation of circulation ratio and tube wall

temperature versus heat flux with five tubes plugged. The results indicate that the critical

circulation was attained at a critical heat flux value of 2.2E5 kCal/(hr.m^2).

Figure 6-17: Circulation ratio and tube wall temperature versus heat flux in the critical section of the D-Tubes (Circuit 3C) with five tubes plugged

Figure 6-18 and Figure 6-19 show that variation of circulation ratio and tube wall

temperature versus heat flux with 10 and 15 tubes plugged respectively. The results

indicate similar trends to those observed in Figure 6-17; except that the value of the

critical heat flux decreases and the value of tube wall temperature increases with the

increase of the number of plugged tubes.
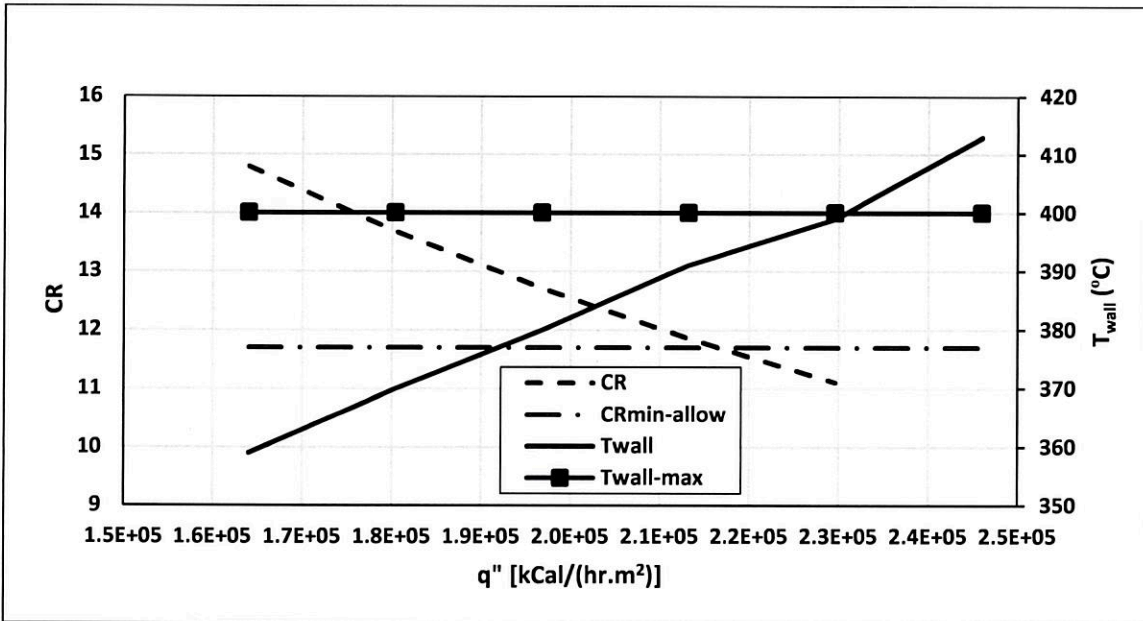
Figure 6-18: Circulation ratio and tube wall temperature versus heat flux in the critical section of the D-Tubes (Circuit 3C) with ten tubes plugged

Figure 6-20 shows the variation of circulation ratio and tube wall temperature versus heat flux in the critical section of the D-tubes (Circuit 3C) with zero to 15 tubes plugged. This is about 5% of the total number of tubes of Circuit 3C which is 107 tubes. The results confirm the observation that the circulation ratio decreases and the tube wall temperature increases with increasing the heat flux and increasing the number of plugged tubes.
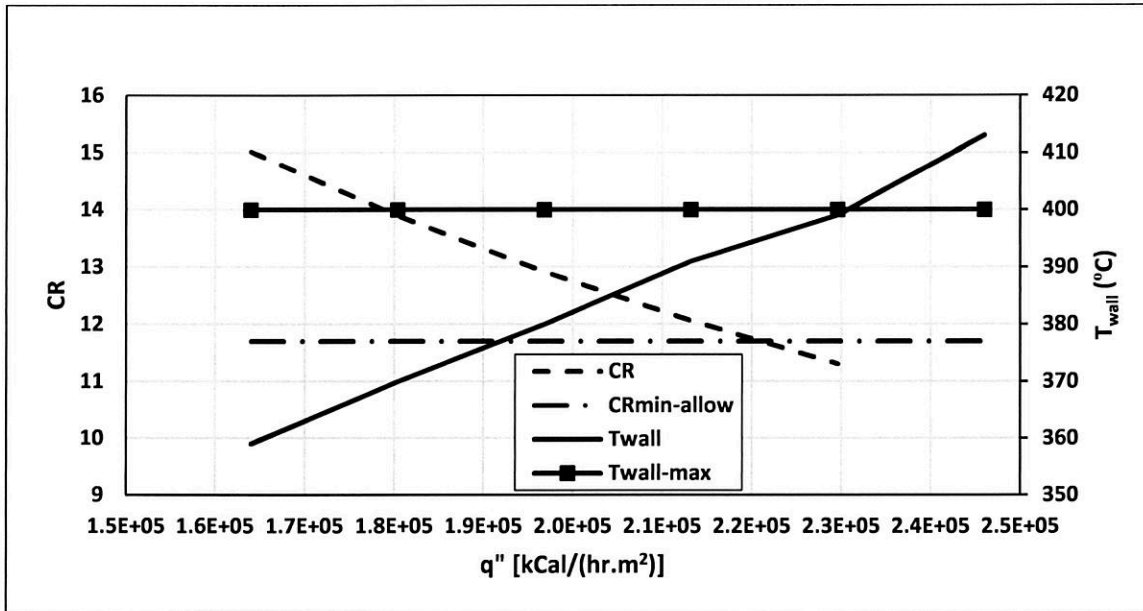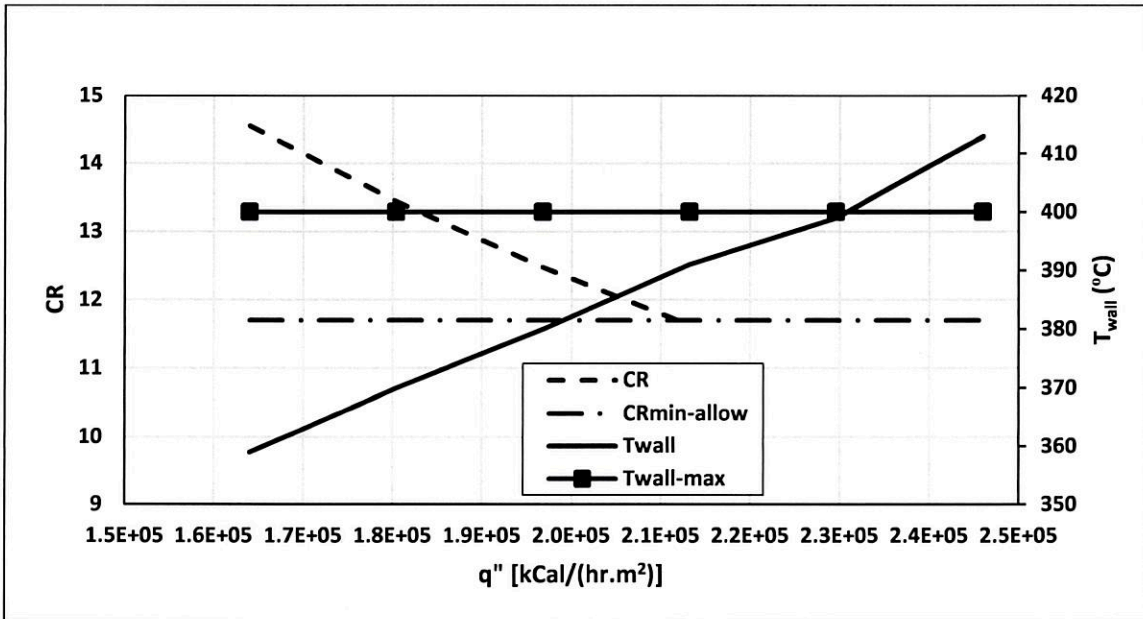
Figure 6-19: Circulation ratio and tube wall temperature versus in the critical section of the D-Tubes (Circuit 3C) with fifteen tubes plugged
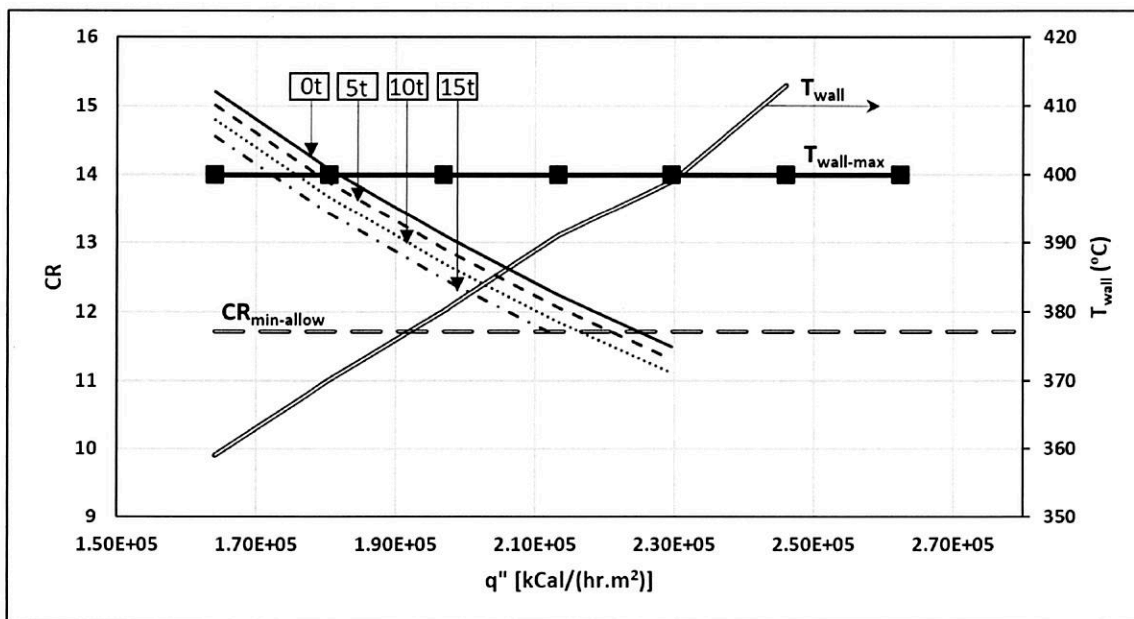
Figure 6-20: Circulation ratio and tube wall temperature in the critical section of the D-Tubes (Circuit 3C) with increasing the number of tubes plugged

6.4   Combined Effect on Velocity and Mass Flow Rate in Circuit 3C

The effect of tube plugging and increase of heat flux on the inlet, outlet, and average velocities of water mixture as well as mass flow rate has been studied in the critical section of the D-Tubes circuit (Circuit 3C). The results are plotted in Figure 6-21. Figure 6-21(a) shows the variation of velocities with variation in heat flux in Circuit 3C with no tubes plugged. As can be seen, the velocity values at the inlet of the circuit is lower than the corresponding ones at the outlet as the density is lower at the inlet of the circuit.

Increasing the heat flux from 1.63E5 to 2.3E5 Kcal/(hr.m^2), results in an increase in the inlet velocity in the range of 2.17 to 2.71 m/s, an increase in the outlet velocity in the range of 2.76 to 3.56 m/s, and an increase in the mixture average velocity in the range of 2.45 to 3.11 m/s.
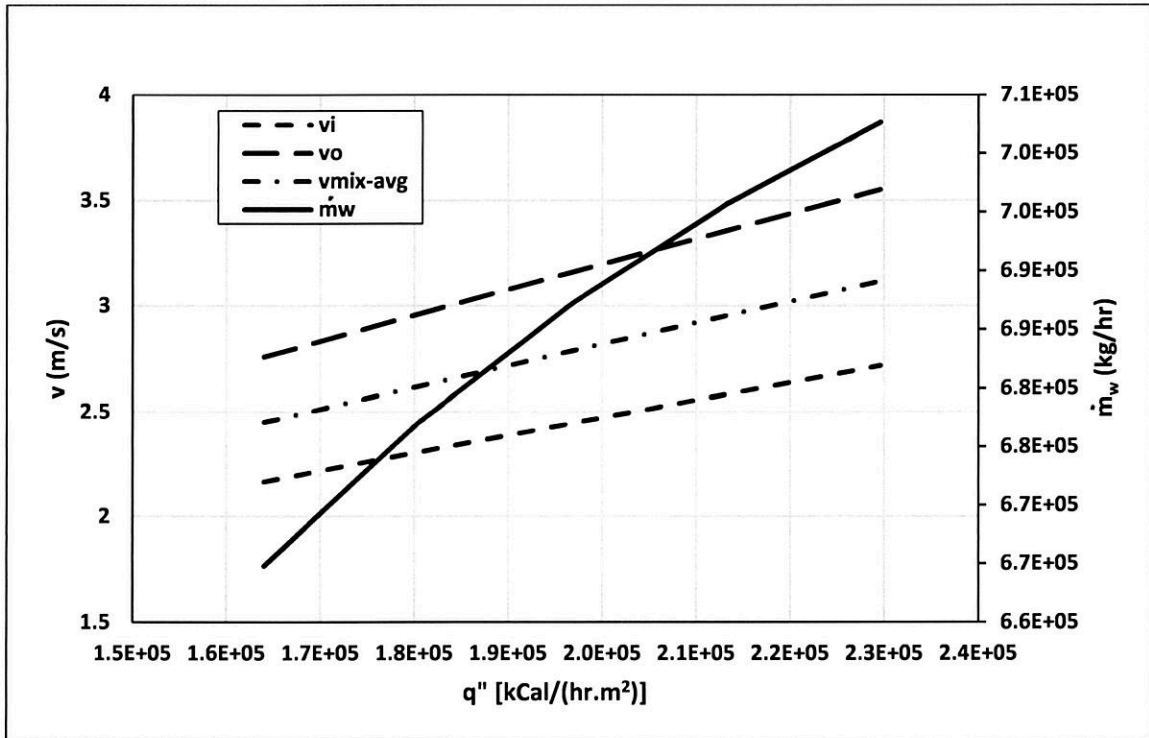
Figure 6-21a: Variation of the inlet, outlet and mixture-average velocities and the mass flow rate in Circuit 3C with no tubes plugged

Figure 6-21b, 6-21c and 6-21d show the impact of heat flux and plugging of tubes on the velocities in Circuit 3C. The results indicate a similar trend to the one observed in Figure 6-21a; except that there is slight increase in the magnitude of the mass flow rate with the increased number of plugged tubes.
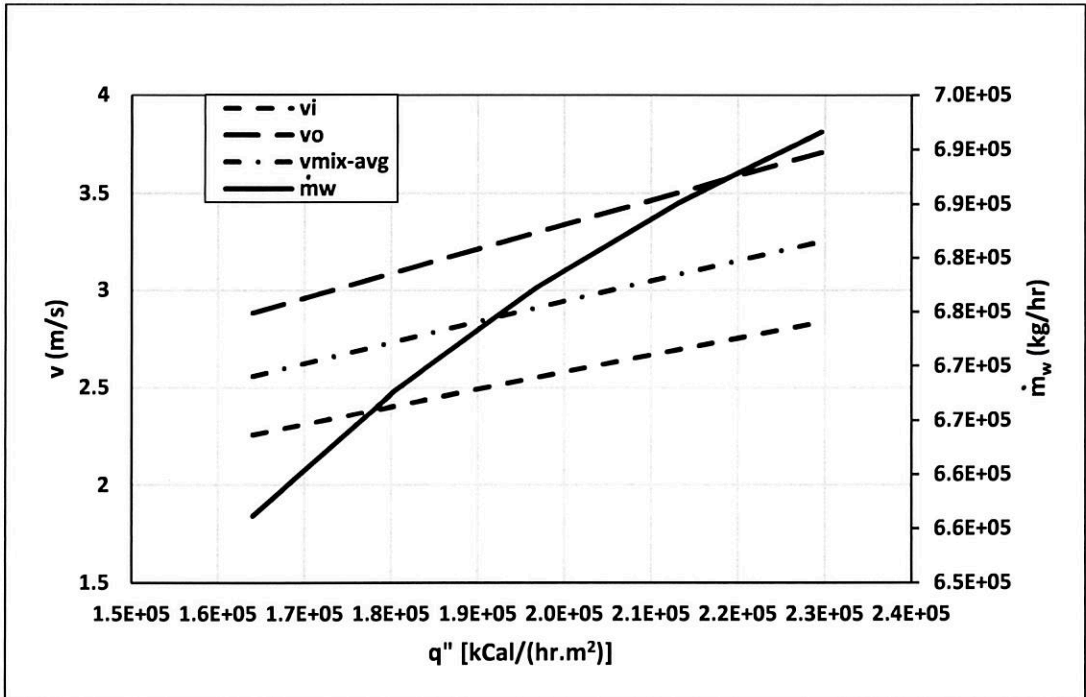
Figure 6-21b: The impact of increasing heat flux on the inlet, outlet and mixture-average velocities and the mass flow rate in Circuit 3C with five tubes plugged
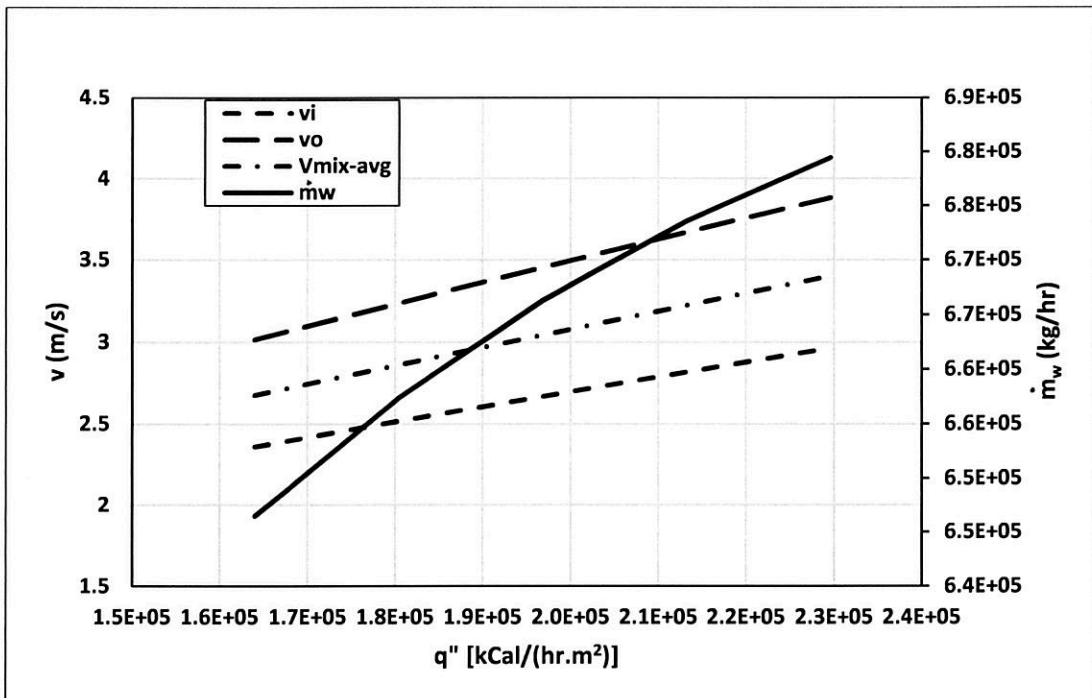
Figure 6-21c: The impact of increasing heat flux on the inlet, outlet and mixture-average velocities and the mass flow rate in Circuit 3C with ten tubes plugged

Figure 6-21d: The impact of increasing heat flux on the inlet, outlet and mixture-average velocities in Circuit 3C with fifteen tubes plugged

Figure 6-22a, 6-22b, 6-22c show the impact of increasing the heat flux and the number of plugged tubes from 0 to 15 on the inlet, outlet and mixture velocity. Once again, the results indicate that the velocities increase with the increase in number of plugged tubes. However, the mixture average and outlet velocity should not exceed the maximum recommended velocity which is 3.6 m/s to avoid erosion of the tubes [28].
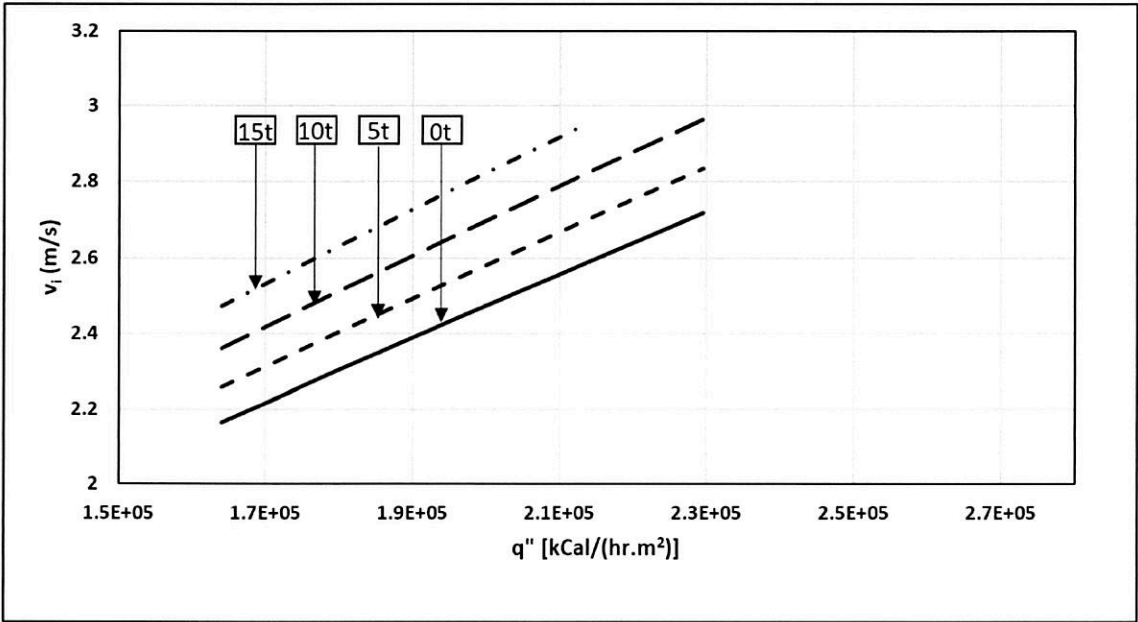
Figure 6-22 a: The impact of increasing heat flux and tube plugging on the inlet velocities in Circuit 3C (number of plugged tubes was varied from 0 to 15)
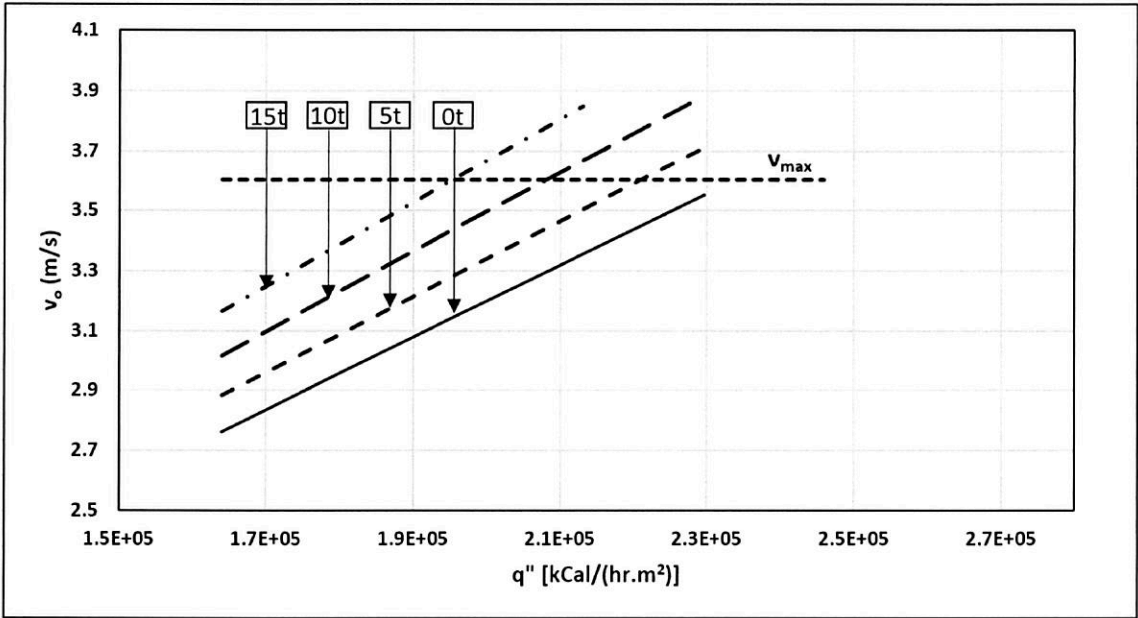
Figure 6-22b: The impact of increasing heat flux and tube plugging on the outlet velocities in Circuit 3C (number of plugged tubes was varied from 0 to 15)
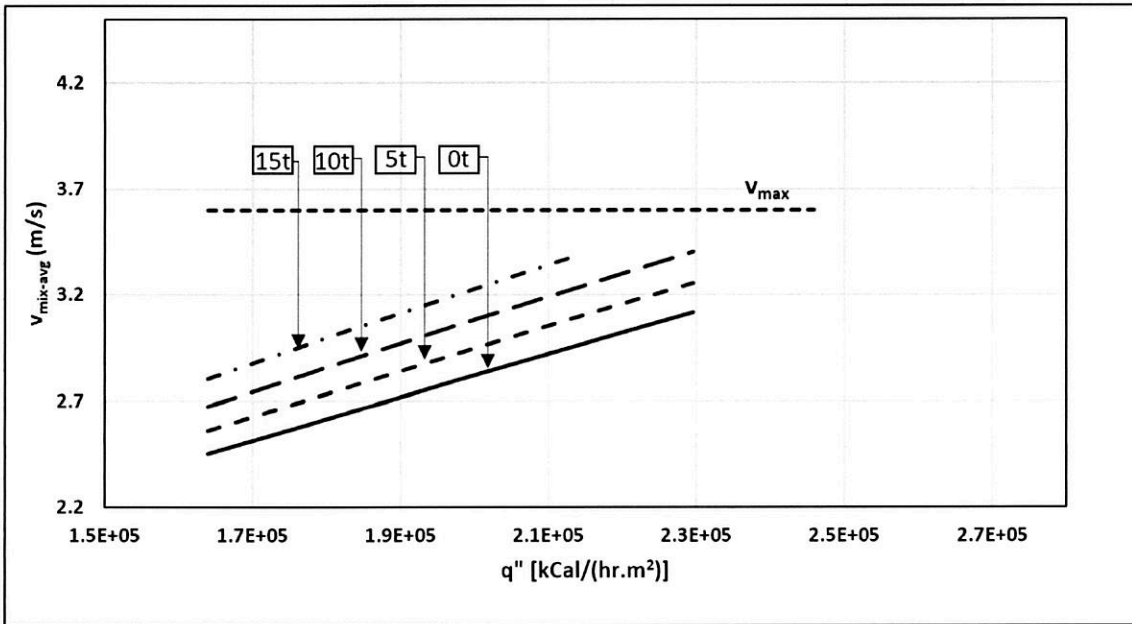
Figure 6-22c: The impact of increasing heat flux and tube plugging on the mixture average velocities in Circuit 3C (number of plugged tubes was varied from 0 to 15)

Similarly, the impact of increasing the heat flux and number of plugged tubes from 0 to 15 on the mass flow rate are shown in Figure 6-23. As can be seen from the figure the mass flow rate increases with the increase in the heat flux even with plugging some of the tubes in the circuit. However, the rate of increase decreases with the increase in the number of plugged tubes.
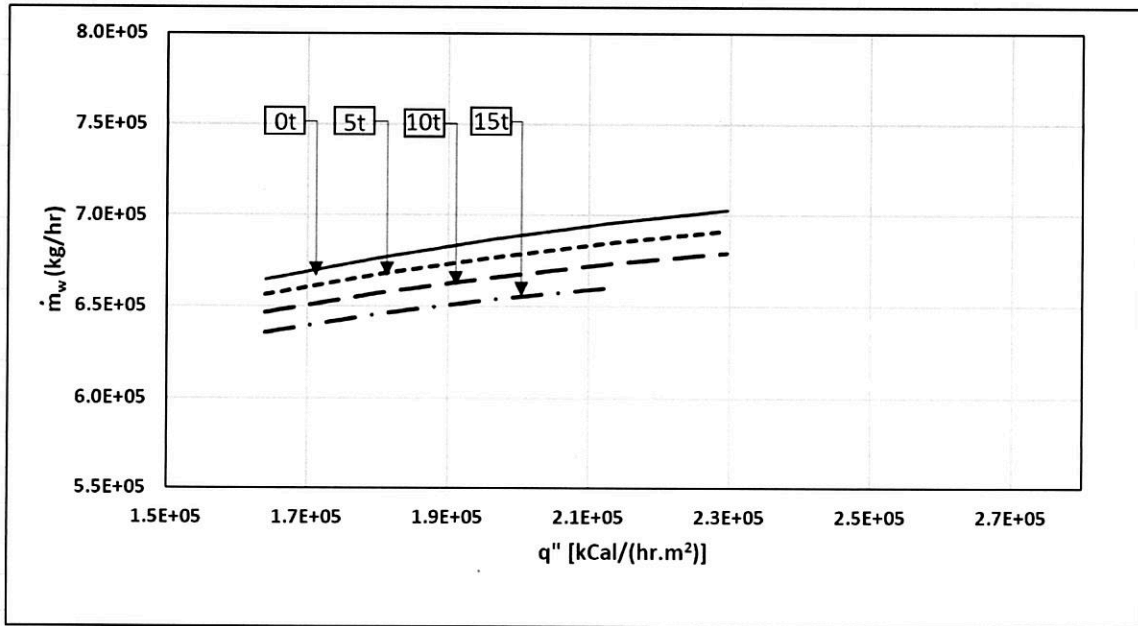
Figure 6-23: The impact of increasing heat flux and tube plugging on the mass flow rate (number of plugged tubes was varied from 0 to 15)

6.5 Investigating Plugging Evaporator (Boiler Bank) Tubes

The impact of heat flux and plugging of furnace tubes on the circulation ratio of Circuit 3C (D-Tubes) has been discussed in details in the previous section. The need for tube plugging occurs due to corrosion or deterioration in the material of the tubes and used as a temporary solution till the next T&I window comes and the tubes are replaced. Other tubes that can be damaged beside the furnace tubes are boiler bank tubes. The impact of varying the heat flux on the circulation ratio and tube wall temperature of boiler bank tubes with some of the tubes plugged will be discussed in this section. The number of plugged tubes will be varied from 1% to 5% of the total number of tubes which is 602 tubes.

Figure 6-24 shows the variation of circulation ratio and tube wall temperature due to variation in heat flux for Circuit 3C with 6 tubes of the boiler bank tubes plugged. The

circulation ratio falls below the minimum allowable value of 11.7 at a heat flux of 2.25E5 kCal/(hr.m^2). The tube wall temperature reaches the maximum allowed value of 400 °C at a heat flux of 2.3E5 kCal/(hr.m^2).

Figure 6-24: Impact of heat flux on circulation ratio and tube wall temperature of Circuit 3C with 6 of the evaporator boiler bank tubes plugged

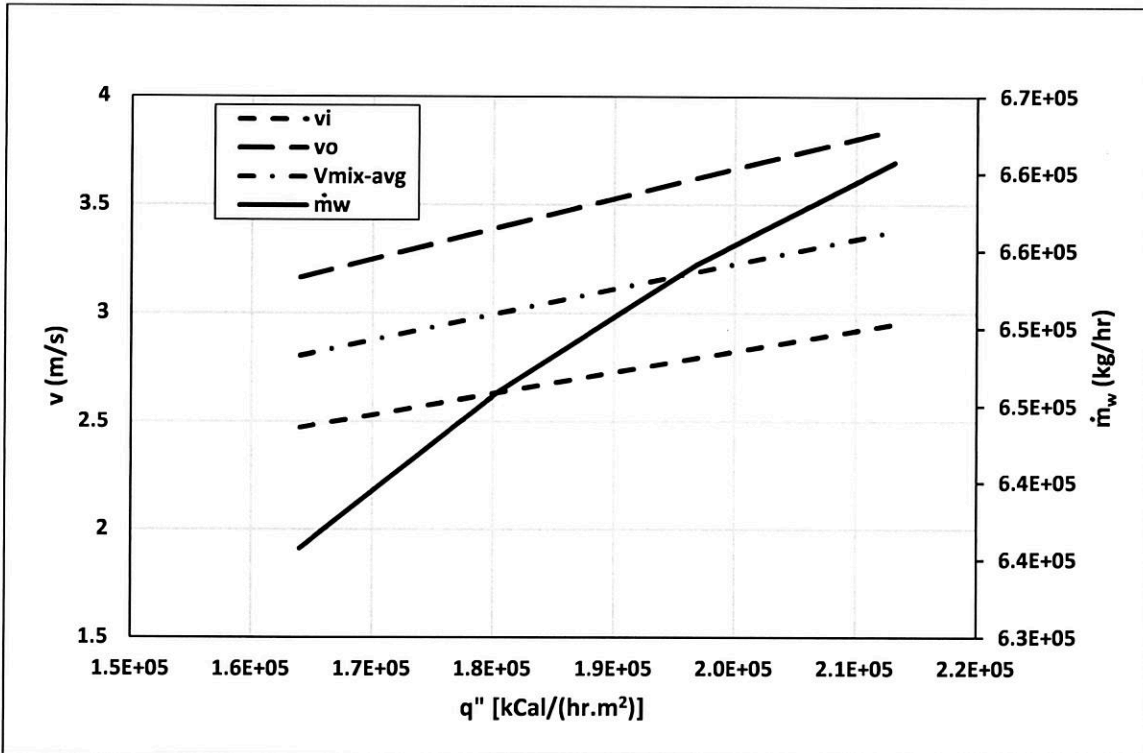Figure 6-25 shows the impact of increasing heat flux on the inlet, outlet and average velocities as well as the mass flow rate of Circuit 3C with 6 tubes of the boiler bank tubes plugged. The velocities of water, mixture and steam as well as the mass flow rate increase with increasing the heat flux exhibiting a similar trend to the case where furnace tubes were plugged. Comparing the values in Figure 6-25 with those in Figure 6-21a indicate that the difference between the values of the velocities is not high. The inlet velocity changes from 2.17 to 2.71 m/s in Figure 6-25 and from 2.17 to 2.71 m/s in

Figure 6-21a. The outlet velocity increases from 2.76 to 3.55 in Figure 6-25 while it increases from 2.76 to 3.56 m/s in Figure 6-21a. Also the mixture average velocity range was 2.45 to 3.12 in Figure 6-25 and 2.45 to 3.16 in Figure 6-21a. Finally, the mass flow rate increases from 6.65 to 7.03E5 kg/hr in both Figures 6-25 and 6-21a. Hence, it can be concluded that the overall effect of tube damage being in the furnace or boiler bank tubes on the D-Tubes is not significant.

Figure 6-25: Impact of heat flux on the mass flow rate and velocities of water, mixture, steam in Circuit 3C with 6 of the evaporator boiler bank tubes plugged

Figure 6-26 shows the impact of increasing heat flux on circulation ratio and tube wall temperature of the Circuit 3C with 18 tubes of the boiler bank tubes plugged. The circulation ratio crosses the minimum value of 11.7 at a heat flux of 2.25E5 $kCal/(hr.m^2)$.

The tube wall temperature reaches the maximum value of 400 °C at a heat flux of 2.3E5 kCal/(hr.m^2).
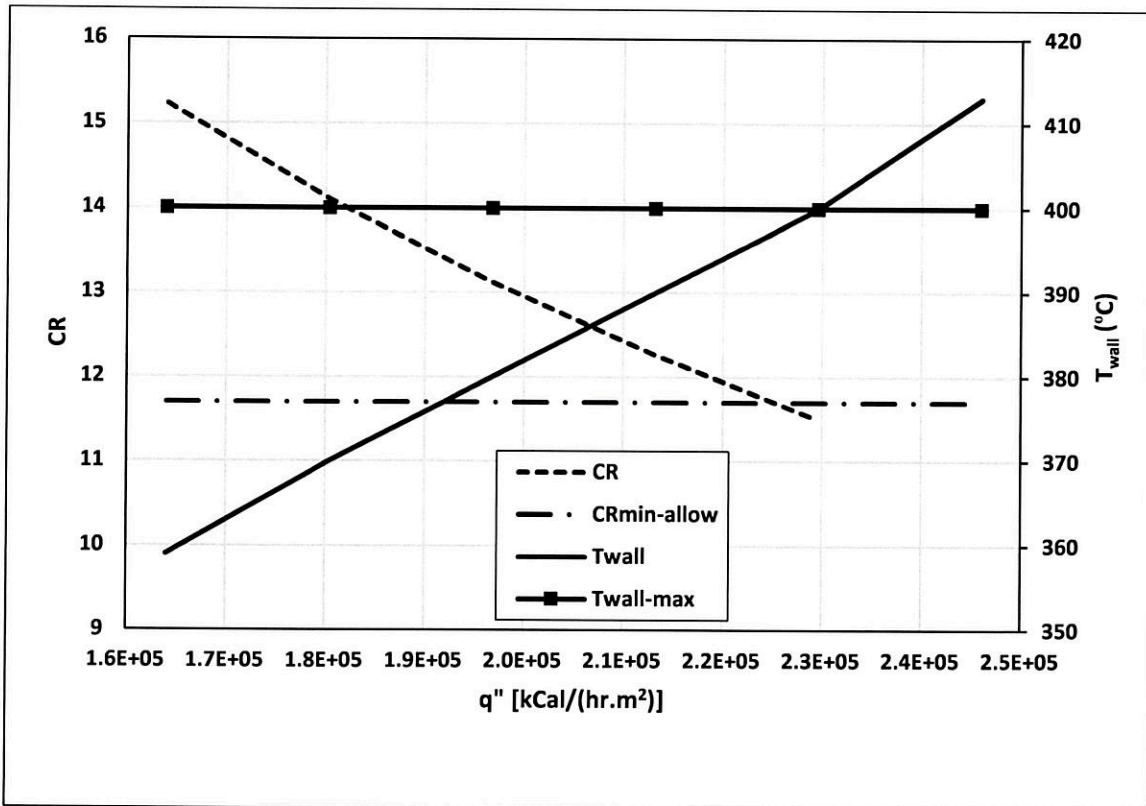
Figure 6-26: Impact of heat flux on circulation ratio and tube wall temperature of Circuit 3C with 18 of the evaporator boiler bank tubes plugged

Figure 6-27 shows the impact of increasing heat flux on the water inlet, outlet and mixture velocities as well as the mass flow rate. The results exhibit similar trend to the ones shown in Figure 6-25 as the heat flux increases with negligible differences in the values of the velocities and the mass flow rate.
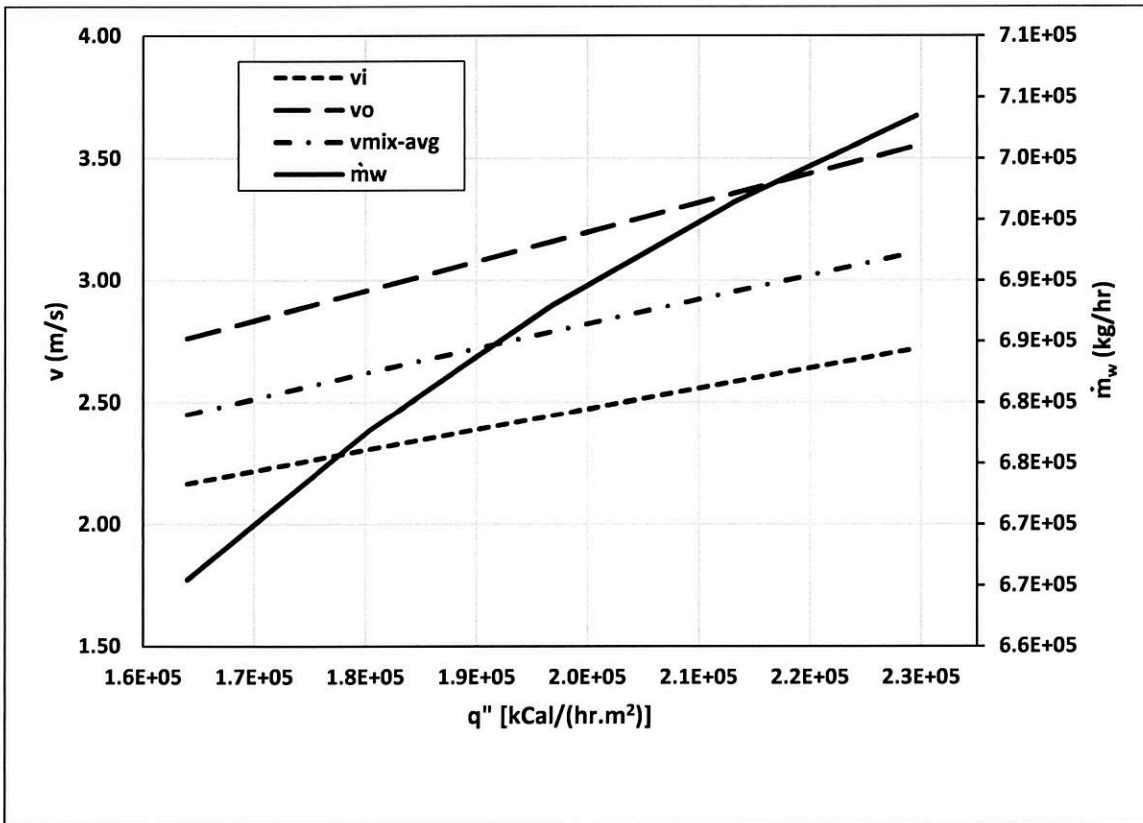
Figure 6-27: Impact of heat flux on the mass flow rate and velocities of water, mixture, and steam velocity in Circuit 3C with 18 of the evaporator boiler bank tubes plugged

Figure 6-28 shows the impact of increasing heat flux on circulation ratio and tube wall temperature for Circuit 3C with 30 tubes of the boiler bank tubes plugged. The circulation ratio crosses the minimum value of 11.7 at a heat flux of 2.25E5 kCal/(hr.m^2). The tube wall temperature reaches the maximum value of 400 C at a heat flux of 2.3E5 kCal/(hr.m^2). Comparing these results with the ones presented for Circuit 3C with 18 tubes of the boiler bank tubes plugged, indicate that increasing the number of plugged tubes does not have significant effect on the circulation and tube wall temperature.
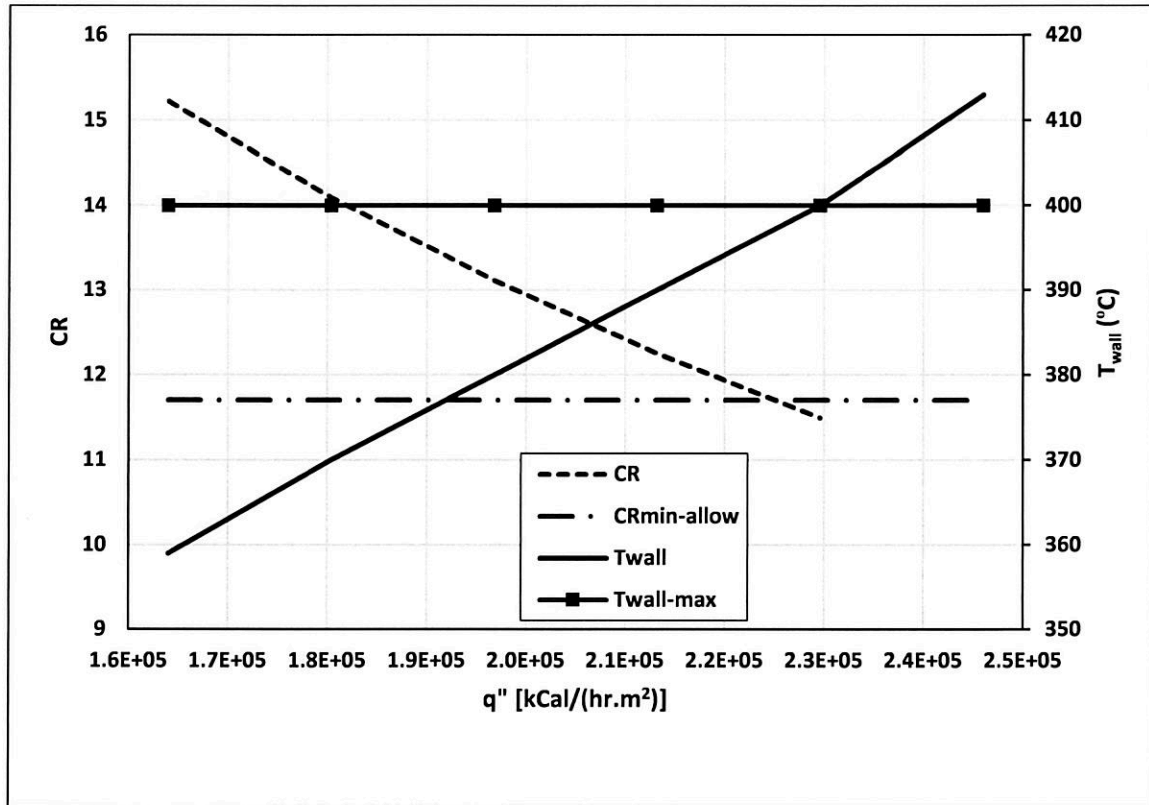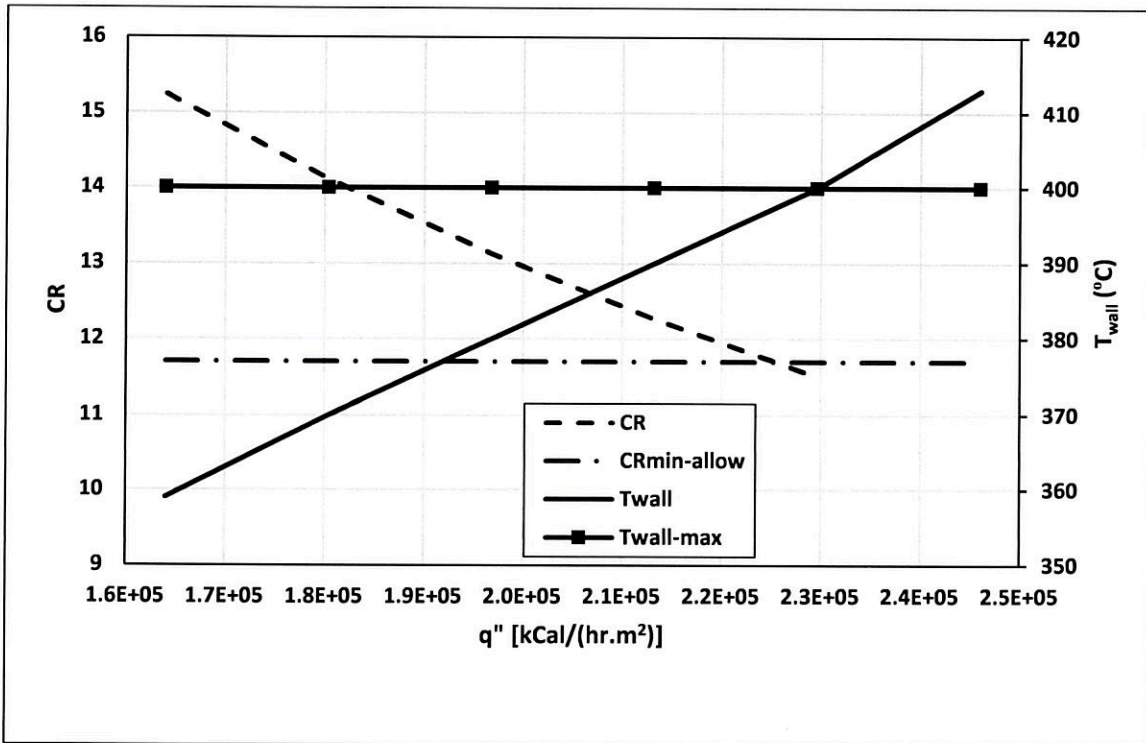
Figure 6-28: Impact of heat flux on circulation ratio and tube wall temperature of Circuit 3C with 30 of the evaporator boiler bank tubes plugged

Figure 6-29 shows the impact of increasing heat flux on the water inlet, outlet and mixture velocities as well as the mass flow rate. The results indicate similar trend to the ones shown in Figure 6-27 as the heat flux increases with minimal differences between the values due to increase in the number of evaporator bank tubes plugged.
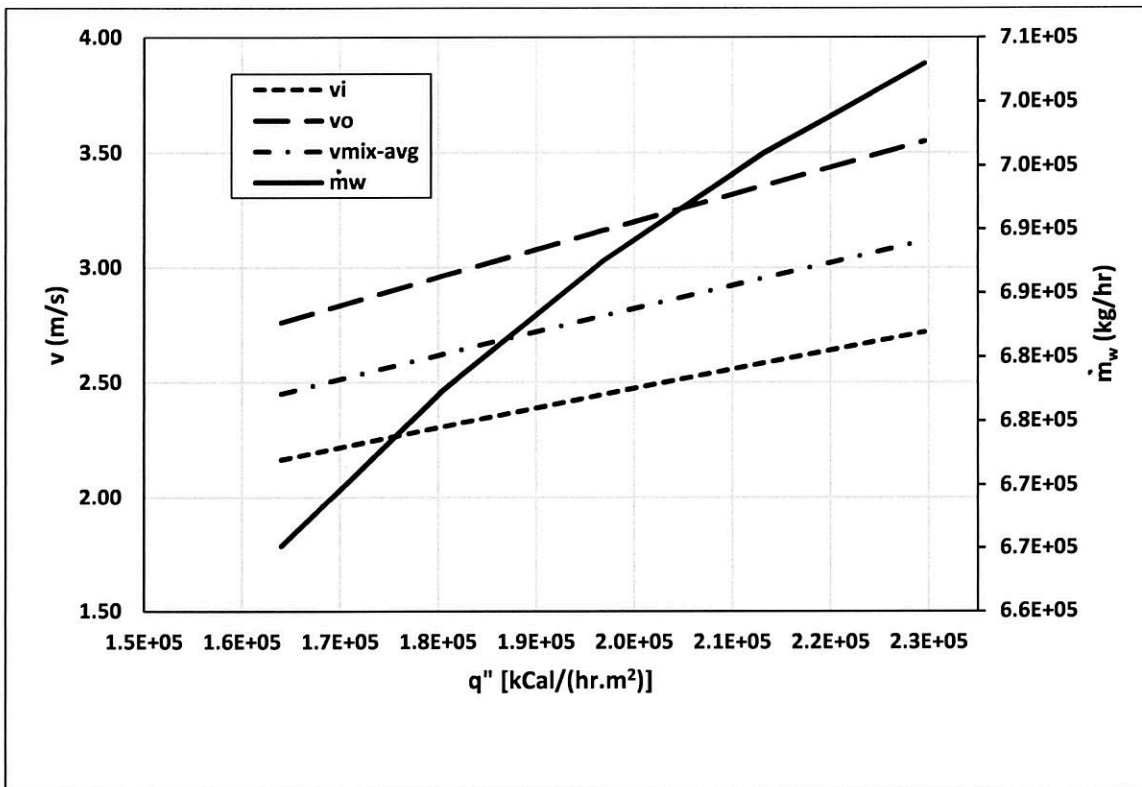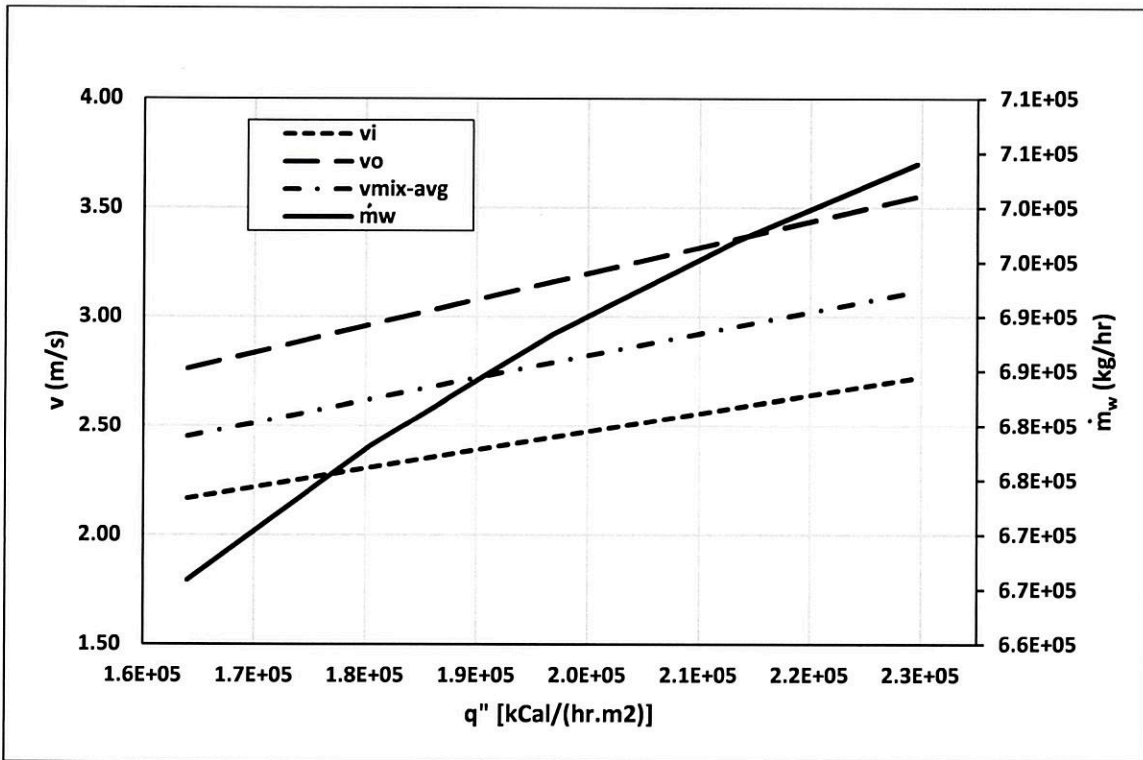
Figure 6-29: Impact of heat flux on the mass flow rate and velocities of water, mixture, and steam velocity in Circuit 3C with 30 of the evaporator boiler bank tubes plugged

Figure 6-30 shows the results of impact of heat flux on circulation ratio and tube wall temperature for the range of 6 to 30 boiler bank tubes being plugged. The results indicate that the minimum circulation ratio is reached at a heat flux of 2.25E5 kCal/(hr.m^2), the same value with no tubes being plugged. It is also observed that the impact of increasing the number of plugged tubes up to 5% of the total number of tubes is not visible. The impact on the tube wall temperature is also not significant. The maximum wall temperature is reached at a heat flux of 2.3E5 kCal/(hr.m^2), the same as without any tubes plugged (Figure 6-21a).
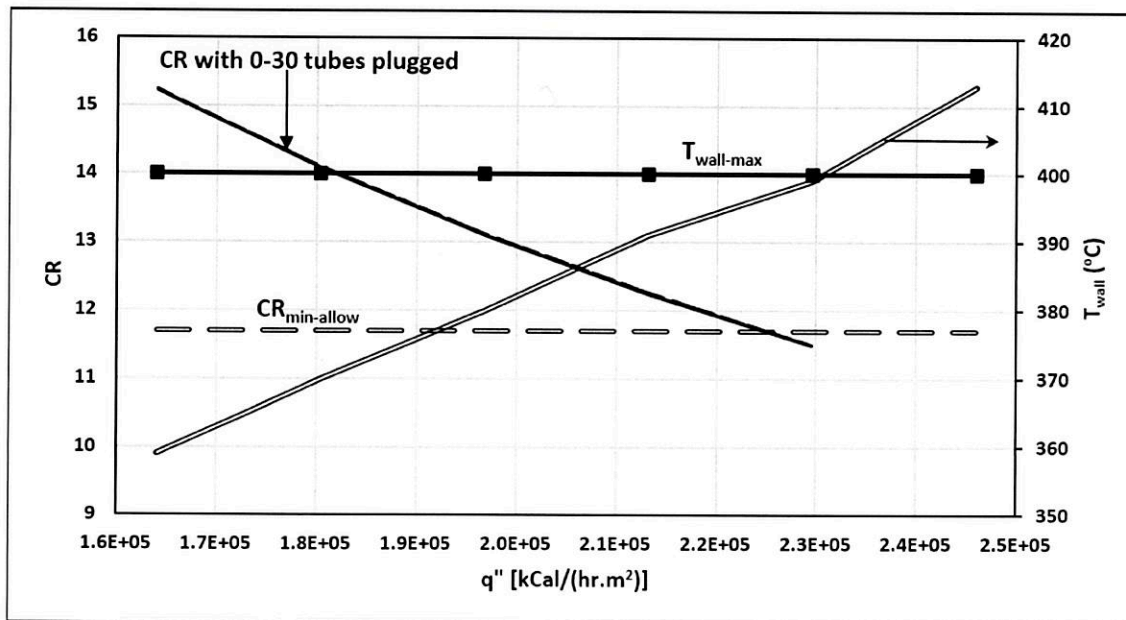
Figure 6-30: Variation of the circulation ratio and the tube wall temperature of Circuit 3C with 6 to 30 of the evaporator boiler bank tubes plugged

Figure 6-31 show the impact of increasing heat flux on the water inlet, outlet and mixture velocities for Circuit 3C if the up to 30 tubes of the boiler bank tubes are plugged. As can be seen, plugging the evaporator boiler bank tubes does not make a big impact on the velocity inside the D-tubes. The outlet velocity does not reach the velocity limit of 3.6 m/s [28].
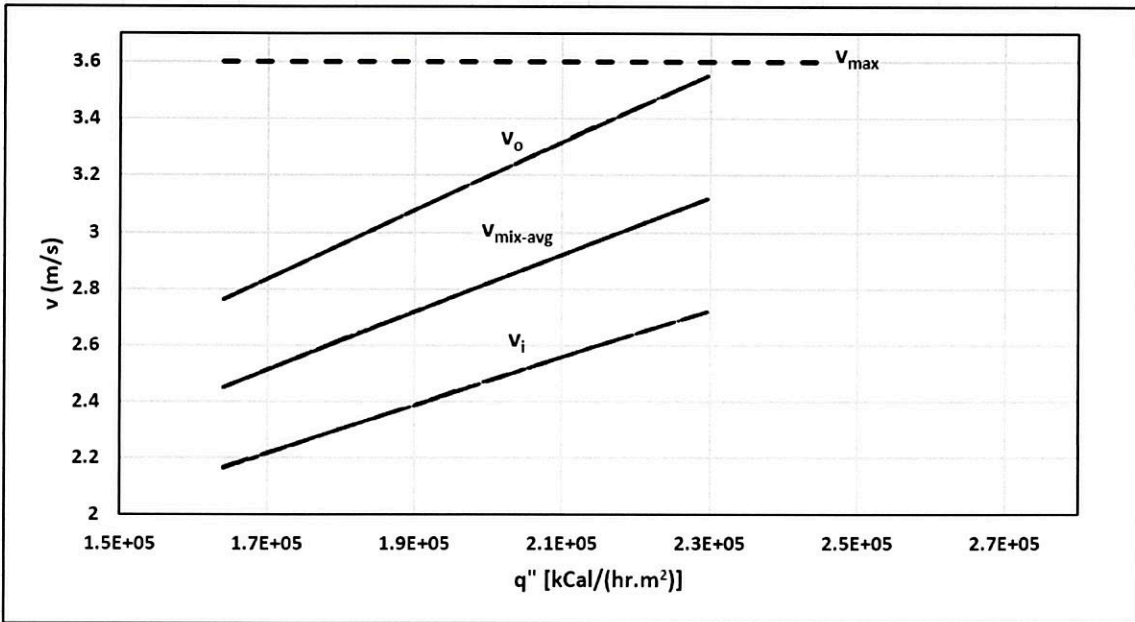
Figure 6-31: Impact of heat flux on the water inlet, outlet and steam-water mixture velocities in Circuit 3C with 6 to 30 of the evaporator boiler bank tubes plugged

Figure 6-32 shows the impact of varying heat flux on the mass flow rate in Circuit 3C with up to 30 tubes of the boiler bank tubes being plugged. The impact of varying heat flux on the mass flow rate is estimated by a decrease of 5% in the mass flow rate of the boiler riser tubes (front wall, rear wall, D-Tubes, division wall, and evaporator circuits).
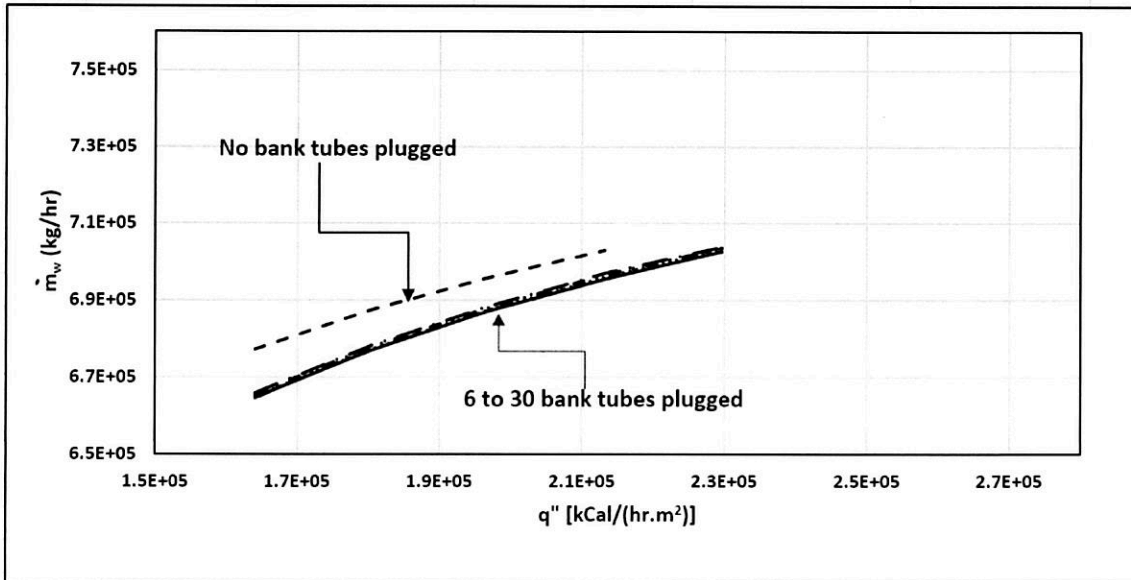
Figure 6-32: Impact of heat flux on the mass flow rate in Circuit 3C with 6 to 30 tubes of the evaporator boiler bank tubes plugged

6.6 Comparing Results for Two Boilers with Different Specifications

The program was used to determine circulation parameters for two boilers with different capacities to observe the trend of the results considering the differences in the specifications of the two boilers.

The difference in parameter values extracted from the data sheets of both boilers are summarized in Table 6-1 [57]. The program was used to determine the heat flux, mass flow rate, and circulation ratio for each boiler and plotted as shown in Figures 6-33, 6-34, and 6-35. The comparison shows both boiler results exhibit the same trend. The observed differences are attributed mainly to the difference in boiler capacity, geometry, and fuel specifications.

93

Table 6-1: Validation of 112,000 kg/hr to 130,000 kg/hr package boilers

Parameter	Boiler # 1	Boiler # 2
Feed Water temperature (°C)	140	115
Steam output (kg/hr)	112,000	130,000
Fuel LHV (kCal/m^3)	9,166	8,665
Furnace exit area (m^2)	6.11	4.71
EPRS (m^2)	198	186
Furnace volume (m^3)	214	196.5
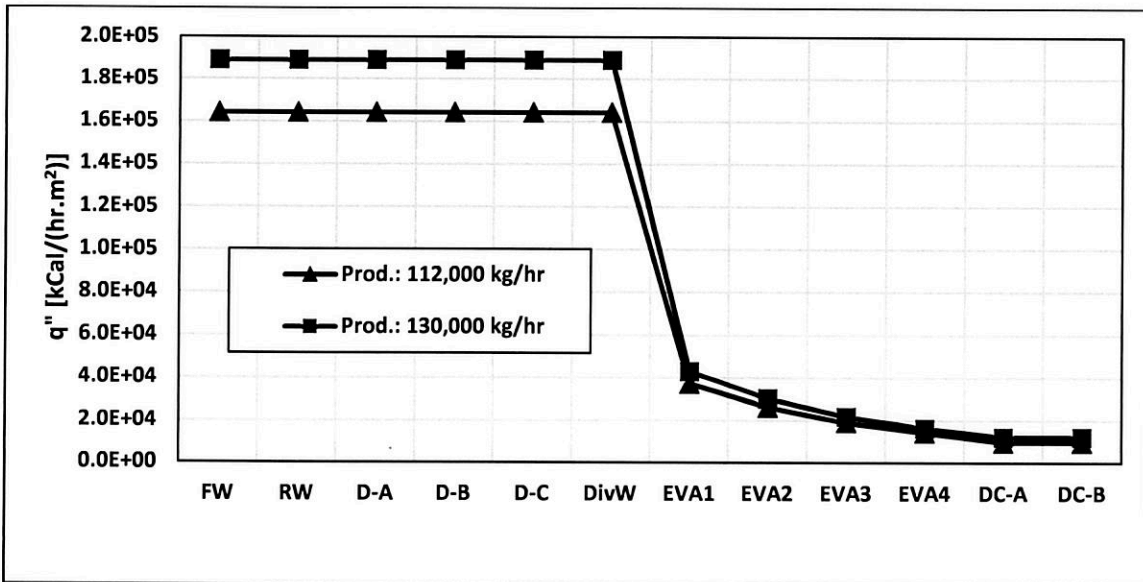
Figure 6-33: Comparing heat flux results for all boiler circuits
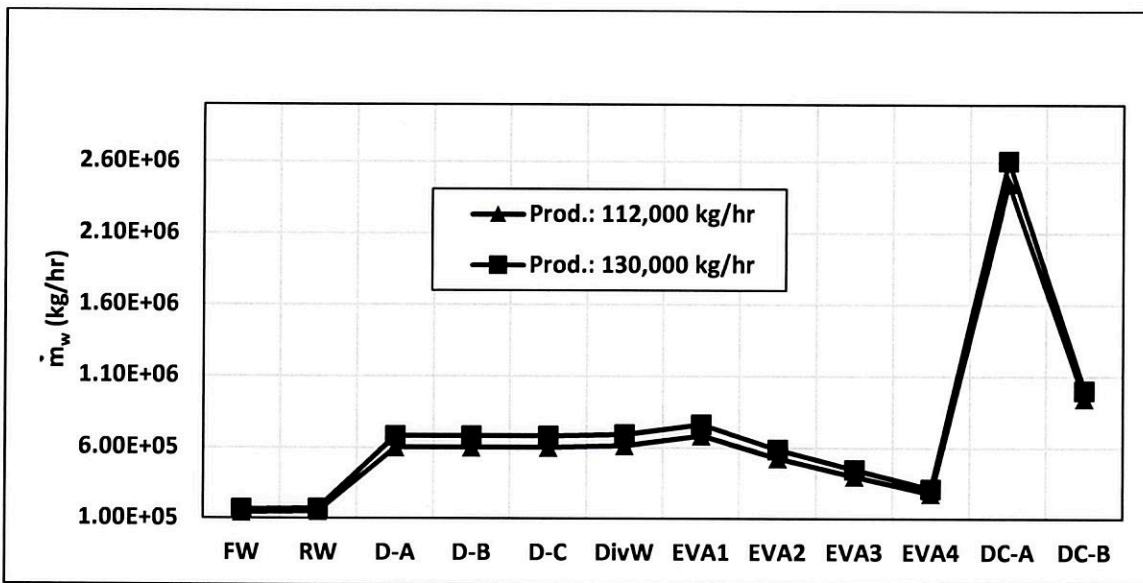
Figure 6-34: Comparing mass flow rate values for all boiler circuits
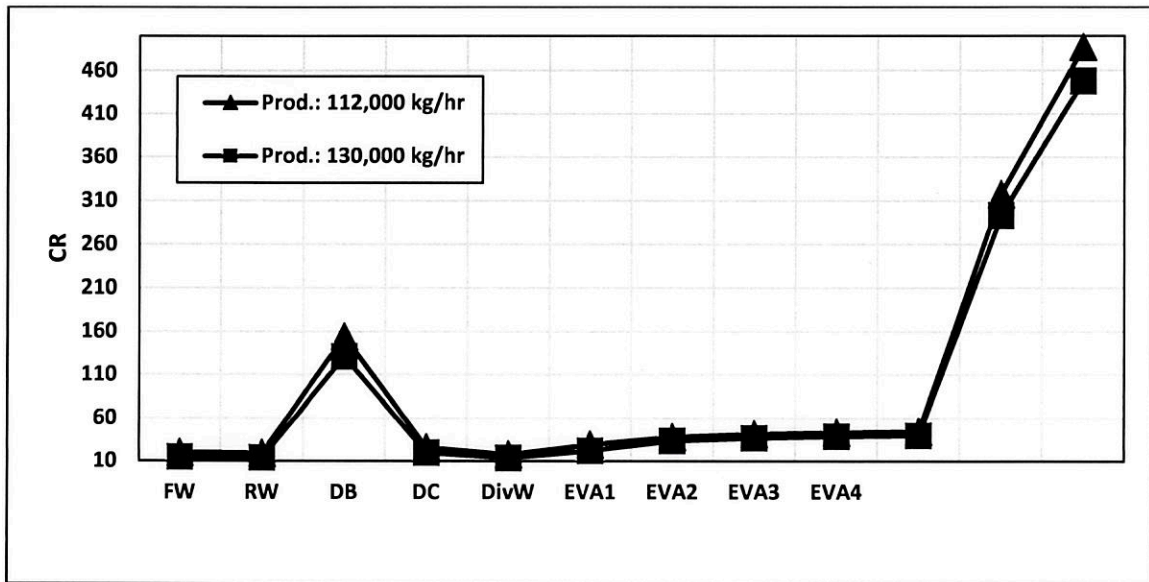
Figure 6-35: Comparing circulation ratio values for all boiler circuits

CHAPTER 7

CONCULSIONS AND RECOMMENDATIONS

7.1 Conclusions

Based on the dissertation study results, the following can be concluded:

1) A program that utilizes Excel as a platform and Visual Basic to establish the program logic was developed to size and analyze the performance of package boilers.

2) The program is capable of conducting detailed analysis of package boilers, is user-friendly, and does not require high computing capacity or additional software.

3) The program can be used as a quick on-site diagnostic tool to evaluate the impact of plugging some tubes or increasing the heat flux to achieve a higher boiler load.

4) The program results were validated with actual measured data of package boilers. Excellent agreement was observed between the two results.

5) The impact of heat flux on circulation parameters and wall temperature was determined for each circuit in 112,000 kg/hr capacity package boiler.

6) The impact of pressure drop (internal friction) on circulation parameters and wall temperature was determined for each circuit in in 112,000 kg/hr package boiler.

7) The impact studies results identified that the D-Tubes (Circuit 3) are the most critical circuit where the circulation ratio decreases beyond the minimum allowable limit at lower heat flux values.

8) Plugging tubes of the D-Tubes (Circuit 3) has significant effect on circulation ratio and wall temperature. It reduces the first and increases the second respectively.

9) Plugging the boiler bank tubes has no significant effect on circulation parameters, but it does impact the production rate.

10) Further analysis on the effect of heat flux variation indicated that the roof tubes of the D-Tubes are the most critical ones as the circulation ratio in these tubes reaches the minimum allowable value at a smaller heat flux values compared to other tubes in other circuits.

11) Distributed pressure drops play an adverse impact on circulation. The available driving head decreases as these pressure drops increase.

7.2   Recommendations

The main recommendations extracted from the study can be categorized into the following:

Boiler Operators and Analysts

1) Ensure that all boiler circuit tubes are designed with a circulation ratio well above the minimum allowable value of the boiler under consideration

2) Special considerations need to be made to the D-Tubes (roof tubes section) of the package boiler and should be carefully designed to avoid overheating of the tubes in that section.

3) Despite the fact that Circuit 3 was found to be the most critical in package boilers, analysis should be made for all circuits and the results should be analyzed and addressed accordingly.

4) During the analysis, a number of modifications can be made to achieve a reliable circulation design. For example, the number of tubes, tube geometry, water flow rate, furnace dimensions, number of burners, fuel specifications can be modified to satisfy design requirements. These include steam production, circulation ratios above the minimum allowable, tube wall temperature below the maximum, and a balanced net driving head between downcomers and other circuits.

5) Plugging package boiler tubes needs to be avoided as much as possible in the furnace tubes but could be accepted in the boiler bank tubes for a temporary period and up to 5% of the tubes.

6) Monitor water treatment programs and chemical cleaning of boilers tubes closely to minimize the impact of internal friction and pressure drop across the circuit tubes.

Future Work

1) Expand the analysis to large, field-erected boilers to avoid circulation problems in those boilers that experience such problems frequently.

2) Integrate this model with other transient performance monitoring programs to monitor boiler performance in real time.

REFERENCES

1. Zvirin, Y. Nuclear Eng. And Design, Vol. 67, p. 203. 1, 1981.

2. Ganapathy, V. Boiler circulation calculations, Hydrocarbon Processing, Vol. 77, pp. 101-106, 1998.

3. Kok, H.V. and T.H.J.J. Van Der Hagen (1999). Modeling the statics of a natural-circulation boiling water reactor loop, Nuclear Technology, Vol. 127, pp. 38-48, 1999.

4. Van De Graaf, R., Van Der Hagen, T.H.J.J. and Mudde, R.F. Scaling laws and design aspects of a natural-circulation-cooled simulated boiling water reactor fuel assembly, Nuclear Technology, Vol. 105, pp. 190-200, 1994.

5. Wu, S. R., Jia, H. J. Jiang, S.Y. and Zhang, Y. J. Investigation on two-phase flow stability in a natural circulation system, Kerntechnik, Vol. 65, No. 5-6, pp. 222-226, 2000.

6. Ha, K. S., Park, R. J., Kim, H. Y., Kim, S. B., Kim, H. D. A study on the two-phase natural circulation flow through the annular gap between a reactor vessel and insulation system, Int. Comm. Heat Mass Transfer, Vol 31, No1, pp. 43-52, 2004.

7. Ganapathy, V. Understanding Boiler Circulation. Chemical Engineering, Oct., page 52-58, 2013.

8. Roslyakov, P. V., Pleshanov, K. A., and Sterkhov, K. V. A Study of Natural Circulation in the Evaporator of a Horizontal Tube Heat Recovery Steam G, Thermal Engineering, 2014, Vol. 61, No. 7, pp. 465–472, 2014.

9. de Mesquita, R. N., Castro, L. F., Torres, W. M., Rocha, M. da S., Umbehaun, P. E., Andrade, D. A., Sabundjian, G., Masotti, P. H.F. Classification of natural circulation two-phase flow image patterns based on self-organizing maps of full frame DCT coefficients. Nuclear Engineering and Design 15 August: 335:161-171, 2018.

10. Pereyra, E. J., Shah, B. A. and Edwards, L. L. Circulation rates and tube burnout in natural circulation boilers, Tappi Journal, Vol. 72, pp. 143-148, 1989.

11. Basu, P. and L. Cheng. An experimental and theoretical investigation into the heat transfer of a finned water wall tube in a circulating fluidized bed boiler, Int. J. Energy Research, Vol. 24, pp. 291-308, 2000.

12. Astrom, K. J. and Bell, R. D. Drum-boiler dynamics, Automatica 36 363-378, 2000.

13. Gomez, A., Fueyo, N. and Diez, L. I. Modeling and simulation of fluid flow and heat transfer in the convective zone of a power-generation boiler, Applied Thermal Engineering 28 (2008) 532–546, 2008.

14. Edge, P.J., Heggs, P.J., Pourkashanian, M., Williams, A. An integrated computational fluid dynamics–process model of natural circulation steam generation in a coal-fired power plant, Computers and Chemical Engineering 35 (2011) 2618–2631, 2011.

15. Krzywanski, J. and Nowak, W. Modeling of Heat Transfer Coefficient in the Furnace of CFB Boilers by Artificial Neural Network Approach, International Journal of Heat and Mass Transfer 55 (2012) 4246–4253, 2012.

16. Hou, X., Sun, Z., Su, J., Fan, G. An investigation on flashing instability induced water hammer in an open natural circulation system. Progress Nuclear Energy, November 93: 418-430, 2016.

17. Biasi, L., G. C. Clerici, S. Garribba, R. Sala and A. Tozzi. Studies on burnout: Part 4- A new correlation for round ducts and uniform heating and its comparison with world data, Energia nucleare, Vol. 14, n. 9, pp.530-536, 1967.

18. Leung, J. C., Gallivan, K. A., Henry, R.E. and Bankoff, S. G. Critical heat flux predictions during blowdown transients, International Journal of Multiphase Flow, Vol. 7, No. 6, pp. 677-701, 1981.

19. Taler, Jan. A method of determining local heat flux in boiler Furnaces, Int. J. Heat Mass Transfer. Vol. 35, No. 6, PP. 162S1634, 1991.

20. Monde, M. and Yamaji, K. Critical heat flux during natural convective boiling in a vertical uniformly heated tubes submerged in saturated liquid, ASME Journal of Heat Transfer, Vol. 90, No. 2, pp. 111-116, 1990.

21. Monde, M., Mitsutake, Y. and Kubo, S. Critical heat flux during natural convective boiling on uniformly heated inner tubes in vertical annular tubes submerged in saturated liquid, Worme- und Stoffubertragung, Vol. 29, pp. 271-276, 1994.

22. Monde, M., Mitsutake, Y. and Hayasi, M. Critical heat flux during natural circulation boiling on uniformly heated outer tube in vertical annular tubes submerged in saturated liquid (change in critical heat flux characteristics due to heated equivalent diameter), International Journal of Heat and Mass Transfer, Vol. 42, pp. 3189-3194, 1999.

23. Hall, David D. and Mudawar, I. Critical heat flux (CHF) for water flow in tubes-II; Subcooled CHF correlations, International Journal of Heat and Mass Transfer 43 (2000) 2605-2640, 2000.

24. Taler, J., Duda, P., Weglowski, B., Zima, W., Gradziel, S., Sobota, T., and Taler, D. Identification of local heat flux to membrane water-walls in steam boilers, Fuel 88 (2009) 305–311, 2009.

25. Seung Jun Kim. An Experimental Study of Critical Heat Flux with Surface Modification and Its Analytic Prediction Model Development, Doctor of Philosophy in Nuclear Engineering, University of Illinois at Urbana-Champaign, 2012.

26. Y. Katto and S. Yokoya. Critical Heat Flux of liquid helium in forced convective boiling. International Journal of Multiphase Flow, Volume 10, Issue 4, Pages 401-413, August 1984.

27. Kamel, M. S., Lezsovits, F., Hussein, A. M., Mahian, O., Wongwises, S. Latest developments in boiling critical heat flux using nanofluids: a concise review. International Communications in Heat and Mass Transfer, November 98:59-66, 2018.

28. Babcock and Wilcox. Steam Its Generation and Use. Fortieth Edition, 1992.

29. Hector S. Campbell. The effect of chemical composition of water on corrosion problems in plant, Anti-Corrosion Methods and Materials, Vol. 27, No. 3, pp. 4 – 5. 29, 1993.

30. Romeo, E., Carlos, R., Monzón, A. Improved Explicit Equations for Estimation of the Friction Factor in Rough and Smooth Pipes, Chemical Engineering Journal 86 (2002) 369–374, 2002.

31. Woodruff, E. B., Lammers, H. B., Lammers, T. F. Steam Plant Opeartion, Eighth Edition, 2005.

32. Annaratone, Donatello. Steam Generators Description and Design, 2008.

33. Joseph, D. D. and Yang, B. H. Friction Factor Correlations for Laminar Transition and Turbulent Flow in Smooth Pipes, Physica D 239 (2010) 1318-1328. 33, 2010.

34. Fang, X. and Xu, Y. Correlations for Two-Phase Friction Pressure Drop Under Microgravity, International Journal of Heat and Mass Transfer 56 (2013) 594–605, 2013.

35. Slawomir, G. and Karol, M. Estimation of the pressure drop in the natural circulation boiler evaporator. MATEC Web of Conferences, Vol 240, p 05009, 2018.

36. Lockhart, R.W. and Martinelli, R. C. Proposed correlation of data for isothermal two-phase two-component flow in a pipe. Chem. Eng. Prog., Vol. 45, pp. 39-48, 1949.

37. Martinelli, R.C. and Nelson, D. B. Prediction of pressure drop during forced circulation boiling of water. Trans. ASME, Vol. 70, p. 695, 1948.

38. Chine-Hsiung, L, and C. H. Barkelew. Numerical Analysis of Jet-Stirred Reactions with Turbulent Flows and Homogeneous Reactions, AIChE Journal, Vol. 32, No. 11, November, 1986.

39. Coelho, P. J., and Carvalho, M. J. Evaluation of a Three Dimensional Mathematical Model of a Power station Boiler, Journal of Engineering for Gas Turbines and Power, Vol. 118, pp.887-895, 1996.

40. Fan, J. R., X. D. Zha and K. F. Cen. "Study on Coal Combustion Characteristics in a W-shaped Boiler Furnace," Fuel, Vol. 80, pp. 373-381, 2001.

41. Milkhaliov, A. G. and Batrakov, P. A. Experimental study of the radiative-convective heat transfer in complex shape furnaces of the gas-tube boiler. 2016 Dynamics of Systems, Mechanisms and Machines (Dynamics) Dynamics of Systems, Mechanisms and Machines (Dynamics), 1-4 Nov. 2016.

42. Liu, F., Becker, H. A. and Bindar, Y. A Comparative Study of Radiative Heat Transfer Modeling in Gas-Fired Furnaces Using the Simple Grey and the Weighted-Sum-of-Grey-Gases Models. International J. of Heat and Mass Transfer, Vol. 41, pp. 3357-3371, 1998.

43. Chungen, Y., S. Caillat, J. L. Harion, B. Baudoin and E. Perez. Investigation of the Flow, Combustion, Heat Transfer and Emissions from a 609 MW Utility Tangentially Fired, Pulverized Coal Boiler, Fuel, Vol. 81, pp. 997-1006, 2002.

44. Bader, H., Habib, M., Said, S. Analysis of Water Circulation in Boilers, Report for Saudi Aramco, Dhahran, Saudi Arabia, 2006.

45. Habib, M. A., Said, S., Bader, H. Determination of maximum Boiler Swing Rates, Report for Saudi Aramco, Dhahran, Saudi Arabia, 2009.

46. Moghari, M., Hosseini, S., Shokouhmand, H. Sharifi, S. Izadpanah, S. A numerical study on thermal behavior of a D-type water-cooled steam boiler, Applied Thermal Engineering 37 (2012) 360 -372, 2012.

47. Azimi, S. S. and Nazami, M. H. Modeling of combustion of gas and natural gas in a furnace: Comparison of combustion characteristics. Energy, Volume 93, Part 1, 15 December, Pages 458-465, 2015.

48. Zarrabi, K, Platfoot, R. A., Zhang, H. & Sheth, A. and Rose, I. Estimation of metal temperature variations for scarred boiler tubes, PII: SO308-0161(96)00005-1, 1996.

49. Ranjbar, Khalil (2006). Failure analysis of boiler cold and hot reheater tubes, Engineering Failure Analysis 14 (2007) 620–625, 2007.

50. Khjavi, M.R., Abdolmaeki, A.R., Adibi, N., and Mirfendereski, S. Failure analysis of bank front boiler tubes, Engineering Failure Analysis 14 (2007) 731–738, 2007.

51. Bulloch, J. H., Callagy, A. G., Scully, S., Greene, A. A failure analysis and remnant life assessment of boiler evaporator tubes in two 250 MW boilers, Engineering Failure Analysis 16 (2009) 775–793, 2008.

52. Dominguez, Veronica A., Tedesco, Roberto and Peña, Pablo G. Analysis of Steam Superheater Tubes Failures of Medium-Pressure Boilers, Paper No. 08433, NACE Corrosion 2008 Conference and Expo.

53. Emara-Shabaik, H. E., Habib, M. A., and Al-Zaharna, I. Prediction of risers' tubes temperature in water tube boilers, Applied Mathematical Modelling 33 (2009) 1323–1336, 2009.

54. Purbolaksono, J. Ahmad, J., Khinani, A., Ali, A. A. and Rashid, A. Z. Failure case studies of SA213-T22 steel tubes of boiler through computer simulations, Journal of Loss Prevention in the Process Industries 23 98–105, 2010.

55. Kembaiyan, Kumar; Miller, William D; Kluck, Robin W; Collins, Stephen M; Leach, Matthew;Phillips, Mark. Impact of Circulation and Water Treatment on Boiler Tube Failures, Materials Performance; Apr 2013; 52, 4; ProQuest.

56. Malik, Anees, Meroufel, Abdelkader and Saleh Al-Fozan. Boiler Tubes Failures: A Compendium of Case Studies, J Fail. Anal. and Preven. 15:246–250, 2015.

57. Package Boilers Manuals, Saudi Aramco.

58. Rayaprolu, K. Boilers for Power and Process, 2009.

59. Ganapathy, V. Industrial Boilers and Heat Recovery Steam Generators – Design, Applications, and Calculations, 2003.

60. ASME PTC 4-2008. Fired Steam Generators – Performance Test Codes.

CURRICULUM VITAE

Name	Hamad S. Al Mehthel Al Saqour
Nationality	Saudi Arabia
Date of Birth	6/22/1971
Email	almehths@aramco.coml
Address	Dhahran, Saudi Arabia

Academic Background

B.Sc., Mechanical Engineering, King Fahd University of Petroleum and Minerals, GPA of 3.72 out of 4.0	Jan. 1994
M.Sc., Mechanical Engineering, Rice University, Houston, Texas, the USA, GPA 4.0 out of 4.0	May 2000
Ph.D., Mechanical Engineering, King Fahd University of Petroleum and Minerals	May 2019

Work Experience

Process Equipment Engineer. Consulting Services	Oct. 1994 – Mar. 2006
Supervisor, Process Equipment Unit, Consulting Services Department, Saudi Aramco	Mar. 2006 – Jun. 2009
Assistant to VP, Engineering Services, Saudi Aramco	Jun. 2009 – Jul. 2010
Senior Project Engineer/Project Manager, Yasref Project Execution, Gasoline Block Package	Jul. 2010 – Aug 2012
Coordinator, Professional Engineering Development Division, Saudi Aramco	Aug 2012 – Aug 2013

Division Head, Technology and Engineering Division, Aramco Overseas Company	Sept. 2013 – Sept. 2015
Coordinator, Static Equipment Division, Consulting Services Department, Saudi Aramco	Sept. 2015 – Mar. 2016
Coordinator, Engineering Knowledge and Resources Division, Engineering, Saudi Aramco	Since Mar. 2016

Conferences

1. *Hamad S. Al-Mehthel Al-Saqour.* Aramco Overseas Deepens Relations in Chemicals. IChemE 2014 Global Award Ceremony, Gloucestershire, the UK.

2. *Hamad S. Al-Mehthel Al-Saqour.* Aramco Overseas Technology, Engineering and Procurement. ONS 2014, Stavanger, Norway.

3. *Hamad S. Al-Mehthel Al-Saqour.* Boiler Performance Optimization Program. Petrotech 2002 , Bahrain

4. *Hamad S. Al-Mehthel Al-Saqour.* Girth Flange Analysis in Stabilizer Colum Reboilers. Saudi Aramco Technical Exchange Meeting, July 2003, Dhahran, Saudi Arabia.

5. *Hamad S. Al-Mehthel Al-Saqour.* Engineering Knowledge Management. SPE Upstream Knowledge Management Workshop, Abu Dhabi, UAE, 2017.*Hamad S. Al-Mehthel Al-Saqour.* Technology Strategy - Aramco Overseas Company. AAPG 2015 Conference, Amsterdam, the Netherlands.

APPENDIX A: DETAILED HEAT FLUX CALCULATIONS

Input Data

Variable	Description	Value	Unit
B	Number of burners	2	
BD	% boiler blowdown from SO	1	%
c_{pg}	Specific heat of flue gas at T_g	0.3087	kCal/(kg.°C)
$c_{pg-adia}$	Specific heat of flue gas at the adiabatic flame temperature	0.322	kCal/(kg.°C)
D_F	Furnace depth	9.558	m
D_o	Tube outside diameter	63.5	mm
f_i	Internal fouling factor	0.0002	$(m^2.hr.°C)/kCal$
f_e	External fouling factor	0.0002	$(m^2.hr.°C)/kCal$
H_F	Furnace height	6.32	m
LHV	Lower heating value of fuel gas	9,166	$kCal/m^3$
L_f	Length of fin	0.49	m
P_s	Steam pressure	44.13	barg
P_d	Steam Drum pressure	49.03	barg
P_{fw}	Feed water pressure	64.72	barg

p	Tube pitch	88.5	mm
RL	% Radiation loss of the absorbed heat	0.33	%
SO	Steam output	112,000	kg/hr
T_{sup}	Superheated steam temperature	450	$°C$
T_{fw}	Feed Water Temperature	140	$°C$
T_{fuel}	Fuel gas temperature	25	$°C$
T_{amb}	Ambient air temperature	26	$°C$
t_f	Fin thickness	6	mm
t_w	Tube wall thickness	4.0	mm
$m_{a/f}$	Specific combustion air flow (per fuel volume)	14.316	kg/m^3
$m_{g/f}$	Specific flue gas flow (per fuel volume	15.139	kg/m^3
Tube material		Carbon Steel	
Fin material		Carbon Steel	
W_F	Furnace width	3.54	m
$\rho_{g/fu}$	Flue gas density	1.237	kg/m^3
ξ	Boiler efficiency	91	%

λ	Thermal conductivity of tube and fin	35.5	kCal/(hr.m.°C)
ρ_a	Wet air density	1.283	kg/m³
α_i	Internal heat transfer coefficient	4000	kCal/(hr.m².°C)
δ	Fin factor	0.236	
$\in$	Fuel emissivity	0.378	

Output (Calculations)

Variable	Description	Equation	Value	Unit
T_{sat}	Saturation temperature at drum pressure	Steam tables	262.7	$^{\circ}C$
$h_{sat.s}$	Enthalpy of saturated steam	Steam tables	667.6	kCal/kg
$h_{sat.w}$	Enthalpy of saturated water	Steam tables	274.3	kCal/kg
h_{fw}	Enthalpy at feed water temperature	Steam tables	141.7	kCal/kg
$h_{sup.st}$	Enthalpy of superheated steam	Steam tables	794.3	kCal/kg
Q_{abs}	Absorbed heat output	4.2	73,091,200	kCal/hr
Q_{bd}	Blowdown heat output	4.3	148,512	kCal/hr
Q_{THO}	Total heat output	4.1	73,239,712	kCal/hr
Q_c	Total heat of combustion	4.4	80,483,200	kCal/hr
$\dot{m}_{fuel}$	Total fuel mass flow rate	4.5	8,781	m^3/hr
$\dot{m}_a$	Air mass flow rate	4.6	125,703	kg/hr
$\dot{V}_a$	Volumetric flow rate of combustion air	4.7	97,976	m^3/hr
$\dot{m}_g$	Flue gas mass flow rate	4.8	132,930	kg/hr
$\dot{V}_g$	Volumetric flow rate of combustion air	4.9	107,461	m^3/hr
EPRS	Effective projected radiant surface of the furnace tubes	4.12	199	m^2

V_{fur}	Furnace volume	4.13	214	m^3
Q_{c-EPRS}	Combustion heat load on the furnace EPRS	4.10	404,438	$kCal/(hr.m^2)$
Q_{c-FV}	Combustion heat load on the furnace volume	4.11	376,090	$kCal/(hr.m^3)$
T_{w-fur}	Furnace tube wall temperature	Assumed initially	359.5	$°C$
T_f	Fin temperature	Assumed initially	398.4	$°C$
C_t	Screen tube exposed circumference	4.17	94	mm
E_f	Fin extension on both sides of tube	4.18	25	mm
ESL	Total exposed surface length	4.16	119	mm
T_{t-f}	Mean temperature of tube and fin	4.15	368	$°C$
T_g	Flue gas temperature	Assumed initially	1349.2	$°C$
Q_{rad}	Radiation heat from flue gas to tubes	4.14	25,205,274	$kCal/hr$
α_e	External heat transfer coefficient	4.19	129.05	$kCal/(hr.m^2.°C)$
α_o	Overall heat transfer coefficient in furnace	4.20	117.49	$kCal/hr$
Q_{rad-RL}	Radiation heat considering radiation loss	4.21	25,122,370	$kCal/hr$

112

ΔT_w	Temperature difference across tube wall	4.23	14.22	℃
ΔT_{fi}	Temperature difference across fi	4.24	25.25	℃
ΔT_{fe}	Temperature difference across fe	4.25	25.25	℃
ΔT_{ei}	Temperature difference from external to internal bulk	4.26	31.93	℃
T_i	Temperature of internal bulk	4.30	274.77	℃
T_{w-fur}	Furnace tube wall temperature	4.22 (first check)	359.36	℃
ΔT_f	Temperature difference across the fin	4.28	39.1	℃
T_f	Fin temperature	4.27 (first check)	398.41	℃
q''	Heat flux	4.29	126,227	$kCal/(hr.m^2)$
Q_{fur}	Heat exchanged in the furnace	4.31	25,119,200	kCal/hr
Q_g	Flue gas heat at furnace exit	4.33	55,360,830	kCal/hr
T_g	Flue gas temperature	4.32 (first check)	1349.2	℃
h_{adia}	Adiabatic enthalpy	4.35	605.46	kCal/kg
T_{adia}	Adiabatic flame temperature	4.34	1880.3	℃

113

APPENDIX B: DETAILED CIRCULATION CALCULATIONS

Input Data:

Variable	Description	Value	Unit
EPRS	Effective projected radiant surface of the furnace tubes	199	m^2
D_o	Tube outside diameter	63.5	mm
f_{incon}	Concentrated friction factor at the inlet	0.5	
f_{outcon}	Concentrated friction factor at the outlet	1.0	
L_e	Equivalent tube length	7.25	m
N	Number of the tubes in Circuit 1	34	
P_s	Steam pressure	47.50	barg
$\Delta P_{internals}$	Steam drum internals pressure drop	600	kg/m^2
p	Tube pitch	N/A	
q"	Heat flux	163,986	$kcal/(hr.m^2)$
SO	Steam output	112000	kg/h
SH_i	Static Head at the inlet of the circuit	0.0	m
SH_o	Static Head at the outlet of the circuit	7.25	m
T_{EO}	Water temperature at the economizer outlet	194.70	°C

t_w	Tube thickness	4.0	mm
λ	Thermal conductivity of fin and tube	41.3	W/(m.°C)
α_i	Internal heat transfer coefficient	4,700	W/(m².°C)

Information of feeder tubes from mud drum to front wall (Circuit 1)

D_{oF}	Feeder tubes outside diameter	63.5	mm
N_F	Number of the feeder tubes	14	
SH_{iF}	Static Head at the inlet of the feeder tubes	0.0	m
SH_{oF}	Static Head at the outlet of the feeder tubes	0.0	m
t_{wF}	Feeder tubes thickness	4.0	mm

Information of supply tubes from front wall (Circuit 1) to steam drum

D_{oS}	Supply tubes outside diameter	63.5	mm
N_S	Number of the supply tubes	14	
SH_{iS}	Static Head at the inlet of the supply tubes	0.0	m
SH_{oS}	Static Head at the outlet of the supply tubes	0.0	m
t_{wS}	Supply tubes thickness	4.0	mm

Output (Calculations):

Variable	Description	Equation No.	Value	Unit
T_{sat}	Saturation temperature at drum pressure	Steam tables	262	°C
h_{fw}	Enthalpy at feed water temperature (economizer outlet)	Steam tables	198	kcal/kg
$h_{sat.w}$	Enthalpy of saturated water	Steam tables	273	kcal/kg
$\dot{m}_{s1}$	Steam generation in the circuit	4.42	8469	kg/hr
h_{fg}	Latent heat of vaporization	Steam tables	394.48	kcal/kg
S	Circuit tubes surface area	4.43	20.373	m^2
N	Number of the tubes in Circuit 1 (final)	Assumed initially	34	
$\dot{m}_{s2}$	Steam inlet flow (required for subcooling) per crcuit	4.44	650	kg/hr
$\dot{m}_w$	Water mass flow rate per circuit	Assumed initially	153,861	kg/hr
$\dot{m}_s$	Steam mass flow rate per circuit	4.41	9,119	kg/hr
CR	Circulation ratio	4.45	16.9	

$CR_{min-allow}$	Minimum allowable circulation ratio	B&W and Annaratone model [32]	11.7	
V_P	Mass velocity	4.46	1,870,570	$kg/(hr.m^2)$
Circuit Inlet				
x_i	Ratio of steam at the inlet to steam at the outlet	4.47	0.077	
ρ_{wi}	Inlet water density at the steam drum design pressure	Steam tables subroutine	780.66	kg/m^3
ρ_{si}	Inlet steam density at the steam drum design pressure	Steam tables subroutine	24.60	kg/m^3
ρ_{mix-i}	Inlet mixture density at the steam drum design pressure	4.48	691.31	kg/m^3
μ_{wi}	Inlet water viscosity at the drum design pressure	Steam tables subroutine	0.3749	$kg/(m.hr)$
μ_{si}	Inlet steam viscosity at the drum design pressure	Steam tables subroutine	0.0677	$kg/(m\ hr)$
v_i	Water inlet velocity	4.49	0.75	m/s
Z_i	Inlet velocity head	4.50	20	kg/m^2
Circuit Outlet				

117

x_o	Ratio of steam output to steam at the outlet	4.51	1.0	
ρ_{wo}	Outlet water density at the steam drum design pressure	Steam tables subroutine	780.66	kg/m^3
ρ_{so}	Outlet steam density at the steam drum design pressure	Steam tables subroutine	24.60	kg/m^3
ρ_{mix-o}	Outlet mixture density at the steam drum design pressure	4.52	276.68	kg/m^3
μ_{wo}	Outlet water viscosity at the drum design pressure	Steam tables subroutine	0.3749	$kg/(m.hr)$
μ_{so}	Outlet steam viscosity at the drum design pressure	Steam tables subroutine	0.0677	$kg/(m.hr)$
v_o	Water outlet velocity	4.53	1.88	m/s
Z_o	Outlet velocity head	4.54	50	kg/m^2
Average properties				
$\rho_{mix-avg}$	Average mixture density	4.55	420.78	kg/m^3
τ	Density ratio factor	4.57	0.476	
μ_{w-avg}	Average water viscosity	4.58	0.3749	$Kg/(m\ hr)$
μ_{s-avg}	Average steam viscosity	4.59	0.0677	$Kg/(m\ hr)$

$\mu_{mix-avg}$	Average mixture viscosity	4.56	0.2286	$Kg/(m\,hr)$
Re	Reynolds number	4.60	454,064	
v_{avg}	Mixture average velocity	4.61	1.23	m/s
Z_{avg}	Average velocity head	4.62	32.71	kg/m^2
L_e/D_i	Equivalent tube length to diameter ratio	4.71	132.4	
$\dfrac{E}{D_i}$	Tube roughness factor	4.70	0.000793	
f_{new}	Friction factor for new tube	4.69	0.019461	
f_{fouled}	Friction factor for fouled tube	4.68	0.023353	
ΔP_{dist}	Distributed pressure drop	4.67	101	kg/m^2
ΔP_{incon}	Concentrated pressure drop at the inlet	4.72	10	kg/m^2
ΔP_{outcon}	Concentrated pressure drop at the inlet	4.73	50	kg/m^2
ΔP_{tot}	Total pressure drop in the circuit	4.66	161	kg/m^2
TH	Thermosyphonic head (average mixture density by the static head difference)	4.74	-3051	kg/m^2

119

NDH_1	Net driving head	4.65	-3212	kg/m^2
The pressure drop for the feeder and supply tubes are calculated the same as the above				
NDH_2	Net driving head for the supply tubes	4.65	-403	kg/m^2
NDH_3	Net driving head for the supply tubes	4.65	-1046	kg/m^2
The total net driving head for Circuit 1 including the feeders and supply tubes				
NDH	Total net driving head	$NDH_1 + NDH_2 + NDH_3$	-4660	kg/m^2
Note: the NDH for the downcomers circuits is +4660 kg/m2; hence this NDH is balanced by the NDH of Circuit # 1 (-4660 kg/m2).				